Development of Mid-Infrared Spectroscopic Methods for the Determination of Soil Chemical Quality in Tillage Fields

Konrad Metzger

NUI Galway
OÉ Gaillimh

Supervised by

Dr. Karen Daly, Teagasc Johnstown Castle

Dr. Chaosheng Zhang, NUIGalway

The thesis is submitted to National University of Ireland, Galway in fulfilment of the requirement for the degree of Doctor of Philosophy, School of Geography, Archaeology & Irish studies

Submission date: February 2021

“All civilization is basically dependant upon natural resources. All natural resources, except only subterranean minerals, are soil or derivatives of soil. Farms, Ranges, crops and livestock, forests, irrigation water, and even waterpower resolve themselves into questions of soil. Soil is therefore the basic natural resource”

Aldo Leopold, 18.01.1921

Erosion and prosperity

For my future children

Table of Contents

Declarations

This thesis or any part thereof has not been or is not currently being submitted for any degree at any other university.

Konrad Metzger

This thesis is the result of my own work, except where explicit reference is made to the work of others.

Konrad Metzger

Abstract

Fertile soils with high soil quality are the basis for good agricultural production to feed a growing world population. Managing soil fertility and soil quality precisely requires a profound knowledge of its status in the fields, and in the last decades, precision agriculture (PA) has developed as a means of managing soils for optimum yield. Soils show great variability within the fields caused by natural factors as well as management effects, especially field traffic, which introduces compaction, but also leads to variable distributions of nutrients. Capturing this variability requires a high number of samples, which may not be feasible with conventional sampling methods and laboratory analyses. The cost of processing multiple samples per field is too high, using, potentially harmful chemicals in the analysis, posing a threat to health and environment.

This thesis evaluated the feasibility of MIR spectral models to predict soil chemical parameters at the spatial and temporal resolutions required for precision fertiliser applications. Furthermore, the hypothesis that zone-based sampling in field headlands improves the understanding of these areas in tillage systems and captures the variability in soil chemical quality caused by management was evaluated. was evaluated. Focus of the research in this thesis was on the following tasks:

a) the examination of the application of mid-infrared spectroscopy (MIR) as a rapid method of soil analysis for lime requirement (LR) with a benchtop instrument in sampling zones in tillage systems, and

b) an assessment of the performance of a handheld MIR spectrometer for *in situ* sampling and soil analysis of agricultural soils in a case study of lime requirement and organic matter.

c) an inventory and assessment of the variability of soil chemical quality parameters among different headland zones

Mid-Infrared Diffuse Reflectance Fourier-Transform Spectroscopy (MIR-DRIFTS) is a rapid method that can predict soil parameters by analysing the patterns of infrared light absorption caused by soil constituents such as clay minerals and organic matter. In addition to the soil constituents themselves, dependant (such as LR) and summarizing (such as %OM) soil parameters can be predicted with the help of multivariate models and chemometrics.

Lime requirement, defined as the amount of ground limestone necessary to bring acidified soils back to optimum levels (pH 6.5 for tillage soils) is currently measured

in the laboratory with the “Shoemaker, McLean and Pratt” (SMP) buffer. A substitute for this method is required, as the solution contains carcinogenic chromate posing a threat to health and environment which is soon to be discontinued in line with the EU REACH directive. MIR-DRIFTS is a fast and clean alternative with which a partial least squares regression (PLSR) model was calibrated to predict the LR based on the samples from the field sampling campaign. A subset of the samples from the 41 fields of this study was used to build a calibration model (n=495, 31 of the sampled fields) resulting in a R^2 of 0.89 and a Root Mean Squared Error of Calibration (RMSEC) of 1.56 t/ha. Validation with the remaining samples (n=160, 10 of the sampled fields) resulted in an overall R^2 of 0.76 and Root Mean Squared Error of Prediction (RMSEP) of 1.68t/ha, while for the predictions of the LR for each of the ten validation fields separately resulted in R^2 between 0.41 and 0.72 and RMSEP of 0.48 and 4.2 t/ha. While the error for prediction of the LR for each point in the field is too high, we found this method to be a comparable method to the current laboratory extractions based on averaged values. Averaging the prediction of the replicates in each zone as performed in the generalized mixed model also showed to deliver promising results by delivering similar significant differences.

Recent development of handheld MIR spectrometer allows their use directly in the field, where problems arise due to water content and other *in situ* characteristics such as aggregates, roots, cracks etc. distorting the spectra, which leads to problems with the prediction. The performance of a handheld MIR-DRIFTS instrument (Agilent 4300 handheld FTIR) to bring the MIR-DRIFTS technology one step further to being utilized for in-field analyses was analysed. The possibility of using a calibration model, which was developed on a benchtop instrument, to predict spectra collected with a handheld instrument was researched, but comparison of the methods with a Bland-Altman method comparison statistic confirmed that it is preferable to use spectra from the same instrument.

For the application of the handheld FTIR *in situ*, a simple sample preparation step before scanning soil samples on-site in field-moist condition was developed, in which field-fresh samples are filled into a small dish, their surface is smoothed and they can be scanned directly in the field. Samples from three fields were scanned at decreasing moisture contents, from which seven moisture-specific correction spectra were calculated. The correction spectra applied on the moist spectra greatly improved predictions for LR and %OM with a PLRS model derived from dried and ground handheld scanned spectra. For LR they were delivering results similar to the reference sample at low moisture contents (<10% GMC, below the permanent wilting point), for

%OM they corrected the spectra consistently at all moisture contents, beginning at the field moist samples.

To analyse the management impacts on the headland area soil chemical quality, 41 tillage fields in Ireland were sampled in four different zones around the main headland tramline according to traffic (A: field edge, B: main headland tramline, C: transition zone and D: undisturbed main field). Until effective PA measures for soil chemical quality sampling are developed, the efficiency of managing fields and specifically headlands in zones according to traffic was analysed statistically with regards to soil fertility parameters, especially nutrient status, LR and percent organic matter (%OM). Statistical analysis of the difference between the zones with a generalized linear mixed model (SAS procGLIMMIX) revealed significant ($P<0.05$) differences between the zones, especially those involving the main tramline for Phosphorous (P), Potassium (K), LR and pH, while for %OM only significant differences were found in loamy soils. Similar patterns of significant differences between the zones were found when MIR predicted LR and OM values were analysed with the generalized linear mixed model.

The findings of this research underline, that a zone-based approach to determine soil chemical quality coupled with the application of MIR for rapid soil analysis will improve decision support for soil management in tillage systems. Dividing the headland area into different zones allows for a more targeted management of field traffic induced variability, marking one step toward an efficient PA.

This research contributes to the advancement of MIR soil spectroscopy for the application in PA with the following main findings:

- MIR spectroscopy is a feasible alternative for the use of SMP buffer solution for the determination of LR on a field-wide application based on averages
- MIR spectroscopy can be used for screening in a headland zone-based management setting for LR and %OM
- A simple *ex-situ* sample preparation method was developed which enabled the scanning of field moist, untreated soils
- With moisture-specific correction spectra, the prediction of LR and %OM from field moist samples was greatly improved
- There are statistically significant differences in soil chemical quality parameters between different zones in headlands, which can be used to guide headland-zone-specific management decisions

Acknowledgements

I would like to express my sincere gratitude to my supervisors Dr. Karen Daly and Dr Chaosheng Zhang for their guidance and support during the PhD and for their patience and open ears for my questions. I would also like to thank the Walsh Scholarship and ICT-Agri ERA-Net for the funding of my research, Teagasc for providing the infrastructure for all the experiments and NUIGalway for the scientific support and education. The guidance from the members of my Graduate Research Committee Dr. Maura Farrell, Dermot Forristal and Prof. Kevin McDonnell is much appreciated.

While conducting the fieldwork and the experiments the laboratory staff of Teagasc Johnstown Castle was always available for advice and help during the experiment, and I would like to thank especially Dr. Anna Fenelon, Dr Brendan Healy and Carmel O'Connor as well as the interns and summer students for their help conducting the analyses in the laboratory.

Dr. Mark Ward was a great partner during the fieldwork without whom it wouldn't have been possible to collect the necessary amount of samples, thank you for your help and the great time in the field!

I would like to thank my office partner Ian Kavanagh for the good time in our office, the interesting chats, for teaching me about farming and life in Ireland, and for giving me a lift to and from work!

I am grateful for the love and care from my family: my parents, Luitgard and Hanspeter Metzger who supported me all the way until this point and raised me to be the person who I am today and my siblings Elisabeth and Ekkehard.

Special thanks are due to my in-laws Andréa Estrella, Andrea Cappelletti and Gianlucka for giving us a home for the final writing stage.

And finally, I would like to thank my wonderful wife, Marina Estrella for always being on my side, supporting me and never giving up believing in me! Thank you so much my princess, without you I wouldn't have come so far! I love you!

Publications

This thesis is based on three scientific publications with additional integrating chapters. The scientific publications are as follows:

Paper 1 deals mainly with calibrating a PLSR model for Lime requirement based on the samples from 41 fields.

> **Metzger, K.,** Zhang, C., Ward, M., Daly, K. 2020. Mid-infrared spectroscopy as an alternative to laboratory extraction for the determination of lime requirement in tillage soils. Geoderma, https://doi.org/10.1016/j.geoderma.2020.114171

Paper 2 describes the development of a sampling strategy with a handheld portable MIR scanner in a small trial.

> **Metzger, K.,** Zhang, C., Daly, K., 2021. From benchtop to handheld MIR for soil analysis: Predicting lime requirement and organic matter in agricultural soils. Biosyst. Eng. 204, 257–269. https://doi.org/10.1016/j.biosystemseng.2021.01.025

Paper 3 deals with the analysis of the four sampling zones, examining if there are statistically significant differences and if they can be attributed to certain management types. Additionally, it is explored how well MIR predicted samples display statistically significant differences.

> **Metzger, K.,** Zhang, C., Ward, M., Daly, K. 2021. Variability in Soil Chemical Quality in Traffic-dependent Zones within Field Headlands. *Communications in Soil Science and Plant Analysis.*
>
> https://doi.org/10.1080/00103624.2021.1921191

List of Figures

List of Tables

Abbreviations

%OM	Percentage Organic Matter
°C	Degree Celsius
µ	Mean
Al	Aluminium
Al	Absorbance
ANN	Artificial Neural Network
b	Pathlength (Lambert Beer)
B	Spectral Power Density
BS	Base Saturation
C	Carbon
c	Concentration (Lambert Beer)
Ca	Calcium
$CaCO_3$	Calcium Carbonate (limestone)
CEC	Cation Exchange Capacity
Co	Cobalt
CO_2	Carbon Dioxide
CTF	Controlled Traffic Farming
Cu	Copper
d	Particle Diameter
DA	Discriminant analysis
DR	Diffuse Reflectance
DRIFTS	Diffuse Reflectance Infrared Fourier Transform Spectroscopy
DTGS	Deuterium Triglycine Sulphate Detector
EPO	External Parameter Orthogonalization
EU	European Union
Fe	Iron
FTIR	Fourier Transform Infrared (Spectroscopy)
g	Gravitational Acceleration
GMC	Gravimetric Water Content
GPS	Global Positioning System
H^+	Hydrogen Ion
H2O	Water Molecule
I	Reflected Light Intensity
I'	Intensity of Beam (Interferogram)
I_0	Incident Light Intensity
ICT	Information and Communications Technology
IR	Infrared
K	Potassium
KBr	Potassium Bromide
LLoA	Lower Limit of Agreement
LR	Lime requirement
LV	latent variable
MA	Moving Average Smoothing
MCT	Mercury, Cadmium, Telluride Detector

MDS	Minimum Data Set
Mg	Magnesium
MIR	Mid-Infrared
MIR-DRIFTS	Mid-Infrared Diffuse Reflectance Infrared Fourier Transform Spectroscopy
Mn	Manganese
MSC	Multiplicative Scatter Correction
N	Nitrogen
NAP	Nitrates Action Program
NIPALS	Nonlinear Iterative Partial Alternating Least Squares
NIR	Near-Infrared
NO_3^-	Nitrate
P	Phosphorous
PA	Precision Agriculture
PCA	Principal Component Analysis
PCR	Principal Component Regression
PLS	Partial Least Squares
PLSR	Partial Least Squares Regression
ppm	Parts Per Million
R	Reflectance
R^2	Variance Explained
RCPI	Range Confidence Prediction Indicator
RMSE	Root Mean Squared Error
RMSEC	Root Mean Squared Error of Calibration
RMSECV	Root Mean Squared Error of Cross-Validation
RMSEP	Root Mean Squared Error of Prediction
RSS	Residual Sum of Squares
S	Sulphur
SD1	First Sampling Depth (5-10 cm)
SD2	Second Sampling Depth (25-30 cm)
SDG	UN Sustainable Development Goal
SEP	Standard Error of Prediction
Si	Silicon
SiC	Silicon Carbide
SMP	Shoemaker McLean and Pratt Buffer Solution
SNR	Signal to Noise Ratio
SNV	Standard Normal Variate
SOC	Soil Organic Carbon
SOM	Soil Organic Matter
SQI	Soil Quality Indicator
SSQI	Spectral Soil Quality Indicator
SVHC	Substance of Very High Concern
SWIR	Short Wave Infrared
T	% Transmittance
TSS	Total Sum of Squares
UAA	Utilized Agricultural Area
UK	United Kingdom
ULoA	Upper Limit of Agreement
UN	United Nations

USDA	United States Department of Agriculture
vis-NIR	Visible-Near-Infrared Range
X	Predictor/ Independent Variable Matrix
Y	Response/ Dependent Variable Matrix
Zn	Zinc
δ	Path Length Difference (interferogram)
ε	Molar Absorptivity Constant
η	Viscosity
ν	Wavelength
ρ	Density
σ	Standard Deviation
$\bar{\nu}$	Wavenumber

Chapter 1

Introduction

1.1 Background

1.1.1 Soils and the importance of good soil quality

Soil is a crucial part of our ecosystem and one of the pillars of the well-being of humanity. It plays an important role in reaching many of the sustainable development goals (SDG) defined by the United Nations (UN) (UN General Assembly, 2015). Soils deliver ecosystem services such as food- fibre- and fuel production, forming the basis for recreation and health, recycling or assimilation of pollutants, improvement of water and air quality, regulation of water flow, storage and delivery of nutrients, storage of carbon, stabilization of the ecosystem and being the source of biodiversity (Blume et al., 2010; Friedman et al., 2001; Johnson et al., 1990; Karlen et al., 2003; National Research Council, 1993)). Through delivering these ecosystem services, soils have a direct impact on the SDGs. SDG 2 aims for “zero hunger”, where the soils are the foundation of food production, SDG 3 is demanding “good health and well-being”, where soils are contributing by filtering contaminants in the percolating water, but are also being protected from pollution and degradation so they can still provide the ecosystem services. The aim of SDG 6 is to provide clean drinking water, where the soils again play an important role in filtering the water before it reaches the groundwater. Through SDG 11, “Sustainable cities and communities”, soils are protected from being lost to infrastructure, as they contain cultural and national heritage. SDG 12 “Responsible consumption and production” is relying on soils being managed sustainably, and in SDG 13, “Climate action” the management of soils and soil carbon can contribute to reducing CO_2-levels in the atmosphere. In their diversity they sustain “Life on land” in SDG16 (European Environmental Agency, 2019; Keesstra et al., 2016; UN General Assembly, 2015). Agriculture, as the main user of soils (others being forestry and infrastructure) is facing the challenge to produce more (healthy) food for a growing world population (UNEP, 2012) and simultaneously protecting soils from being degraded in maintaining or improving soil quality for future generations. This calls for a better understanding of soil quality, so we as society can treat the valuable resource soil with the care it deserves as the foundation of a healthy life and a functional ecosystem.

1.1.2 Measurement of soil parameters in the field

Soil formation, a process happening over centuries, is highly influenced by the underlying bedrock, the position in the landscape, climate, water movement, vegetation, and management, which makes soils vary strongly on a small scale. They consist of a complex mixture of weathered bedrock minerals and decomposed organic materials which are introduced from the vegetation on the surface and decomposed by soil life, through which organic compounds and nutrients stored in the organic material are released and incorporated into the soil matrix. Since humans started cultivating the landscape around them by forestry, agriculture and mining, their activities have brought drastic changes onto soils through erosion caused by deforestation, decreasing soil quality through intensive farming and introducing pollutants through atmospheric deposition caused by burning of fossil fuels (European Comission, 2012). To guarantee fertile soils and healthy habitats for future generation means to utilize soils sustainably. To implement management decisions for reaching that goal, the distribution of soil parameters needs to be known at a high spatial resolution. Working with traditional soil sampling strategies this goal cannot be reached in a practical way, as the collection of samples and their analysis in the laboratory (involving numerous physicochemical analyses depending on the parameter of interest) is not feasible, both in terms of time needed for analysis and financially. This calls for a novel way of soil analysis, for which the work presented in this thesis will contribute.

Novel methods will be explored with special focus on headlands in small tillage fields and on the measurement of lime requirement, an important measure to regulate the soil pH.

1.1.3 Precision Agriculture and Controlled Traffic Farming

Precision agriculture (PA) and controlled traffic farming (CTF) are one part of the solution to develop sustainable farming principles. It is considered by the European Commission as a tool to increase agricultural output and efficient use of resources (European Comission, 2012)

The main idea of PA lies in the increased application of information and communications technology (ICT) in all sections of agriculture. This involves recording of all relevant data and analysing them to obtain information about processes which can be improved or (global or local) problems which can subsequently be tackled specifically. Fields of PA application include the use of robots and data analytics in milk production, the use of sensors for weed and disease detection and treatment in fields, for the detection of nutrient status of plants and for the production of soil parameter maps. CTF describes the use of exact position information for adapted cultivation (e.g. contour cultivation for erosion minimization), for variable rate application of fertilizer and pesticides in doses adapted to the present conditions, for precise machinery guidance to limit field traffic to specific areas to reduce soil compaction and for autonomous guidance of machinery (autosteer) (Schrijver et al., 2016).

1.1.4 Soil Spectroscopy

For PA to be effective, good and high-resolution knowledge about the soil properties is essential. This cannot be achieved by analysing soils with traditional, wet chemical laboratory analyses. This type of analysis is too slow, too expensive and produces laboratory waste with negative impact on the environment. Great effort is put into the development of cheaper methods, many involving the attempt to use existing remote and proximal sensing technologies for their application in soil analysis.

The method for the research presented in this thesis is infrared (IR) spectroscopy, a technology developed for food and grain analysis in the 1960s in the near-infrared (NIR) range (Chang et al., 2001). The development of more robust instruments and scanning methods, which allow also the expansion into the mid-infrared (MIR) range and the development of chemometric methods, especially multivariate calibrations, allows for the application in analysing the highly complex system which is present in soils.

1.2 Policy framework

Soil and its management are impacted by a plethora of national, European, and international policies and frameworks. On a worldwide scale, soils play an important part in many of the 17 UN SDGs (UN General Assembly, 2015) (see section 1.1.1), which are guiding the development of sustainable soil management practices. On a European level, soils are an important player in the Water Framework Directive which aims to improve the chemical and biological status of all water bodies within the European Union (EU) (European Comission, 2000). The role of soils within that is mainly to protect the water bodies from pollution. For that, they have to be well managed to guarantee that no nutrients are lost from soils to the receiving water bodies to stop eutrophication. Another task of soils within that framework is the sustainable use of pesticides and to prevent them reaching water bodies. The Water Framework Directive is implemented into Irish law with a special focus on nitrates through the Nitrates Action Program (NAP) (Department of Agriculture Food & the Marine, 2018) and for other nutrients through the Statutory Instrument S.I. No. 605 of 2017 (European Union, 2017).

The use of the Shoemaker McLean and Pratt (SMP) buffer solution for the determination of lime requirement falls under the EU REACH framework for hazardous chemicals as it contains potassium chromate. Potassium chromate is classified as a “Substance of Very High Concern” (SVHC) in Annex XIV of the REACH directive due to its carcinogenic properties and is being phased out (European Chemicals Agency, 2010a, 2020).

1.3 Objectives and key questions

The objective of the research for this thesis was to bring the use of MIR soil spectroscopy one step further towards routine application in sustainable farming technologies and PA. This objective was examined from different perspectives in the process of the development. Focus in this research was on the headland area in tillage fields, an area characterized by high variability of soil parameters, especially on soil chemical quality parameters. To develop an effective traffic- and zone-based sampling for the headlands, the spatial distribution and spatial variability of the parameters of interest has to be known, and a fast and cheap analysis tool, MIR spectroscopy in the case of the present research, is assessed and deployed in the headland traffic zone-based sampling.

Three main research questions with the subsequent tasks form the basis of the research as following:

1) Can MIR spectroscopy be used as alternative to laboratory extractions to determine lime requirement?
    - Develop a calibration model based on a database of soil samples collected in tillage headlands for the prediction of lime requirement with MIR spectroscopy
    - Evaluate the model and validate its precision
    - Use the model data in the headland zone approach and evaluate its feasibility
2) How can a handheld MIR spectrometer be applied directly in the field under field-moist conditions?
    - Develop a sampling approach for a handheld MIR spectrometer in the field
    - Evaluate if data from the handheld spectrometer can be used in models developed with data from a benchtop spectrometer
    - Examine correction strategies for soils in field moist status
3) Is there variability of soil chemical quality parameters in headlands in a headland zone-based sampling approach?
    - Examine if there are statistically significant differences between soil chemical quality parameters within four traffic-based zones in the headland area

- Examine the feasibility of this zone-based approach for the use in sustainable agricultural management decisions

1.4 Structure of the thesis

The thesis is composed of six main chapters:

Chapter 1 introduces the topic of soil quality and its importance to reach the UN sustainable development goals, as well as the emerging technologies in MIR soil spectroscopy.

Chapter 2 presents the current knowledge in the fields of soil quality, spatial variability of soil parameters, PA, soil spectroscopy and chemometric modelling.

Chapter 3 describes the methodology for the sample collection, laboratory analyses, MIR scanning, chemometric modelling and statistical analyses.

Chapter 4 consists of the three scientific papers.

Chapter 5 discusses the findings of the research, relates the work of the three papers to each other and highlights the contributions to the advancement in soil spectroscopic techniques.

Chapter 6 delivers conclusions from the overall work and highlights future research questions.

Chapter 2

Literature Review

2.1 Overview

In this chapter, the current literature and the state of research will be outlined and gaps in the existing literature identified. Maintaining good soil quality is the main task with regards to soil in order to reach the UN SDGs (European Environmental Agency, 2019; Keesstra et al., 2016; UN General Assembly, 2015). As soils are derived from extremely heterogenous materials and are varying on a small geographical scale, soil attributes and their distribution within an agricultural field have to be well known to make a statement about soil quality and to implement correcting measures. To be able to record soil parameters on a small scale and at a high spatial resolution, new methodologies which are able to deal with a high sample throughput have to be developed (Shannon et al., 2018). Traditional, laboratory and wet-chemical analyses are too costly (time and capital) and involve hazardous materials, which is why new technologies have to be developed. The new technology used for the present research is mid-infrared spectroscopy, which is used to develop calibrations for soil quality parameters.

2.2 Soil quality

Soils are the foundation of food production and agriculture, as producer of food and fibre, is dependent on a functioning soil ecosystem to be able to meet the demand of a growing world population (National Research Council, 1993).

To reach sustainable soil utilization (FAO, 2009), soil quality has to be closely monitored to be able to react to declining quality, and put management measures into place where and when needed (FAO, 2017; Karlen et al., 1997).

Warkentin and Fletcher (1977) introduced the concept of **soil quality** as a method to evaluate the different functions soils provide (i.e. agricultural soil use through food, fibre and fuel production, recreation, recycling or assimilation of pollutants, improvement of water and air quality, regulation of water flow, storage and delivery of nutrients, storage of carbon, stabilizing the ecosystem).

Larson and Pierce (1991) defined it as the "*capacity of a soil to function within the ecosystem boundaries and to interact positively with surrounding ecosystems"* (Karlen et al., 2003). Soil quality is specific for each soil (Friedman et al., 2001), and is controlled by both inherent and dynamic properties (Karlen et al., 2003). Doran and Parkin (1994) extended the definition of soil quality to cover productivity, environmental quality and animal health to the following: *"The capacity of a soil to function within ecosystem boundaries to sustain biological productivity, maintain environmental quality and promote plant and animal health"* (Doran and Parkin, 1994).

I**nherent properties** are soil properties which are determined by external factors for soil formation, such as climate, topography, vegetation, parent material, time, mineralogy and resulting texture (Friedman et al., 2001), whereas the **dynamic properties** are describing the change of soil properties evoked by soil management practices (Friedman et al., 2001; Karlen et al., 2003). In order to capture its complexity and spatial variability, soil quality cannot be evaluated with one single parameter (Karlen et al., 2003; Velasquez et al., 2007; Warkentin and Fletcher, 1977) and it is challenging to be defined (Johnson et al., 1990). It can be subdivided into **physical, chemical and biological soil quality** (Friedman et al., 2001; Idowu et al., 2008; Johnson et al., 1990; Karlen et al., 2003; National Research Council, 1993). There are numerous soil parameters to describe each subset of soil quality, however, many parameters from one group are highly correlated with parameters from the other group (Arshad and Martin, 2002; National Research Council, 1993). As Karlen et al. (2003) stressed, there is no ideal soil quality parameter, useful for all demands, but it has to be created to serve a specific, management goal. Table 1 shows a list of parameters used to describe soil quality clustered into the three subgroups of soil quality. Several authors prefer the term soil health instead of soil quality, as the term “health” is integrating various factors which influence a healthy ecosystem such as soils (Doran et al., 1997; Idowu et al., 2008)

Table 1 Parameters describing the three sub-groups of soil quality (adapted after (Blume et al., 2010; Bünemann et al., 2018; Cécillon et al., 2009a; Friedman et al., 2001; Idowu et al., 2008; National Research Council, 1993))

Physical	Chemical	Biological
Soil structure	Soil organic Carbon	Microbial biomass C
Soil and rooting depth	pH	Potentially mineralizable N
Infiltration	Lime Requirement	Soil respiration
Bulk density	Electrical conductivity	Biological activity
Water holding capacity	Available P and K	Soil organic matter
Water content	Salinity	Biodiversity
Hydraulic conductivity	Cation exchange capacity	Root health
Aeration	Total and organic N	
Porosity	Heavy metal content	
Erosion	Salinity	
Compaction		
Penetration resistance		
Aggregate distribution		
Aggregate stability		

Soil quality has been in decline during the last decades, and the demand to determine the state of soils has increased with the arising problems of **soil degradation**, not only in form of **erosion** and **sedimentation**, but also in form of **soil compaction**,

salinization and the **loss of organic matter** and **biological activity** (Andrews et al., 2004a; Cécillon et al., 2009a; Karlen et al., 2003; Larson and Pierce, 1991; National Research Council, 1993). A major factor leading to soil degradation is increasing farm traffic with heavy machinery which has to be managed carefully to maintain or improve soil quality for the future of food production (Batey, 2009; National Research Council, 1993; Pierce et al., 1983; Soane and van Ouwerkerk, 1994).

2.3 Negative influences of traffic on soil quality

2.3.1 Compaction

Soil compaction, as described by Soane and Ouwerkerk (1994) is a *"process of densification in which porosity and permeability are reduced, strength is increased and many changes are induced in the soil fabric and in various behaviour characteristics*." With increasing field traffic, heavier machinery, shorter crop cycles and field traffic on wet soils, soil compaction manifests itself in yield losses and structural soil degradation (Badalíkova, 2010; Bradford and Peterson, 2000; Hamza and Anderson, 2005; Lipiec and Hatano, 2003; Naderi-Boldaji and Keller, 2016; Soane and van Ouwerkerk, 1994)

Increasing traffic has to be adapted to prevent the worst damages, and with good knowledge of the soil physical condition in a high spatial resolution, the problem can be tackled by means of PA (Hamza and Anderson, 2005; Lipiec and Håkansson, 2000; Sørensen and Dalsgaard, 2005).

When approaching soil compaction, it has to be considered that the applied stresses of passing tractors are highly dynamic and last for a short time only (Cui et al., 2010; Horn et al., 1995; Keller et al., 2013). To which extent soils are affected by imposed stresses through the applied load depends on the **soil strength** (Défossez and Richard, 2002; Dexter, 1997; Lipiec and Hatano, 2003). Soil strength, and thus **compactibility**, is depending on many soil properties such as **soil texture** and **grain size distribution** (Naderi-Boldaji et al., 2013; Olson, 1990), **bulk density** (Bennie and Burger, 1988; Mossadeghi-Björklund et al., 2016; Naderi-Boldaji et al., 2013), **pore size distribution** (Badalíkova, 2010; Griffith et al., 1992; Olson, 1990), **soil organic matter** content (Dexter, 2004; Mosaddeghi et al., 2000) and the **water content** during compaction (Badalíkova, 2010; Busscher et al., 1997; Dexter, 1997; Dickey et al., 1985; Greacen, 1960; Mirreh and Ketchenson, 1972; Mosaddeghi et al., 2000; Naderi-Boldaji et al., 2013).

Generally, soil compaction should be treated as a matter of **soil structure**. Many publications identified the biggest impact of compaction to be a breakdown of

macropores towards smaller pores and a decrease in macroporosity (Blume et al., 2010; Cui et al., 2010; Kooistra et al., 1994; Lipiec and Hatano, 2003; Servadio et al., 2001).

The key problems associated with soil compaction are **bad workability** (Dexter, 2004; Hamza and Anderson, 2005), **inhibited root growth** due to mechanical resistance (Bengough et al., 2011; Bengough and Mullins, 1990; Lipiec and Stępniewski, 1995) and **diminished water infiltration** and **hydraulic conductivity** with its consequences such as excessive **surface runoff** and **soil erosion** (Batey, 2009; Kulli et al., 2003; Naderi-Boldaji et al., 2016).

2.3.2 Soil fertility and soil chemical quality

Soil fertility as main driver for economic yields of agricultural fields (Bünemann et al., 2018; Du and Zhou, 2009; Velasquez et al., 2007) is strongly depending on the **chemical soil quality**, especially on the availability of nutrients, most importantly nitrogen (N), phosphorus (P) potassium (K) and magnesium (Mg), as well as a well-balanced cation exchange capacity (CEC) to hold and release the nutrients when they are needed (Bünemann et al., 2018). A fertile soil fulfils its function of supporting plant growth and food production by delivering sufficient macro-and micro-nutrients, thus guaranteeing good yields (Bünemann et al., 2018). In an Irish context, the availability of fertilizers for crops is evaluated with an index system, grouping the amount of available (i.e. extractable) nutrient into four indices ranging from index 1 to index 4. National advice is to bring the fertilizer index to index 3, guaranteeing an adequate yield response without overapplying fertilizer with negative environmental impacts. (Wall and Plunkett, 2016). The index system for Irish tillage soils is displayed in Table 2. For available N, no index system based on measurements is available, and the required N supply is estimated through the cropping history of the field. (Wall and Plunkett, 2016)

Table 2 Irish soil index system for tillage soils for the three main fertilizer P, K and Mg, as measured in soil extractions with Morgan's extraction

Soil index	Description	Response to fertilizer	P [mg/l]	K [mg/l]	Mg [mg/l]
1	Very low	Definite	0.0-3.0	0-50	0-25
2	Low	Likely	3.1-6.0	51-100	26-50
3	Medium/adequate	Unlikely	6.1-10	101-150	51-100
4	High	None	>10	>150	>100

2.3.3 Soil pH and lime requirement

One soil parameter with specific importance for soil chemical quality is the soil pH, which is crucial for the release and plant availability of nutrients. The pH is the measurement of the activity of H^+ ions in solution ($pH = -\log_{10} [H^+]$). In humid climate, soils tend to acidify naturally due to the slight acidity of the rain in equilibrium with the atmospheric carbon dioxide (CO_2) (McLean, 1982). The acidic water percolates the soil and neutralizes with the basic cations in solution and transports these cations away from plant roots. In addition to the leaching of bases, at lower pH values (below pH 4.7 (Sparks, 2003)), aluminium (Al) adsorbed to clay minerals gets exchanged with the H^+ in the solution. Once the Al ion is in solution, it is coordinated by H_2O molecules, which then, depending on the pH, hydrolyse and release H^+ ions. Below pH 4.7, Al^{3+} is the dominant species, which, in comparison to the $Al(OH)_2$ present until pH 6.5, is soluble and toxic to the plant root system (Sparks, 2003).

In productive agricultural systems the most important source of soil acidity is the application of chemical fertilizer based on ammonium N (Goulding, 2016). Added to soil, N-fertilizer is nitrified (Barak et al., 1997; Goulding, 2016), and if the resulting NO_3^- isn't taken up by the crops, it will get leached, causing acidification (Barak et al., 1997). The soil itself works as a buffer by exchanging the acid forming cations with basic cations which are adsorbed to the surface (clay minerals, organic matter). This buffering capacity is strongly dependant on the type and amount of clay minerals and organic matter (OM), as these factors govern the CEC (Thomas and Hargrove, 1984). Once this buffer system is exhausted, the pH drops rapidly with additional acidity introduced. With lower pH, nutrients such as P, K, Mg, calcium (Ca) and Sulphur (S) will no longer be available for plant uptake. In addition, the availability of metals such as Iron (Fe), Manganese (Mn), Copper (Cu), Zinc (Zn), Cobalt (Co) and Al also increases to toxic levels (Sparks, 2003; The Fertilizer Association of Ireland, 2016).

For Irish agricultural crops, the following optimum pH values are given in Table 3

Table 3 Optimum pH values for Irish agricultural crops as given in Soil pH & Lime technical bulletin (The Fertilizer Association of Ireland, 2016)

Crop	Optimum pH
Beet, Beans, Peas, Oilseed	7.0
Cereals and Maize	6.5
Potatoes	6.0
Peaty soils	5.8

Lime is a crucial soil conditioner in both tillage and grassland systems. It helps to bring the soil pH to the optimum level for crop production. By applying lime ($CaCO_3$) to the soil, it neutralizes the acidity, and so helps to improve soil structure (and thus drainage), the solubility of nutrients and provides optimum growth conditions for soil microorganisms (Goulding, 2016). The general neutralization reaction of acidity with lime is shown in Equation 1 (Goulding, 2016), which leads to an exchange of the adsorbed H^+ ions with the Ca^{2+} ions.

$$\mathrm{CaCO_3} + 2\mathrm{H^+} \rightarrow \mathrm{Ca2^+} + \mathrm{CO_2} + \mathrm{H_2O} \qquad (1)$$

Or, taking the acidifying effect of Al^{3+} into consideration the overall reaction is described by Equation 2 (Sparks, 2003).

$$2\mathrm{Al} - \mathrm{soil} + 3\mathrm{CaCO_3} + 3\mathrm{H_2O} \rightarrow 3\mathrm{Ca} - \mathrm{soil} + 2\mathrm{Al(OH)_3} + 2\mathrm{CO_2} \qquad (2)$$

While the impact of field traffic on soil physical quality has been in the focus of many studies (Emmet-Booth et al., 2020; Koch et al., 2008; Soane and van Ouwerkerk, 1995), its impact on the soil chemical quality or soil fertility, consisting of fertilizer status, acidity and trace elements (Idowu et al., 2008) hasn’t received much attention as of now.

2.3.4 Measuring soil chemical quality

As soil quality and its varying aspects are influenced by more than one measurable soil parameter, methods to reduce the number of parameters describing soil quality are applied. One often used approach is to find a **minimum data set (MDS)** with which the minimum amount of parameters which still describe soil quality accurately is determined (Arshad and Martin, 2002; Blume et al., 2010; Cécillon et al., 2009a; Sparling et al., 2004). The selection of suitable parameters for the MDS is dependent on the soil function of interest (Andrews et al., 2004b; Cécillon et al., 2009a). Paz-Kagan et al. (2014) used visible-near-infrared (vis-NIR) spectroscopy to detect changes in soil quality and soil degradation with a spectral soil quality indicator (SSQI) based on a scoring function derived from spectral classification. It correlated well with a laboratory-based soil quality indicator (SQI), making it a useful tool to assess changes in soil quality.

Soil acidification as important factor for soil pH is influenced by numerous soil parameters, which are difficult to measure with simple laboratory measurements and thus it is typically summarized by the soil lime requirement (LR). The LR is expressed as the amount of lime needed to bring the soil to the target pH (in t/ha, usually measured in the top 10 cm of soil. It is a recommendation based on intrinsic soil properties such as CEC, clay mineralogy and %OM which govern soil acidity (McLean, 1982). The strong dependence on these intrinsic soil parameters becomes apparent where soils with the same pH value can have different LR, largely because cation exchange mechanisms differ greatly among soil types. The exact LR is measured in time consuming incubation trials, where lime and soil are mixed and left to react and the resulting pH is measured. This test is not used routinely anymore but is still used to calibrate laboratory methods (McLean, 1982). In commercial soil laboratories, routine methods are deployed that involve titration of the soil solution with a base (soil-base titration) or measuring the resulting pH after mixing the soil with a buffer (soil-buffer equilibration) (McLean, 1970). In the soil-buffer equilibration methods the soil is left to react with a solution made up from different buffers which in combination lead to linear change in pH with neutralized acidity (Sikora, 2006). Prominent buffer methods include the “Adams and Evans” buffer (Adams and Evans, 1962) the “Shoemaker, McLean and Pratt” buffer (SMP) (Shoemaker et al., 1961), the “Sikora” buffer, an alternative to the SMP buffer without hazardous chemicals (Sikora, 2006) and the “Mehlich” buffer which was developed for a soil pH range from 6.6 to 3.8 (Mehlich, 1976). Other methods include the LR determination by titration with calcium hydroxide ($Ca(OH)_2$) (Kissel et al., 2007) and texture and crop dependent models developed from long term trials in the United Kingdom (UK) (ROTH lime) (Goulding, 2016). Of the routine laboratory procedures, the SMP buffer method delivers the most accurate results in the pH and LR ranges usually present in agricultural soils in temperate climates (Tunney et al., 2010). However, SMP buffer solution contains hazardous substances such as potassium chromate (K2CrO4) and 4-nitrophenol, which are a threat to health and safety, making waste disposal an important financial factor. Potassium chromate is designated as a “Substance of Very High Concern’’ (SVHC) and included in the candidate list for authorization within the REACH framework (European Chemicals Agency, 2010b). As this compound will be phased out, there are several efforts to find an alternative method to determine the LR, with reliable results for agricultural soils (McLean et al., 1966; Tunney et al., 2010).

2.4 Soil Spectroscopy

One tool to record a high number of samples in a short time while recording the entire information about soil parameters simultaneously is infrared spectroscopy. Firstly developed for the analysis of grains and milk, infrared spectroscopy has been developed into a time-and cost-efficient, non-destructive analysis tool for numerous soil parameters (Janik et al., 1998; Nocita et al., 2015; Soriano-Disla et al., 2014; Viscarra Rossel et al., 2006).

2.4.1 Basic principle, electromagnetic radiation

The main principle of IR spectroscopy is based on the vibration in form of stretching and bending of an atomic bond. When the compound is irradiated with infrared radiation from an IR emitting source, bonds which vibrate at a specific frequency of the spectrum, absorb this part of the radiation (Sherman Hsu, 1997; Stuart, 2004). The remaining light which did not get absorbed (i.e. transmitted or reflected) is detected and displayed in a graph with the wavenumber or wavelength on the x-axis and either the transmission or absorbance on the y-axis.

The IR-spectrum ranges from the red end of the visible spectrum to the microwave region and can be grouped into three sub regions measured either by the wavelength ν [nm] or by the wavenumber $\bar{\nu}$ [cm^{-1}] (Sherman Hsu, 1997).Wavelength and wavenumber are related to each other as shown in the following Equation 3.

$$\bar{\nu} = \frac{1}{\nu} \qquad (3)$$

The corresponding wavenumbers and wavelengths for the regions of the infrared spectrum are displayed in **Error! Reference source not found.**.

Table 4 Sub-regions of the IR spectrum and corresponding wavenumbers [cm-1] and wavelengths [µm and nm] after Sherman Hsu (1997)

	Near IR	**Mid IR**	**Far IR**
Wavenumber [cm^{-1}]	13,000-4,000	4,000-200	200-10
Wavelength [µm]	0.78-2.5	2.5-50	50-1,000
Wavelength [nm]	780-2,500	2,500-50,000	50,000-1,000,000

2.4.2 Soil spectroscopy

One of the first applications of infrared spectroscopy in soil science is described in Dalal and Henry (1986), where they used NIR to predict soil moisture, organic C and organic N based on three wavelengths which were used for the prediction with multiple regression. Soil spectroscopy was first developed using NIR, but with the development of Fourier transform infrared spectrometers (FTIR), enabling smaller instruments and faster scanning times, the MIR range has gained recognition for this application (Sherman Hsu, 1997; Stuart, 2004). The best method to obtain spectra from *soil samples* with little sample preparation is provided through the **diffuse reflectance (DR)** technique (Du and Zhou, 2009; Janik et al., 1998; Sherman Hsu, 1997). **Diffuse Reflectance Infrared Fourier Transform Spectroscopy (DRIFTS)** is the combination of the two techniques into a powerful method with *"potential to add considerable value to soil analysis"* (Janik et al., 1998) (Du and Zhou, 2009; Janik et al., 1998; Janik and Skjemstad, 1995; Reeves, 2010).

For soil spectroscopy, the NIR region and the MIR region are utilized. The **mid IR (MIR)** region (4000-400 cm^{-1} (2500 nm - 25000 nm)) is mainly dominated by fundamental vibrations and first overtones of covalent bonds in organic compounds which can be used for the discrimination of organic matter and constituents of clay (Awiti et al., 2008; McCarty et al., 2002; Shepherd and Walsh, 2002). Below 2000 cm^{-1} the spectrum is characterized by broad absorption peaks of inorganic soil compounds (O-Si-O stretching, quartz) which dominate any other effects, but above 2000 cm^{-1} it is free of any interference of quartz (Janik et al., 1998; Shepherd and Walsh, 2007; Viscarra Rossel et al., 2006).

The **near IR (NIR)** region (700-2500 nm (14000-4000 cm^{-1})) is dominated by combinations and overtones and thus shows broader peaks than in the MIR (McCarty et al., 2002; Shepherd and Walsh, 2007, 2002; Sherman Hsu, 1997; Sørensen and Dalsgaard, 2005) and weak intensities for organic carbon (Janik et al., 1998). Despite its disadvantages the NIR region is used often for a quick analysis with no need for very high accuracy (Janik et al., 1998). The NIR region could be utilized first for analytical purposes, as it was easier to generate the beam and recording of the spectra was relatively simple compared to measurements in the MIR region.

Viscarra Rossel et al. (2006) give good overview over the visible and infrared spectra of soils as shown in Figure 1.

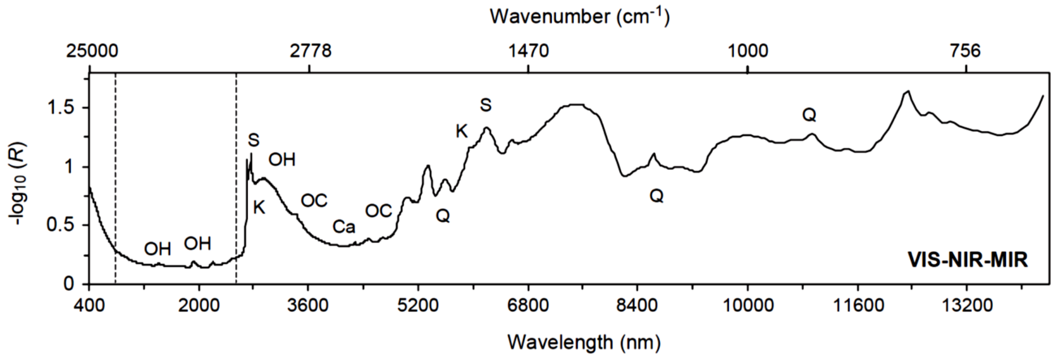

Figure 1 Representation of the visible and infrared (VIS-NIR-MIR) spectra of a soil displayed in absorbance units ($-\log_{10}(R)$) and in wavelength (bottom x-axis) and wavenumber (top x-axis). Source: Viscarra Rossel et al. (2006)

2.4.3 Soil spectroscopy- absorbing soil constituents

The main soil components which absorb IR radiation are organic matter (aliphatic, aromatic and amide vibrations), clay minerals (lattice water, O-H, Si-O and Al-O vibrations), sand (quartz, Si-O, lattice vibration), carbonates (X-H vibration) and Fe-oxides (Fe-O/H vibrations) (Janik et al., 1998; Nocita et al., 2015; Soriano-Disla et al., 2014; Stenberg and Viscarra Rossel, 2010; Vohland et al., 2014). These spectrally active components occur in variable combinations and concentrations in the analysed soil, depending on soil genetics, soil formation and land use interact with each other, creating a complex pattern of fundamental- overtone- and combination absorptions. Table 5 gives an overview over the soil parameters which could be predicted with IR spectroscopy.

While the NIR range is dominated by broad overtone and combination patterns, the MIR range shows more fundamental absorptions and a clearer peak resolution (Hutengs et al., 2019). And while for some applications it is advantageous that the NIR range is insensitive to quartz, the MIR range is sensitive to quartz and other silicates, which gives it the possibility to also detect inorganic soil fractions such as clays and sand (i.e. quartz) (Reeves, 2010; Reeves et al., 2005).

Table 5 wavelengths, range and possible assigned vibration in the NIR (N) and MIR (M) region of soil constituents with the literature where the vibrations are mentioned

Parameter	Wavelength [nm]*	Range	Assignment	Reference
Water	1400, 1900	N	Adsorbed water-O-H bending & stretching	(Ben-Dor and Banin, 1995; Dalal and Henry, 1986; Viscarra Rossel et al., 2006; Viscarra Rossel and Behrens, 2010)
	1450, 2200	N	Lattice water	(Ben-Dor and Banin, 1995; Dalal and Henry, 1986; Viscarra Rossel et al., 2006)
Water content/ moisture	100-2500	N	Air dry water content	(Ben-Dor and Banin, 1995)
		N	Water content 1.5 Mpa	(Chang et al., 2001)
	1926, 1954, 2150	N		(Dalal and Henry, 1986)
OM	700-2500	N	chromophores , O-H, C-H, N-H, vibrational modes, combinations and overtones	(Ben-Dor and Banin, 1995; Viscarra Rossel and Behrens, 2010)
	2500-20000	M		(Masserschmidt et al., 1999)
OC	1744, 1870, 2052	N		(Dalal and Henry, 1986)
	660, 816, 1824, 1904, 2016, 2208	N		(Viscarra Rossel and Behrens, 2010)
	6250, 6660	M	aromatic	(Janik and Skjemstad, 1995)
	5780	M	carboxylic	(Janik and Skjemstad, 1995)
	2860, 4650	M	carbohydrate	(Janik and Skjemstad, 1995)

		M	organic compounds	(Viscarra Rossel et al., 2006)
Clay	608, 988, 1392, 1908, 2184, 2208, 2236, 2432	N	metal-OH bend, O-H stretch, C-O	(Viscarra Rossel and Behrens, 2010)
	1600, 1800, 2000, 2200	N		(Viscarra Rossel and McBratney, 1998)
	1400, 1900, 2200	N		(Ben-Dor and Banin, 1995)
		N		(Chang et al., 2001)
	2755,2940, 6130	M	Smectite, (Quartz, Organic acids)	(Janik and Skjemstad, 1995)
Quartz	9091-10,000	M	O-Si-O stretching, masking other effects	(Janik et al., 1998)
Others	2330	N	CO3	(Ben-Dor and Banin, 1995)
	1050	N	Fe-oxides	(Ben-Dor and Banin, 1995)
		N	Aggregation	(Chang et al., 2001)

* If no wavelength is specified the whole range is meant

2.4.4 Chemometric modelling

As the whole spectrum is recorded by FTIR in one single measurement, it is influenced by numerous compounds, overtones, and combinations. In order to retrieve information about single parameters and to build a calibration model, **chemometric** techniques have to be applied (Geladi, 2003; Kalivas, 2005). Commonly used regression methods are **principal component regression (PCR)** and **partial least squares regression (PLSR),** established methods to reduce the dimensionality of the predictor dataset in which hundreds of wavenumbers are the variables, and use the reduced set for regression analysis (Janik et al., 1998; Viscarra Rossel et al., 2006). More advanced data mining methods such as *random forest*, *boosted regression trees*, *support vector machines* and *artificial neural networks* (Ng et al., 2019; Viscarra Rossel et al., 2006; Viscarra Rossel and Behrens, 2010) and deep learning algorithms (Padarian et al., 2019) are becoming more popular and show good results.

Another crucial part in chemometric modelling is the pre-treatment of the spectra. Hereby the goal is to increase the information content of the spectra and decrease the influence of random noise and scattering, i.e. improving the signal to noise ratio (SNR) (Esbensen and Swarbrick, 2018; Savitzky and Golay, 1964).

Common pre-treatment measures are smoothing of the spectra, where several points of the spectrum are averaged to reduce the influence of random noise, using derivatives of the spectra (usually first or second derivative) to enhance the peaks (Savitzky and Golay, 1964), corrections for multiplicative effects on the spectra such as multiplicative scatter correction (MSC) (Geladi et al., 1985) and standard normal variate (SNV) (Barnes et al., 1989), normalization to make the different spectra comparable, and baseline corrections to compensate for an offset in the spectra due to differences during measurement (Esbensen and Swarbrick, 2018). Trimming the spectra can also improve the information content of the spectra as regions of the spectrum which contain no viable information and only add to the noise can be cut out (Engel et al., 2013; O'Rourke et al., 2016; Rinnan et al., 2009). After successful pre-treatment, the model should have a small number of explanatory variables (be parsimonious), maximize the variance explained by the model (R^2) and minimize the prediction error (root mean square error, RMSE) (Esbensen and Swarbrick, 2018).

2.4.5 Application of soil spectroscopy

Various attempts have been made to use soil spectroscopy, especially DRIFTS, to analyse soil parameters and soil quality parameters. Especially the opportunity to obtain analytical values for MDS of soil quality indices makes spectroscopic analyses a promising tool (Awiti et al., 2008; Cohen et al., 2006). Most of the work has been done predicting soil chemical and biological quality with NIRS DRIFTS.

Velasquez et al. (2005) showed the power of NIRS and principal component analysis (PCA) to distinguish between different land use types in south America. Using the first two principal components of the recorded spectra they could distinguish between intact land with good organic, chemical and biological condition (i.e. land with intact plant cover) and eroded land and fields with intensive agriculture. Cécillon et al. (2009b) used PCA and discriminant analysis (DA) to predict parts of the General Indicator of Soil Quality (GISQ) (Velasquez et al., 2007). They could successfully discriminate different degrees of wildfire disturbance on soil biological and chemical quality. Awiti et al. (2008) implemented an effective approach to manage soil resources. Applying a multivariate analysis of variance on spectrally detected chemical parameters they showed significant differences between three age classes of converted forest land. With a proportional odds logistic model, they could distinguish the samples into three spectral classes and used PCA to predict the membership to one of the classes. Ben-Dor et al. (2008) reviewed the capacity of *imaging spectroscopy* to classify soils regarding erosion, degradation, salinization, soil genesis and formation, soil contamination, soil chemistry and water content from aerial and satellite imagery. They concluded it holds considerable information about soil parameters and titled the method *"a giant that still needs to wake up"*, as further research, especially in image processing and the development of a spectral database is still to be done. Cohen et al. (2006) researched soil ecological condition based on biogeochemical predictors and stated, that both ordinal logistic regression models and classification tree models delivered more accurate predictions when applied to processed visible-NIR spectra than applied on laboratory values. Odlare et al. (2005) used the first principal components of the NIR spectra to model the spatial distribution on clay content, pH and total carbon in a field with the geostatistical method of kriging. Vågen et al. (2006) showed the suitability of VIS-NIR to predict a soil fertility index consisting of ten physicochemical parameters.

2.4.6 Lime requirement in spectroscopy

Even if the lime requirement (LR) isn't a soil parameter *per se* (there is no molecule indicating LR, much less a spectrally active one), it can still be predicted, as it is strongly dependent on the CEC and hence clay content, clay type and OM (Chang et al., 2001; Janik et al., 1998; Soriano-Disla et al., 2014).

There are previously reported approaches in predicting the LR with IR spectroscopy. Tekin et al. (2013) developed an on-the-go NIR sensor, which was calibrated for pH. From the pH they developed a LR map according to DEFRA fertilizer manual (Department for Environment Food and Rural Affairs, 2010). Demattê et al. (2019) researched the precision of vis-NIR-SWIR spectroscopy (short wave IR) to predict LR based on CEC and base saturation (BS). They found high correlation between laboratory derived LR and spectral LR, proposing a hybrid approach with 20% of the samples analysed in the lab and the remaining 80% analysed spectrally. These approaches derived lime recommendations from proxy soil parameters, the only studies on LR derived from buffer pH were conducted by Viscarra Rossel et al. (2001) and Viscarra Rossel and McBratney (2001). They investigated the LR measured with a Mehlich-buffer response model measured at 122 points in a field in Australia. The MIR calibration resulted in an R^2 of 0.75 and a RMSE of 0.61 t/ha. Merry and Janik (1999) researched the potential of MIR to predict LR in different regions in Australia and could predict the LR on a large scale. A follow-up analysis of this report from

1999, or an indication of actual routine use of MIR for LR in Australia couldn't be found.

2.4.7 Portable instruments

NIR spectrometers are relatively easy to minimize for use in a portable version as they usually don't contain interferometers with moving parts, however, handheld MIR spectrometers are not as widely used, are more expensive, and have only recently become available. Their performance to predict dried and ground soil samples has been reviewed for example by Soriano-Disla et al. (2017) as a comparative study of several portable infrared instruments, and the authors found, that MIR instruments using the full MIR range deliver similar results to the benchtop instrument. Several other studies used small, portable instruments as an alternative to benchtop instruments and found that, despite losses in signal to noise ratio, range and stability, these instruments especially in the MIR range offer a good alternative to benchtop analyses (Hutengs et al., 2019, 2018; Martínez-España et al., 2019; Soriano-Disla et al., 2019). Calibrations directly based on the field moist spectra collected with a prototype MIR spectrometer with a limited spectral range delivered promising results, but with lower accuracy than the same samples measured dried and ground (Dhawale et al., 2015; Ji et al., 2016).

Another important factor to consider in the development of portable MIR instruments for soil sensing is, that MIR radiation interacting with the soil moisture and causing distorted spectra due to specular reflectance and broad peaks of water absorption, which overlap weaker features (Janik et al., 2016), making the application of MIR spectroscopy on fresh soil samples more complicated than that of dried soils in the laboratory. The soil moisture, as well as other irregularities on the *in situ* samples in addition to other influences such as weather, lead to considerable distortions in the spectra, which renders it extremely complicated to compare scans from fresh samples with a spectral database usually built from dried and ground samples (Hutengs et al., 2019; Soriano-Disla et al., 2017).

Starting from visible and NIR spectra, where the influence of soil water, even though weaker than in MIR spectra, still caused problems with prediction, methodologies to remove the distorting influence of "*in situ* conditions" (Soriano-Disla et al., 2017) are being developed by several groups. Direct standardization (Ji et al., 2015) , grouping the samples by moisture content to eliminate the moisture contribution to the spectra (Mouazen et al., 2006) and a truly chemometric approach, the external parameter orthogonalization (EPO) (Minasny et al., 2011; Roger et al., 2003) are among the most used methods for NIR samples.

With the more accessible hardware (handheld FTIR spectrometer) and possible methodologies to tackle the problem of *in situ* conditions, research has started to explore the application of portable MIR soil spectroscopy. The first attempts in using portable MIR directly in the field developed predictions of carbon (C) and N using different spectrometers and (IR) ranges in addition to three different soil states (field moist, dried and sieved, dried, sieved and finely ground), but they built separate calibration for each instrument and soil state, which resulted in relatively good predictions of soil C content (Reeves et al., 2010). Hutengs et al. (2019) conducted a comparative study with the same handheld MIR scanner used in the present study (Agilent FTIR 4300) to predict soil organic carbon. They scanned the soil directly in the field and compared the spectral predictions with those derived from dried and sieved samples as well as dried, sieved and finely ground samples. The same samples were also scanned in the NIR range. For each of the three states of sample they created a calibration model and evaluated their performance. They found better predictions for soil organic carbon (SOC) in MIR than in NIR, where the scans directly in the field resulted in RMSEs close to the ones of NIR predictions of ground samples (RMSE 0.16% – 0.18% SOC), with an improvement in the RMSE of the ground samples (RMSE 0.11 % SOC).

In the presented studies for the use of handheld MIR spectrometers, separate calibrations were built for each type of scan. Corrections for moisture and *in situ* characteristics like the ones described for vis-NIR spectra are not yet applied in MIR spectra.

2.5 Spatial variability

During the last decades the demand to determine the state of soils has increased with the arising problems of soil degradation, not only in form of erosion and sedimentation, but also in form of soil compaction, salinization and the loss of organic matter and biological activity (Andrews et al., 2004a; Cécillon et al., 2009a; Karlen et al., 2003; Larson and Pierce, 1991; National Research Council, 1993). Soil degradation in tillage systems can be caused by field traffic and heavy machinery (National Research Council, 1993; Pierce et al., 1983; Soane and van Ouwerkerk, 1994).

In tillage systems the field area which receives the most traffic is called the turning headland, described as the area of the field where turning of machinery occurs. Usually the direction of drilling is parallel to the field edge and thus perpendicular to the main field drilling orientation (Sparkes et al., 1998). Increased traffic, especially in the headland close to the field gate, can negatively impact soil quality due to compaction from frequent wheeling (Koch et al., 2008; Sparkes et al., 1998; Withers et al., 2006) and this can have a negative influence on crop growth and yields due to reduced pore space and water infiltration (Antille et al., 2019; Batey, 2009; Hamza and Anderson, 2005; Soane and van Ouwerkerk, 1995, 1994). Sparkes et al. (1998) found that in addition to yield reduction and plant destruction from headland traffic, the influence of hedges and trees on the field edge decreased yields through shading and competition for water. Often overlooked is the irregular application of fertilizer caused by the turning patterns which can also reduce yield in the headlands. While headland settings exist for most fertilizer spreaders, the precision of application is generally lower than in the regular patterns in the main field. Sometimes farmers try to compensate for this irregularity by applying additional fertilizer in the headland, often on areas of compacted soil making fertilizer utilization inefficient (Soane and van Ouwerkerk, 1995). These factors either in isolation or combination can lead to a decrease in soil chemical quality (Karlen et al., 2003) in different zones of the headlands. Around the main headland tramline, the effects of compaction through increased traffic and of suboptimal fertilizer are prevalent, while the area between headland tramline and the field edge is more affected by bordering vegetation and irregular fertilizer application due to machinery turning patterns.

One promising remote sensing technology is infrared spectroscopy. First developed for food and pharmaceutical analysis, with the development of multivariate statistical models, it has been researched for its application in soil sensing over the last decades (Janik et al., 1998; Nocita et al., 2015; Soriano-Disla et al., 2014; Viscarra Rossel et al., 2006). When soils are irradiated with infrared light, soil compounds containing covalent bonds, such as clay minerals and organic matter, absorb that light at different wavelengths specific for a chemical compound. From the characteristic spectrum consisting of the absorptions of the compounds plus interaction- and overtone effects, the concentration of the compound can be inferred with the help of multivariate modelling. In addition to components which directly absorb infrared radiation, dependent soil parameters such as texture, pH and lime requirement (buffer capacity as a factor of type and amount of organic matter and clay) can be predicted as well (Geladi, 2003; Janik et al., 1998; Kalivas, 2005; Sherman Hsu, 1997; Stuart, 2004). However, for the nutrient status, especially N, P and K the prediction is more complicated as the molecules don’t absorb in the IR range. However, Dunne et al. (2020) developed a calibration for P sorption indices which is a step towards using infrared spectroscopy for nutrient status analysis of soils.

With an average size of Irish tillage farms of 58 ha (Central Statistics Office, 2016) and more than 75% of Irish farms having a size under 100 ha of utilized agricultural area (UAA) (Eurostat, 2016), the countrywide average lies well below the average in the European Union where <50% of the farms are smaller than 100 ha. The small farm size and the high cultural and environmental value given to field borders such as hedgerows (Department of Agriculture Food & the Marine, 2015), which are a valuable habitat and carbon storage (Deverell et al., 2009) and cannot be removed to create bigger fields, causes a small field size in comparison to other countries (Deverell et al., 2009). This leads to a bigger proportion of the field being disturbed by traffic, making that area a special area of interest in the specific context of Irish agriculture.

2.6 Precision agriculture and controlled traffic farming

One way of reducing the problems caused by both irregular fertilizer application and frequent field traffic is the implementation of PA (Earl et al., 2003; Håkansson and Lipiec, 2000; Hamza and Anderson, 2005; Sørensen and Dalsgaard, 2005). The use of PA to target applications in specific areas of fields, can optimise crop yields by improving efficiency and utilization of soil functions (Ortega and Santibáñez, 2007). This is achieved through the increased use of information technology, especially GPS (Global Positioning System) aided navigation systems for field operations. In doing so, the placement of seeds, fertilizer and pesticides is controlled precisely, making sure that the right amount is put in the right place, maximizing yields while minimizing environmental impacts (Godwin et al., 2003; Ortega and Santibáñez, 2007). Controlled traffic farming as a special case of PA is concerned with minimizing soil compaction caused by field traffic by precisely guiding machinery on fixed tracks (tramlines) (Antille et al., 2019; Batey, 2009; Vermeulen et al., 2020). For PA measures to be efficient, the variability of the soil parameters of interest has to be known with higher spatial resolution than current methods allow (Bölenius et al., 2017; Clay et al., 2017; Earl et al., 2003; Franzen, 2018) so that management of problematic areas can be targeted. This is not feasible with traditional composite sampling and analysis due to the coarse spatial resolution and time delays in receiving results. An alternative to field composite sampling is to delineate field zones based on traffic and recorded yields in a targeted sampling approach in management (Clay et al., 2017; Ortega and Santibáñez, 2007). These zones offer potential to use remote or proximal sensing technologies to obtain soil information.

2.7 Soil spectroscopy within the broader field of geography

Besides use in an agricultural context, soil spectroscopy also finds application in the broader field of earth sciences and geography, as soil is linked to many processes ranging from the groundwater (provision of clean water) to the atmosphere (sequestration or release of carbon) (UN General Assembly, 2015). Within this range of possibilities, spectroscopy has been used to answer geomorphological questions by analysing underlying erosion processes in the Chinese loess plateau (Ni et al., 2019) and to distinguish different fluvial terraces (Louw et al., 2021). Work has been done to use spectroscopy in a pedological context to determine soil types and soil classes in national soil classification systems (Teng et al., 2018; Zeng et al., 2016). Other work has been conducted to analyse soil contamination with toxic metals and hydrocarbons (Gholizadeh et al., 2018; Shi et al., 2018). This pedological, geochemical and geomorphological information can then be used as the basis for planning and the selection of high-value areas to be protected, as well as lower-value areas to be commissioned for construction etc.(Zambon et al., 2018).

In the interaction of soils with the atmosphere, special focus is on the exploration of the potential of soil to sequester carbon, where spectroscopy can play a crucial role to quantify the potential in a high spatial resolution (Bellon-Maurel and McBratney, 2011; Janik et al., 2007; Lal et al., 2018; Minasny et al., 2017).

2.8 Summary

This chapter gave an overview over the current state of the literature for soil quality, the measurement of soil quality parameters with new methodologies (i.e. infrared spectroscopy) and the problematics of the distribution of these parameters in field headlands, especially in small tillage fields.

This literature review identified gaps in the knowledge of the distribution of soil quality parameters in the headlands and the impact traffic patterns have on their distribution in that specific area, in the application of MIR spectroscopy in the lab analysis for the direct prediction of SMP buffer LR and the potential to substitute common lab extractions, as well as in the application of portable MIR instruments directly in the field and how to deal with the *in situ* conditions of the sample.

Chapter 3

Methodology

3.1 Overview over papers and datasets

The research done is published in three papers.

Paper 1 deals mainly with calibrating a PLSR model for Lime requirement based on the samples from 41 fields.

> **Metzger, K.,** Zhang, C., Ward, M., Daly, K. 2020. Mid-infrared spectroscopy as an alternative to laboratory extraction for the determination of lime requirement in tillage soils. Geoderma, https://doi.org/10.1016/j.geoderma.2020.114171

Paper 2 describes the development of a sampling strategy with a handheld portable MIR scanner in a small trial.

> **Metzger, K.,** Zhang, C., Daly, K., 2021. From benchtop to handheld MIR for soil analysis: Predicting lime requirement and organic matter in agricultural soils. Biosyst. Eng. 204, 257–269. https://doi.org/10.1016/j.biosystemseng.2021.01.025

Paper 3 deals with the analysis of the four sampling zones, examining if there are statistically significant differences and if they can be attributed to certain management types. Additionally, it is explored how well MIR predicted samples display statistically significant differences.

> **Metzger, K.,** Zhang, C., Ward, M., Daly, K. 2021. Variability in Soil Chemical Quality in Traffic-dependent Zones within Field Headlands. *Communications in Soil Science and Plant Analysis.*
>
> https://doi.org/10.1080/00103624.2021.1921191

The datasets used for the different papers and the analyses applied to them are described in Table 6.

A database containing information about all used samples and corresponding laboratory results as well as spectral data, and the results of the statistical analyses can be found in the digital appendix.

Table 6 Datasets used for the three papers and the analyses performed on them

Number	Name	Origin	n	Paper	Analysis performed
1a	Calibration	sampling campaign	495	1	MIR LR prediction
1b	Validation	sampling campaign	160	1	MIR LR prediction
2a	Calibration scanned with handheld	sampling campaign (set 1b)	100	2	Calibration for LR and %OM with small set
2b	Validation scanned with handheld	sampling campaign (set 1b)	60	2	Validation for LR and %OM with small set
2c	Trial set for *in situ*	Field moist samples	9	2	Prediction with model from set 3a
1	Calibration and validation	sampling campaign (set 1a and 1b)	655	1	statistical analysis of zones MIR prediction

3.2 Study area and field sampling

3.2.1 Sampling campaign

41 tillage fields from 25 farms in the Republic of Ireland were selected as sites for this study. All fields were cereal fields (spring barley: 25, winter barley: 8, winter wheat: 8) and under continuous cereal tillage for the previous three years. The fields were selected in correspondence with Teagasc tillage advisors (Ward et al., 2020) and are situated across the main tillage regions in Ireland ranging from the south (Co. Waterford) to the northern border (Co. Louth). The location of the fields is displayed in Figure 2. The size of the fields ranged from 2 ha to 37 ha, with a median size of 8 ha, with the majority of the fields showing sandy loam (16) and loam (18) US Department of Agriculture (USDA) (NRCS, 2018) textures in the topsoil. The dominant soil great groups according to the Irish Soil Information System (Simo et al., 2007) represented in the dataset are Luvisols (21) and Brown earths (12). Detailed summary statistics are given in Table 7 and Table 8.

Table 7 Summary statistics for the 41 sampled fields for %OM, pH, lime requirement and texture classes and a breakdown of the distribution of texture classes within the sampled fields

	OM [%]	pH	LR [t/ha]	Texture by field		
min	2.0	5.0	-10.5	**USDA texture class**	**n (fields)**	**%**
max	10.2	8.2	10.0	sandy loam	16	39%
average	5.8	6.6	-3.0	loam	18	44%
median	5.6	6.6	-2.5	clay loam	6	15%
range	8.3	3.2	20.5	sandy clay loam	1	2%

Table 8 Soil great groups of the examined fields according to the Irish soil information system and the number of fields in each great group

Soil great group	n (fields)
Luvisol	21
Brown earth	12
Groundwater Gley	1
Surface water Gley	2
Brown Podzolic	2
Alluvial	1
Other	2

The fields were divided into four sampling zones running parallel to the headland tramline, guided by assumed headland traffic patterns. The hypothesized impacts of traffic include all field traffic being led through the main headland tramline, turning traffic from tractors exiting one in-field tramline and moving to the next one (fertilization, spraying) as well as irregular fertilizer inputs caused by turning. This leads to the following design: Zone A represents an area of the field where irregular traffic occurs during turning operations which could lead to irregular inputs.

In addition to the irregular inputs, there could also be disturbances from the field edge and possibly a hedge row, manifested by shading, water competition, weeds, and introduction of organic matter through roots and leaves. Zone B is defined to be directly on and around the headland tramline where the highest impacts of field traffic are expected, especially a drastic deterioration of soil physical quality through compaction. Zone C was defined as a transition zone between the headland tramline and the main field. In this zone the biggest source of irregularities was postulated to be through the input pattern due to switching fertilizer spreaders and sprayers on or off at the end and beginning of the turning process. Zone D characterises the main field excluded from the influence of field traffic and serves as reference for normal field conditions. Inputs in the main field are assumed to be regular and the impact of traffic is minimal and limited to few passes in the infield tramlines for fertilizing and spraying operations. One sampling point was placed in each zone, forming a transect from the field edge to the main field. Four replicate transects were placed in between the infield tramlines which are determined by the width of the boom sprayer (usually 24 m) resulting in 16 sampling points per field. Each sampling point was sampled in two depths which are determined by ploughing operations: the first sampling depth (SD1) reached from 5-10 cm, representing the area of the soil profile which is annually loosened through ploughing, and the second sampling depth (SD2) reached from 25-30 cm to represent the area of the soil profile which isn't regularly disturbed through

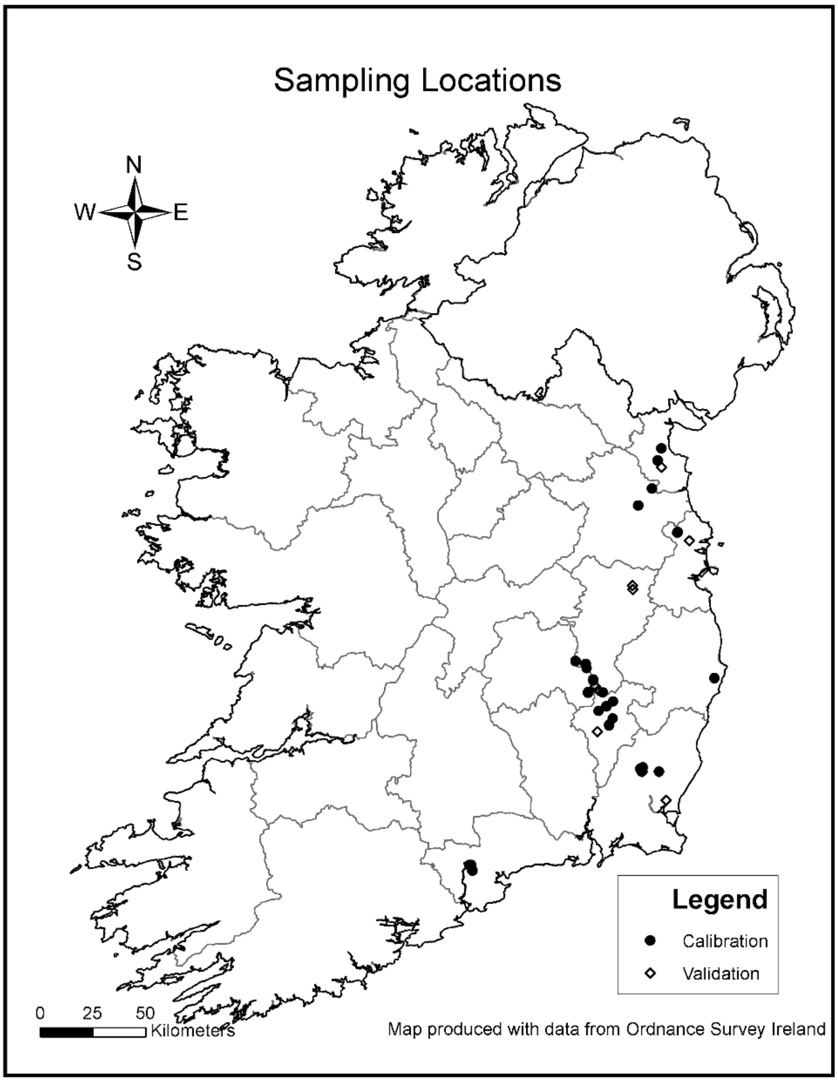

Figure 2 Location of the sampled fields. A closed point depicts a field which was used for the calibration set in the LR research, an open point depicts a field used in the validation set

ploughing and thus is more impacted by compaction building up with every pass (subsoil compaction). In every point, a small sampling pit was dug (ca. 50 cm deep, 50 cm wide and 1 m long) from where samples could be collected. At each point and in both sampling depths an undisturbed sample was taken in a stainless-steel cylinder (ca. 100 cm^3 volume) which was wrapped in tinfoil and sealed in a bag to be stored in a cold room until further analysis. Around the position of the cylinder, a disturbed sample was collected into a coated cardboard box for further laboratory analysis. The total sampling setup resulted in 656 sampling points (in one point no sample could be taken) and 1312 undisturbed and 1312 disturbed samples. The schematic including the sampling zones, replicates and sampling points is given in Figure 3.

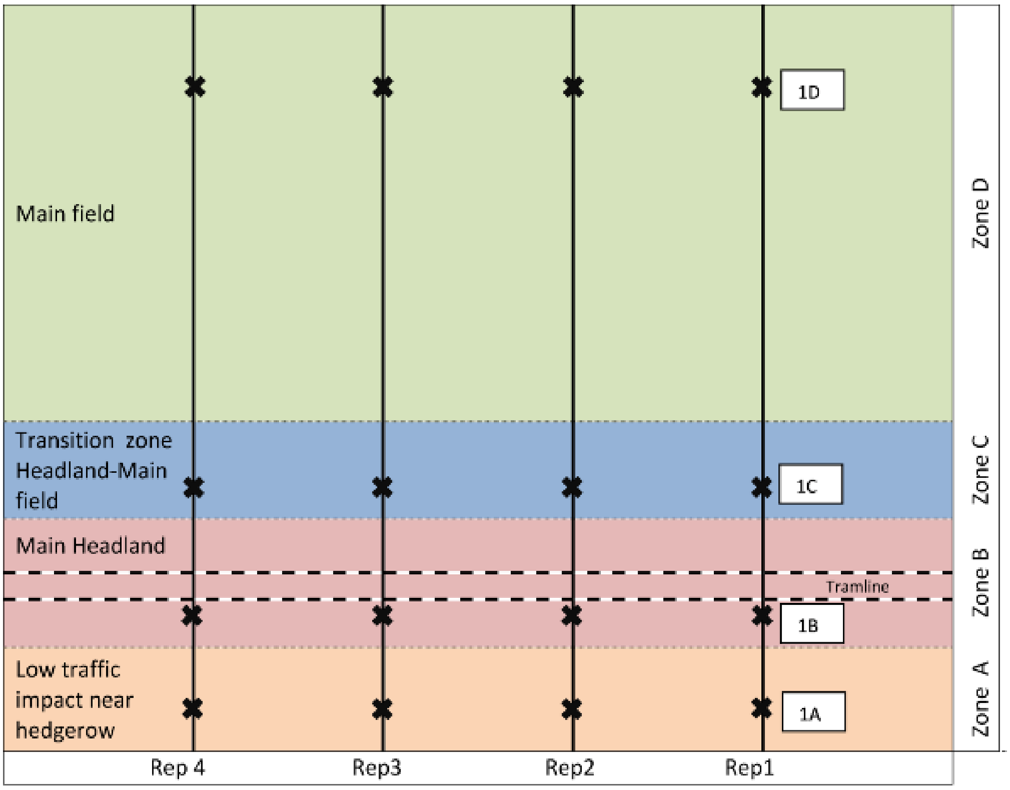

Figure 3 Sampling setup for a schematic field with the zones, replicates and sampling points displayed

3.2.2 Sampling for trials with the handheld MIR scanner

For the analysis with the portable MIR instrument, three sites in the vicinity of the Teagasc Johnstown Castle Research Centre in Wexford, Ireland were selected as test sites for the new sampling strategy. The texture classes were known from previous analyses: two fields, Field A and Field C, are sandy loams, the remaining Field B is a loam. The sandy loam fields A and C varied in the proportions of sand and clay, with Field A showing 62% sand and Field C showing 55% sand. The amounts of clay changed respectively, with the amount of silt being constant. The samples were collected in a sampling depth of 5-10 cm through digging a small pit with a spade, clearing the top 5 cm of soil after which the sample was scooped out with a spatula and stored in a 1 l plastic container with a screw cap to retain the moisture and stored in a cold room until use. The texture classes of the fields are displayed in Table 9, including the USDA texture class and the percentages of sand, silt, and clay.

Table 9 Summary statistics of the three fields used for the analysis with the portable instrument for texture, moisture content, lime requirement and pH

Field	Texture Class	Sand [%]	Silt [%]	Clay [%]	Moisture [% w/w]	% OM	LR [t/ha]	pH
Field A	Sandy loam	62.3	15.3	22.3	38.3	7.5	1.5	6.2
Field B	Loam	47.3	17.7	35.0	22.4	6.2	0.5	6.3
Field C	Sandy loam	55.0	15.9	29.1	54.7	9.2	6.5	5.5

3.3 Laboratory analyses

3.3.1 Sample preparation

The disturbed samples in the cardboard boxes were brought to the laboratory where they were dried at 40 °C for ca. one week. After drying they were mechanically sieved to 2 mm, filled back into the cardboard boxes and stored in sets of 89 samples in the Johnstown Castle sample storage system, where each sample was assigned a unique sample number and a specific position in the set. When the samples are placed in the set, after every 9th sample, an in-house quality control sample with known concentrations is added and analysed with the other samples. For these in-house quality control samples, a range of accepted results is defined in a control chart, and when the result of the analysis is outside of the defined specifications, the analysis must be repeated. This provides certainty that the analysis is delivering reliable results.

3.3.2 Particle size distribution

Particle size distribution was determined on a composite sample for each field to describe the texture class at each field. The composites were formed for each SD (SD1 and SD2) by taking 20 g of dried and sieved soil from each of the four replicates taken in zone D (main field) and mixing them well to form one sample. This resulted in 82 samples to be analysed (41 samples per SD). They were analysed with the sieve pipette method using 20 g samples for the USDA particle size classification (Gee and Bauder, 1986; Massey et al., 2007). The organic matter in the sample was removed by oxidizing it with hydrogen peroxide, after which the clay aggregates were dispersed with sodium hexametaphosphate overnight. The dispersed sample was then transferred into a 50 µm sieve in which the sand fraction (>50 µm) is retained while the remaining sample is wet sieved into a 1 l cylinder. The cylinder is filled up with deionized water to measure 1 l. The determination of the particle size < 50 µm is based on Stoke's law, which relates the sinking velocity of a particle to its diameter and is a standard procedure in particle size analysis. It is described in the following equation for the terminal velocity of a particle with a given diameter (Gee and Bauder, 1986):

$$v = \frac{g(\rho_s - \rho_l)d^2}{18\eta} \quad (4)$$

with v being the terminal settling velocity of the particle with diameter d, ρ_s and ρ_l the densities of the particle and the liquid respectively and η the viscosity of the water at a given temperature. From the terminal velocity the sampling time at 10 cm can be calculated.

After reaching a stable temperature (21°C) the cylinder was shaken to disperse the sample equally, set down, and after 44 s, a subsample was taken with a pipette at a depth of 10 cm. This subsample is an aliquot of the sample which contains only samples < 50 µm (silt and clay). The cylinder is then left to settle for 5 hours and 40 minutes after which another subsample is taken (at 7.5 cm to reduce sampling time). This subsample contains, utilizing Stoke's law, only particles < 2 µm (clay fraction). The aliquots are transferred into a crucible and the water is dried off at 105°C overnight, together with the sand fraction >50 µm. The resulting dry masses together with the known volume of the aliquot can then be used to calculate the percentages of sand, silt, and clay. The USDA particle size classification for the fine soil fraction is displayed in Table 10

Table 10 USDA particle size limits as used for the derivation of the texture classes

Fraction	Particle size [µm]	Particle size [mm]
Sand	50 - 2000	0.05 - 2
Silt	2 - 50	0.002 – 0.05
Clay	<2	<0.002

With the concentrations of sand, silt and clay, each soil can be plotted in a ternary diagram, the so-called "soil texture triangle" which is done for the 41 fields in the two SDs as displayed in Figure 4.

3.3.3 %Organic matter

The percentage organic matter was determined by loss on ignition, as the difference in weight after heating the dried soil sample to 500°C for 12 h. For that, ca. 5 g of soil were filled into a crucible, dried overnight at 105°C to remove residual moisture. After weighing the water-free samples they were put into a furnace and kept at 500°C to volatilize all organic materials present in the soil for 12 hours. After cooling down the samples were weighed again, and the percentage of organic matter (%OM) can be calculated with Equation 5.

$$\%\mathrm{OM} = \frac{\text{weight (sample dried)} - \text{weight (sample 500°C)}}{\text{weight (sample dried)}} * 100 \qquad (5)$$

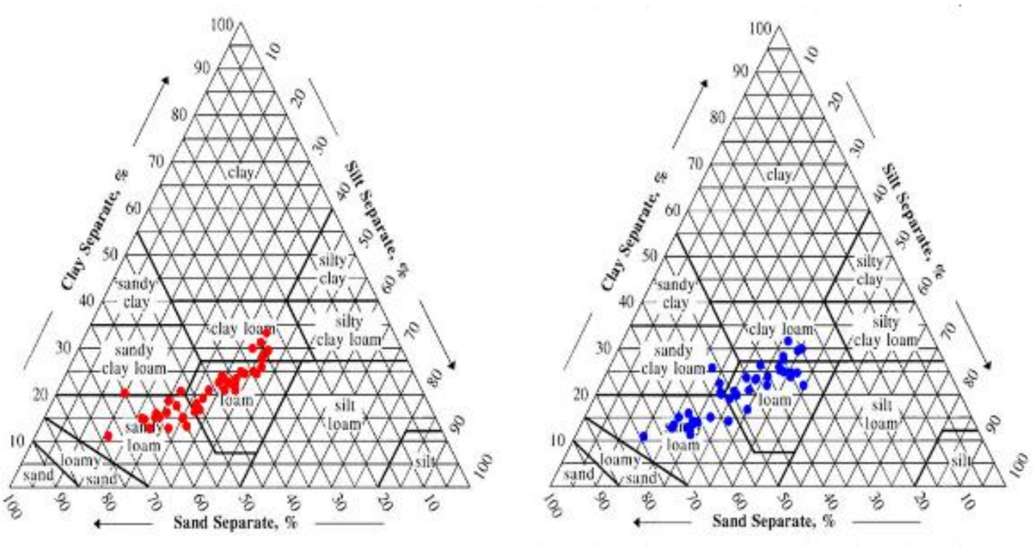

Figure 4 The 41 samples of this study plotted in the soil texture triangle for SD1 (red, left plot) and SD2 (blue, right plot), plots created with the NRCS texture calculator (NRCS, 2018)

3.3.4 Lime requirement and pH

Soil pH was measured on 10 ml soil mixed with 20 ml deionized water (1:2 ratio) and pH measured with a Mettler Toledo “in Lab Routine” pH electrode. Lime requirement (LR), an important measurement of the amount of lime needed to bring the soil back to a pH ideal for the crop to be grown (pH 6.5 for cereals) was determined by extracting 10 ml of soil in 20 ml “Shoemaker McLean and Pratt” (SMP) buffer solution (McLean, 1982; Shoemaker et al., 1961) which was placed on a gyratory shaker for 30 min before filtering through a Whatman No.2 filter This buffer solution serves as an acidity exchanger with the soil, and once the extraction and filtration is finished, the pH of the solution is measured with a pH electrode. The required SMP pH is defined for different crop groups, depending on the optimum pH (optimum pH for cereals: 6.5, target SMP pH for cereals: 6,9), and from the difference between target SMP pH and actual SMP pH the amount of lime (in the form of ground $CaCO_3$) needed can be calculated with the following formula (Teagasc and Plunkett, 2016).

$$\mathrm{LR}\ [\mathrm{t/ha}] = (\text{target SMP pH} - \text{actual SMP pH}) * 12.5\ \mathrm{t/ha} \qquad (6)$$

The SMP buffer solution contains potassium chromate and 4-nitrophenol, classified as hazardous materials (European Chemicals Agency, 2010b) which makes handling the SMP solution dangerous and the disposal of the waste expensive in order to avoid negative environmental impacts.

3.3.5 Nutrient analysis: Phosphorus, Potassium, Magnesium

Plant available major nutrients Phosphorous (P), Potassium (K) and Magnesium (Mg) were measured with Morgan's extraction; 3 ml of soil were extracted with 15 ml of Morgan's solution (sodium acetate buffered at pH 4.8) by shaking the solution in a round bottom flask for 30 min on a gyratory shaker and then filtered through a Whatman No 2 filter in a filter bed. The filtrate is collected and used for the further analysis.

The Morgan's solution is designed to extract the proportion of P, K and Mg which is available for plants. P and K are analysed colorimetrically. For the P (present as orthophosphate PO_4^{3-}) analysis, the extract is put to react with ammonium molybdate and antimony potassium tartrate, forming a complex with the phosphate ion which is absorbing light at 880 nm. The absorption is proportional to the concentration of P in the solution, and a calibration with known concentrations can be obtained, typically valid in the range of 0.5 – 30 parts per million (ppm) P. K is analysed in a Sherwood Flame Photometer, where the sample with the extracted K is atomized in the flame. In the flame, the K atoms are excited and then emit light at 766.5 nm. This emission is proportional to the concentration of K in the solution, so that a calibration from known concentrations (usually in a range of 20 – 500 ppm K) is built, from which the concentration of the unknown sample can be derived. Plant available Mg is measured colorimetrically. The Mg in solution forms a complex with Xylidyl blue, which absorbs light at 520 nm. The calibration range for Mg is usually from 20 – 500 ppm Mg. The analysis was run with a "Lachat QuickChem ® 8500 Series 2" flow injection analyser with a multichannel manifold, in which the extract is mixed with the complex forming reagent in the case of P and Mg, or with deionized water in the case of K and then transported automatically to the detectors (Daly and Casey, 2003; JOHN, 1970; Morgan, 1941).

3.4 Spectral data acquisition benchtop instrument

3.4.1 Instrument and software

The instrument used for the benchtop study was a Perkin Elmer "Spectrum 400 FT-IR and FT-NIR Spectrometer" (Perkin Elmer, Waltham, MA, USA) equipped with a PIKE Technologies "AutoDiff" Diffuse Reflectance autosampler (PIKE Technologies, Madison, WI, USA). The instrument is run with the "Spectrum 10" software (Perkin Elmer, Waltham, MA, USA), the autosampler with "AutoPRO 5.1" (PIKE Technologies, Madison, WI, USA).

Chemometric and multivariate modelling was executed in UNSCRAMBER X (Camo Software AS, Oslo, Norway).

3.4.2 Sample preparation

From each sample in SD1, a subsample of the dried and sieved soil was ball milled at a frequency of 25/s for three minutes in a ball mill to reach a uniform particle size (< 10 µm). Three subsamples of 1 g of the milled soil was filled into a sample cup for the “Pike AutoDiff” accessory for diffuse reflectance sampling (PIKE Technologies, Madison, WI, USA) (diameter 10 mm) and their surface was smoothed with a blade. The triplicate scans per sample are referred to as spectral replicate. The filled sample cups were then loaded into the “AutoDiff” autosampler in batches of 60 cups.

3.4.3 MIR spectrometer

The "Spectrum 400 FT-IR” works on the principles of Fourier Transform Infrared Spectroscopy (FTIR) which will be described in the following.

The heart of the FTIR spectrometer is the Michaelson Interferometer. Thanks to this technique in combination with Fourier analysis, the scan can be performed faster and more stable compared to dispersive instruments working with monochromators (prism/ gratings), as the spectrum can be recorded faster and with a better signal-to-noise ratio (SNR) (Felgett-advantage: the ability to reach a good SNR in short time, Jacquinot-advantage: more energy is available to interact with sample which allows faster scanning, Connes-advantage: internal laser reference makes external calibration unnecessary) (Janik et al., 1998; Stuart, 2004).

The interferometer consists of two mirrors placed perpendicular to each other and one beam splitter lying diagonally between the two mirrors. The beam splitter consists of a material which doesn’t react with IR radiation (Potassium Bromide (KBr)) and is coated with Germanium or Iron Oxide which gives it the desired properties: the beam splitter lets 50% of the incoming radiation pass onto one of the mirrors, while the remaining 50% are reflected to the other mirror. Both parts of the beam are reflected from the mirrors and then recombine in the beam splitter, from where the recombined beam is sent to the sample and eventually to the detector. One of the mirrors is fixed while the other is moving, which enables a change of the pathlength of one half of the beam. When the two halves of the beam arrive again at the beam splitter, the one half of the beam arrives with a phase-difference (depending on the difference in path length) which causes interferences at recombination. Depending on the path difference, the interference can be either constructive or destructive, and thus, by moving the mirror (changing the optical path difference) the transmitted beam (the beam sent to the sample) can be modulated. In the case of a monochromatic beam with only one frequency the modulation will result in a sinusoidal function with changing path length, in the case of a full MIR beam (polychromatic,4000 – 400 cm^{-1}), the interference pattern becomes more complex, as each frequency interferes at a different optical path difference. The resulting output, the interferogram is a display of the intensity of the transmitted beam plotted over the time of the scan (directly related to the path difference with a constantly moving mirror). This interferogram is formed by overlaying the sinusoidal curves resulting from interferences of each wavelength. It contains information about the entire spectrum displayed as a time domain spectrum. Figure 5 and Figure 6, (modified from Stuart (2004)), give an overview over the optical path in a Michelson Interferometer and the resulting interferograms for a monochromatic and polychromatic beam with the Intensity (I') as a function of the path length difference (δ). The path length is measured independently by a laser, which allows for a precise measurement.

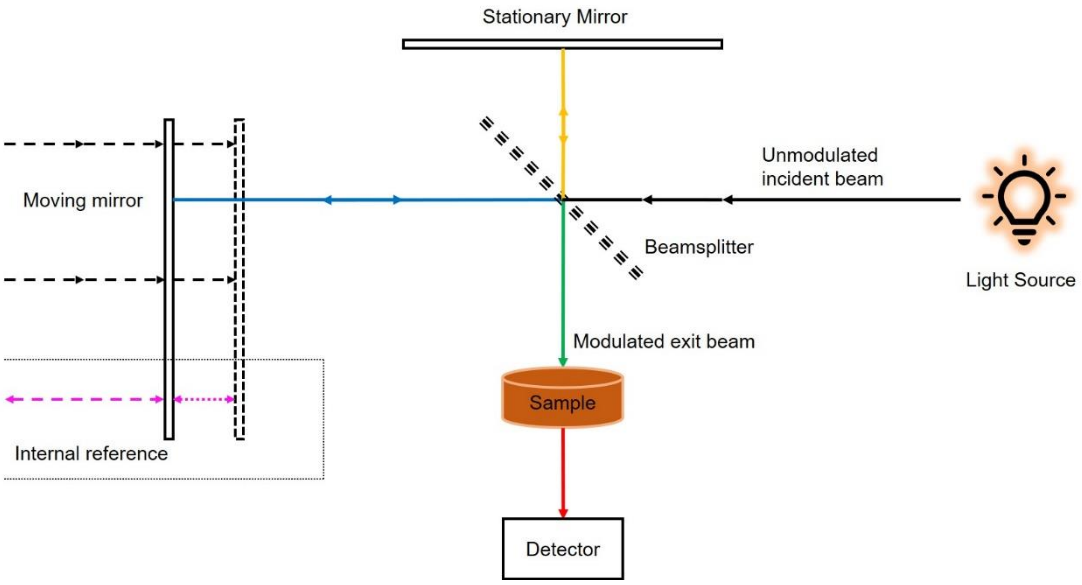

Figure 5 Schematics of a Michelson interferometer with the light path from source through the interferometer and sample to the detector. Modified from Stuart (2004)

With Fourier transformation, time domain spectra can be translated into frequency domain spectra which display the intensity of the transmitted beam over the frequency range. The Fourier pair, the two equations enabling the transformation from one domain to another are given with the following equations (Stuart, 2004).

$$\mathrm{I}(\delta) = \int_0^{+\infty} \mathrm{B}(\bar{\nu}) \cos(2\pi\bar{\nu}\delta)\, d\bar{\nu} \qquad (7)$$

$$\mathrm{B}(\bar{\nu}) = \int_{-\infty}^{+\infty} \mathrm{I}(\delta) \cos(2\pi\bar{\nu}\delta)\, d\delta \qquad (8)$$

Where Equation 7 describes the intensity of the interferogram (I(δ)) as a function of the spectral power density ($B(\bar{\nu})$) at a given wavenumber $\bar{\nu}$, and Equation 8 describes the spectral power density as a function of the intensity of the interferogram at a given path length difference δ. To obtain the spectrum of a sample, first the interferogram without a sample in the beam is recorded (background, silicon carbide (SiC) disk for the instrument used here) and transformed resulting in the incident light intensity (I_0). When the sample is in the beam, the interferogram is changed due to absorption at certain wavenumbers, which is in turn also represented in the Fourier transformed spectrum (I). By calculating the ratio of the sample spectrum to the background spectrum, the final spectrum is obtained, depending on the method as reflectance ($R=I/I_0$) for reflectance measurements or transmittance ($T=I/I_0$) for transmission measurements. The method used for soils is Diffuse Reflectance

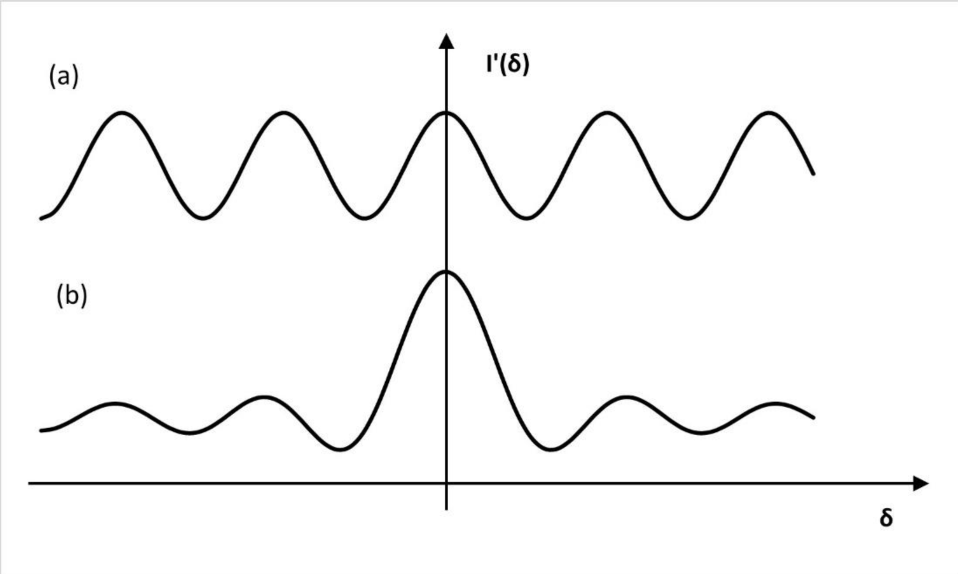

Figure 6 Interferograms resulting from a monochromatic (a) and polychromatic (b) beam, with the detected intensity (I'(δ)) plotted over the pathlength difference (δ) as time domain spectra. Modified from Stuart (2004)

(DR), where a solid sample is irradiated with the beam. When the sample is irradiated, part of the radiation, depending on the wavenumber, is absorbed by the sample components, the remainder is reflected. As the sample consists of soil particles and voids between the particles, the reflected beam can either hit another particle or leave the sample to be collected by a spherical mirror and sent to the detector. A schematic path of the beam through the sample is displayed in Figure 7. The combination of the Fourier Transform Infrared (FTIR) spectroscopy and the Diffuse Reflectance sampling form the basics of the Diffuse Reflectance Infrared Fourier Transform Spectroscopy (DRIFTS). Before the use of DRIFTS, soil samples for mineralogical analysis had to be mixed with KBr to dilute the samples and be pressed into halide disks and used in transmission spectroscopy, which slowed down the analysis process considerably (Janik et al., 1998).

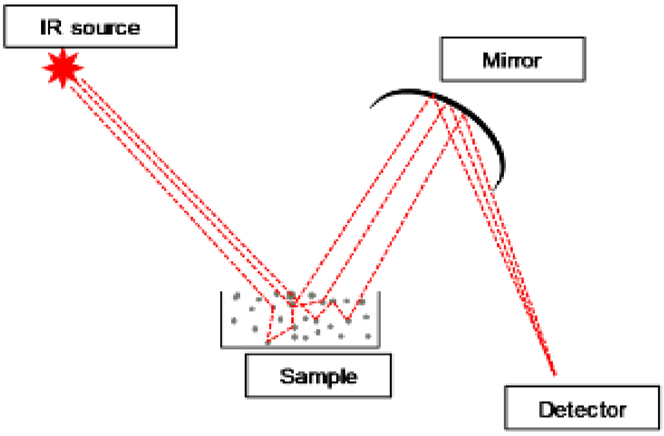

Figure 7 Schematic beam path from the source through the sample where diffuse reflection occurs, to the mirror which focuses the light onto the detector

The Source of radiation for MIR is usually a Nernst or Globar thermal light source and the detector a nitrogen cooled HgCdTe (mercury, cadmium telluride, MCT) or a deuterium triglycine sulphate (DTGS) where cooling is not feasible or the sensitivity is sufficient (as it is the case for NIR scans). To be able to relate the concentration in the sample to the amount of reflected light, a linear relationship must exist between the amount of light and the concentration in the sample, which is given through the Lambert-Beer equation in Equation 9

$$A = \varepsilon bc \qquad (9)$$

In this equation, A describes the absorbance at each wavelength, ε is a constant (molar absorptivity constant), b describes the pathlength and c the concentration. To obtain absorbance values from reflectance (or transmittance), the data must be transformed with Equation 10 after which the spectrum is ready for further processing.

$$A = \log\left(\frac{1}{R}\right) \text{ or } A = \log\left(\frac{1}{T}\right) \qquad (10)$$

3.4.4 Sample scanning

The batch of 60 samples (20x3 spectral replicates) in the autosampler is scanned in diffuse reflectance mode at full range from 4,000 – 450 cm^{-1} in a 2 cm^{-1} sampling interval. 16 co-added scans of each sample cup are collected, and the results are displayed in absorbance units (A). Before every run of 60 samples, the background was calibrated with a SiC reference disk. Information about the conceptual framework of a spectrometer is taken from Esbensen and Swarbrick (2018), Sherman Hsu (1997) and Stuart (2004).

3.4.5 Spectral quality check

The spectral replicates of each sample were analysed for their uniformity by calculating the overall standard deviation of the replicates. First the standard deviation in each wavenumber of the triplicates was calculated, then, the standard deviation of the values of all standard deviations across all wavenumbers was calculated. A threshold value of 0.1 was set as criterion for removing spectral reps from the dataset or repeat the measurement.

3.5 Spectral data acquisition handheld instrument

The portable, handheld instrument used for the research in Paper 2 is a “Agilent 4300 FTIR” (Agilent Technologies, Santa Clara, CA, USA) equipped with a DRIFTS sampling accessory and a DTGS detector. The instrument weighs approximately 2 kg and can be run on batteries for in-field applications.

3.5.1 Laboratory samples (dried and ground)

To evaluate the application of calibrations derived from benchtop spectra to spectra from handheld instruments, the validation set used in the research for Paper 1 was scanned again with the handheld instrument. For that, the sample was filled in the sampling cup of the AutoDiff accessory as described in Section 3.4.2. The handheld instrument was placed into a stand which allows it to be used similarly to a benchtop instrument. It is fixed in a frame and can be lowered onto the sample as shown in Figure 8. The background was scanned every 15 min from a gold-coated reference cap and the samples were scanned in 32 co-added scans in DRIFTS mode with a spectral resolution of 4 cm^{-1}. To obtain spectral replicates (3 scans per sample), the sample cup was rotated 120° after each scan and the stability of the spectra was evaluated with the spectral standard deviation as described for the benchtop data in Section 3.4.53.4.5 .

Figure 8 Handheld instrument fixated in the stand while scanning a sample cup

3.5.2 Field samples

To assess the feasibility of the handheld MIR under field conditions, a field sampling template was constructed (Figure 9) to scan the soil surface and sides in a shallow soil profile, in addition to fresh, loose soil *in situ*. This methodology was tested out on three fields described above Section 3.2.2.

The sampling template was constructed to consist of two plywood plates joined in a right angle with five holes in a W-shaped pattern in each face of the board to ensure regular sampling in five replicates. The template in Figure 9 was deployed to record spectra from the top and the side of the soil profile at a depth of 5-10 cm. The profile was dug to have a flat horizontal surface at a depth of 5 cm and one vertical surface reaching down from 5 to 15 cm so the template could be placed flat on it.

Figure 9 Sampling template at its position in the small soil pit for scanning the surface from above and from the side

The handheld FTIR was placed in the first hole to collect spectra with the following settings: 16 co-added background spectra are scanned from a gold-plated reference cap. After the Background was scanned and scanning of the actual sample (soil) was supposed to start, the instrument didn't start scanning. After ensuring the functionality of the instrument on other materials (wood), the instrument still didn't scan. Consulting the live readings of on the instrument screen showed the scale measuring the absorbance reaching the maximum, leading to the conclusion that all the incoming IR radiation was completely absorbed by the soil surface.

Following that finding, the further sample collection had to be adapted. For a scouting experiment, a block of the sample was taken to the spectroscopy lab to be tried to scan again. Different sample pre-processing methods were applied, including a) scanning one point of the block which had been flattened, b) scanning a piece of the block with the instrument fixed in the instrument stand, c) one subsample cleared of big stones and roots, rolled to a small ball and flattened, and d), a sieved (2 mm) and re-wetted subsample with the instrument in the stand. Scanning the block of soil with the instrument held in the hands failed initially, only after letting the sample dry overnight the instrument recorded a spectrum. Scanning the untreated subsample with the instrument in the stand, however, produced a spectrum in field moist stadium, while the rolled and flattened subsample made the acquisition of spectra easier. Based on these intermediate results from the scouting experiment, a new sampling strategy was devised as described following:

From each point in the field to be sampled, soil was collected and filled into three small petri dishes and the surface was flattened. From each dish, triplicate scans are collected with the handheld spectrometer. To keep the instrument stable, it is placed in the instrument stand, where it is fixed and can be lowered to the sample as shown in Figure 10. The scanning settings were the same as in the approach for the scan directly in the soil pit, with the only difference being, that the background was only collected every 15 min. For ease of access, the scanning was done inside the laboratory, but it is to emphasize that the entire setup, including the instrument stand, can also be used directly in the field.

Figure 10 Handheld FTIR while scanning the sample in the petri dish

3.5.3 Moisture content calculations

Part of the study with the handheld spectrometer was to evaluate the influence of water content on the quality of spectra and prediction. For that, the spectra in the petri dishes were dried gradually, with the moisture content of the samples measured 14 times. Every time the moisture was measured, a corresponding spectrum of the sample was obtained.

The water content was measured gravimetrically (gravimetric moisture content (GMC)), relating the weight of water remaining in the sample to the weight of the dried sample as follows:

$$\mathrm{GMC}\ [\%] = \frac{\mathrm{weight_{wet}} - \mathrm{weight_{dry}}}{\mathrm{weight_{dry}}} * 100 \tag{11}$$

After the 14th weighing, the sample was dried at 105 °C for 24 hr and weighed again to obtain the reference weight ($\mathrm{weight_{dry}}$). This sample was scanned (step 15), as well as a dried, sieved and ball-milled sample as reference (step 16).

3.6 Spectral pre-processing methods

Spectroscopic data require to be pre-processed to reveal more detailed features contained in the spectra, which are hidden by noise, multiplicative and additive effects (Esbensen and Swarbrick, 2018). The pre-processing techniques used for this research will be presented in the following.

3.6.1 Smoothing

While scanning the samples there is always some introduction of instrument noise into the spectrum. Smoothing reduces this noise, by re-calculating a point in the spectrum incorporating the values of the points surrounding the point of interest.

The Moving Average (MA) smoothing is a simple way of smoothing, where a smoothing window with a defined size is placed around one point. From the surrounding points the average is calculated, which replaces the original point. After this operation, the smoothing window will be moved to the next point where the calculation is repeated.

Savitzky-Golay smoothing is a more sophisticated approach where a polynomial is fitted through the points within the smoothing window and the value of the point to be smoothed is replaced by an estimated value from the polynomial (Savitzky and Golay, 1964).

3.6.2 Derivative

Derivatives of spectra are useful to increase the importance of their peaks and changes in their slope. By definition, the derivative $f'(x)$ describes the slope of the original function. In the case of spectra, especially the second derivative $f''(x)$ is of interest, describing the curvature of the spectra while correcting for quadratic baseline shifts (→ $f''(x^2) = 2$ → linearized) and remains interpretable, as the peaks are on the same position like the peaks in the original spectrum. Through their effect of intensifying peaks and changes in the spectra, derivatives are prone to inflate noise present in the spectra. This can be avoided by smoothing spectra before a derivative is calculated.

Savitzky and Golay (1964) developed a method widely used in spectroscopic applications combining the two steps of smoothing and derivatization. This method is a combination of the smoothing described in Section 3.6.1 and a calculation of the derivative spectrum. Firstly, a polynomial is fitted through the points within the smoothing window from which point A is estimated. The smoothing window is moved forward for one point, where point B is estimated from the new polynomial. This process is repeated throughout all points of the spectrum. The first and second derivative through points A, B, C is calculated as following, with $\Delta\overline{\nu}$ being the spectra resolution

$$\frac{\partial \mathrm{y}}{\partial \mathrm{x}} = \frac{\mathrm{B}-\mathrm{A}}{\Delta\overline{\nu}} \tag{12}$$

$$\frac{\partial^2 \mathrm{y}}{\partial \mathrm{x}^2} = \frac{(\mathrm{C}-\mathrm{B})-(\mathrm{B}-\mathrm{A})}{\Delta\overline{\nu}} \tag{13}$$

3.6.3 Normalization

In the process of normalization, spectra are scaled to a common size , through which the influence of additive effects changing the overall intensity of the spectra (e.g. colour of the sample, scanned under slightly different conditions, different height of spectra, path length differences) is minimized and thus the details within the spectra become more important. The normalization is achieved by a column-wise pre-processing, where a statistic is calculated over one column (i.e. in one wavenumber) and then each element of the column is scaled with that statistic. The statistics can be the area, range, average or the height of a standard peak.

3.6.4 Scatter corrections

Especially when dealing with solid samples in powdered form, multiplicative scattering effects with different strengths are present throughout the spectrum depending on the wavenumber. Scattering effects occur when the incoming light has a wavelength similar to the size of the particles in the sample as well as specular reflection (total reflection of the light where the sample behaves like a mirror), which leads to nonlinear baseline effects. Standard Normal Variate (SNV) correction is a method used frequently to correct for scattering effects.

In SNV (Barnes et al., 1989), the spectral data are centred to the average of the entire dataset and scaled to unit variance with

$$\mathbf{X}^*_{i,j} = \frac{\mathrm{x_j} - \overline{\mathrm{x_i}}}{\mathrm{s_i}} \tag{14}$$

where $\mathbf{X^*_{i,j}}$ represents the SNV corrected spectrum for a sample i at a wavenumber j, $\mathbf{X_j}$ the absorbance at wavenumber j, $\overline{\mathbf{X}}_i$ the mean absorbance over the entire wavenumber range of the sample i and s_i the standard deviation for sample i over the entire range. Subtracting the mean spectrum from each wavenumber eliminates additive effects, while dividing by the standard deviation reduces the remaining scatter effects.

3.7 Chemometric modelling

3.7.1 Partial Least Squares Regression

The Partial Least Squares Regression sometimes also referred to as Projection to Latent Structures Regression (PLSR) is the most common and reliable multivariate method used for spectral calibration. It was developed by Herman Wold and further developed by Svante Wold and Harald Martens (Esbensen and Swarbrick, 2018; Wold et al., 2001) In simple terms, it utilizes two matrices, **Y**, the dependent variables/response variables, in the case of spectroscopy the laboratory values and **X**, the predictors/X-variables, in this case the spectra, a matrix spanned by the samples (1…n) and the wavenumbers as variables (4000…450 for MIR), which are being decomposed into score and loading vectors. The principle of decomposing a matrix into score and loading vectors is conceptually the same as in principal component analysis (PCA), consisting of a drastic reduction of dimensionality (number of variables describing the system) guided by the multivariate directions of maximum variance. The multivariate directions of maximum variance are the basis of a new coordinate system spanned by orthogonal factors (in the case of PCA) or latent variables (LV, in the case of PLSR), which eliminate problems of multicollinearity arising from highly correlated spectral data and enable the system to be used for subsequent modelling. The basic way to describe the two matrices **X** and **Y** decomposed by scores and loadings is given in Equation. 15 and 16,

$$\mathbf{X} = \mathbf{TP^T} + \mathbf{E} \tag{15}$$

$$\mathbf{Y} = \mathbf{UQ^T} + \mathbf{F} \tag{16}$$

where **X** and **Y** are the predictor- and response (in the general case of more than one response variable) matrices, **T** and **U** the matrices containing the score vectors $\mathbf{t}_i$ and $\mathbf{u}_i$ for **X** and **Y** respectively, **P** and **Q** the matrices containing the loading vectors $\mathbf{p}_i$ and $\mathbf{q}_i$ for **X** and **Y** respectively and **E** and **F** containing the residuals, the remaining variance which couldn't be described by the linear combinations of scores and loadings. This decomposition causes especially the set of X-variables to be described by far less variables (LVs, usually <10) than the original variables (wavenumbers, usually >>100). The scores describe the relation of the sample to the new "coordinate system" while the loadings describe the weight each variable has in calculating the scores. The ultimate goal of PLSR in the calibration step is to maximize the covariance between the **Y** scores **u** (or in the case of only one variable just the vector **y** containing the response variables) and **X** scores **t**. Doing so, a linear regression between **t** and **u** can be created and used for the prediction of new, unknown samples. This linear regression is called the "inner relation", while the decomposition of **X** and **Y** is called the "outer relation" of the PLSR. The main difference to PCA (and principal component regression directly relying on the PCA of the two matrices) is, that PLSR actively uses the information available in **Y** to guide the calculation of the **t**-scores, hence creating a direct link between **X** and **Y**. The mathematical process developed by Herman Wold in 1966 (Wold, 1973) to perform the decomposition of the matrices is called "Nonlinear Iterative PArtial Least Squares" or "Nonlinear Iterative Partial Alternating Least Squares" (NIPALS) and the main steps for the case of only one response variable (**y**) based on the geometric description in Esbensen and Swabrick (2018), the method reference of the UNSCRAMBER X (CAMO Software AS, 2011) and in Adams (1995) is given in the following:

The matrix **X** and the vector **y** are mean centred and standard deviation scaled

1) Indexing starts at one: $\mathbf{X_1}$=**X**, $\mathbf{y_1}$=**y**
2) The loading weight $\mathbf{w_1}$ is calculated with

$$\mathbf{w_1} = \frac{\mathrm{X}_1^{\mathrm{T}}\,\mathrm{y}_1}{|\mathbf{X}_1^{\mathrm{T}}\,\mathbf{y}_1|} \tag{17}$$

this maximizes the covariance between $\mathbf{X}^{\mathrm{T}}$ and **y** and normalizes **w**

3) Through a projection of $\mathbf{X_1}$ on $\mathbf{w_1}$, the corresponding score vector $\mathbf{t_1}$ is calculated

$$\mathbf{t_1} = \mathbf{X_1 w_1} \tag{18}$$

this step is the projection of the object vector onto the latent variable in **X**

4) The **Y**-loadings **q** are calculated by regressing **y** onto **t**

$$\mathbf{q_1} = \frac{\mathrm{t}_1^{\mathrm{T}}\,\mathrm{y}_1}{|\mathbf{t}_1^{\mathrm{T}}\,\mathbf{y}_1|} \tag{19}$$

5) And similarly, the **X**-loadings **p** are calculated by regressing **X** onto **t**

$$\mathbf{p_1} = \frac{\mathrm{X}_1^{\mathrm{T}}\mathbf{t}_1}{|\mathbf{t}_1^{\mathrm{T}}\,\mathbf{t}_1|} \tag{20}$$

6) Now, the direction of maximum variability in **X** and **y** can be described with the scores and loadings associated with the first latent variable (LV1) and the variance can be removed from the initial matrices $\mathbf{X_1}$ and $\mathbf{y_1}$ by deflating them as follows:

$$\mathbf{X}_2 = \mathbf{X}_1 - \mathbf{t_1}\mathbf{p}_1^{\mathrm{T}} \tag{21}$$

$$\mathbf{y}_2 = \mathbf{y}_1 - \mathbf{q_1}\mathbf{t}_1^{\mathrm{T}} \tag{22}$$

<u>Note:</u> as **y** was directly used to in the calculation of **w** and consequently **t** with Equation 18, in the case of one **y**-variable, the scores **t** are the same for **X** and **y** (**U** → **y**, **Q**=1 in the notation from Equation 16).

7) After the deflation, $\mathbf{X_2}$ and $\mathbf{y_2}$ contain the remaining information (variance) in the system which couldn't be described by the scores and loadings for LV1. Steps 3) to 7) are repeated A times, thus increasing the number of LVs and decreasing the information remaining in $\mathbf{X_A}$ and $\mathbf{y_A}$. The sufficient amount of A LVs is determined by cross-validation (leaving a subset of samples out of the calibration and calculate model performance parameter like R^2 and RMSE to evaluate the prediction of the subset), after which the remaining $\mathbf{X_A}$ and $\mathbf{y_A}$ are defined as the residuals **E** and **f**.
8) The regression coefficients **b** satisfying the formal regression equation $\hat{\boldsymbol{y}} = \boldsymbol{X}\hat{\boldsymbol{b}}$**,** are calculated as follows

$$\mathbf{b} = \mathbf{W}(\mathbf{X^T W})^{-1}\mathbf{q} \tag{23}$$

When the model is calibrated with a sufficient number of LVs, it can be used to predict unknown response variables $\mathbf{\hat{y}_i}$ from new X-variables $\mathbf{X_i}$ in the following steps.

1) The new matrix $\mathbf{X_i}$ has to be scaled and the centre of the calibration data $\mathbf{\bar{X}}$ is subtracted

$$\mathbf{X}_{\mathbf{i},\mathbf{1}}^{\mathrm{T}} = \mathbf{X}_{\mathbf{i},}^{\mathrm{T}} - \mathbf{\bar{X}^T} \tag{24}$$

2) From the new $\mathbf{X_i}$, the score vector $\mathbf{t_i}$ is calculated corresponding to Equation 18 with the loading weight vector $\mathbf{w_1}$ from the calibration model

$$\mathbf{t}_{\mathbf{i},\mathbf{1}} = \mathbf{X}_{\mathbf{i},\mathbf{1}}\mathbf{w_1} \tag{25}$$

3) $\mathbf{X_{i,1}}$ is deflated using the loading vector $\mathbf{p_1}$ from the calibration model and the new scores vector $\mathbf{t_{i,1}}$ to

$$\mathbf{X}_{\mathbf{i},\mathbf{2}} = \mathbf{X}_{\mathbf{i},\mathbf{1}} - \mathbf{t}_{\mathbf{i},\mathbf{1}}\mathbf{p}_{\mathbf{1}}^{\mathrm{T}} \quad (26)$$

Steps 2) and 3) are repeated until the optimum number of LVs A determined during the calibration is reached and $\mathbf{X}_{i,A}$ is the residual matrix $\mathbf{E}_i$

4) The prediction of the response variable $\hat{\mathbf{y}}_i$ is then calculated as follows, with $\bar{\mathbf{y}}$ being the average of the response variables and A being the number of LVs

$$\hat{\mathbf{y}}_{\mathrm{i}} = \bar{\mathbf{y}} + \sum_{\mathrm{a}=1}^{\mathrm{A}} \mathbf{t}_{\mathrm{i,a}}\mathbf{q}_{\mathrm{a}} \quad (27)$$

5) Alternatively (short prediction), $\hat{\mathbf{y}}_i$ can also be predicted using the regression coefficients **b**

$$\hat{\mathbf{y}}_{\mathrm{i}} = \mathbf{X}_{\mathrm{i}}^{\mathbf{T}}\mathbf{b} \quad (28)$$

The short prediction in step 5) is used for practical applications, while the full prediction (calibration) is used for model development, as the loading weights in spectra can be directly related to absorptions at a specific wavenumber, which gives the PLSR superior interpretability.

3.7.2 Performance indicators and performance evaluation

The performance of the calibration model and the prediction is measured with several performance indicators which will be described in the following (Adams, 1995; Bellon-Maurel et al., 2010; Esbensen and Swarbrick, 2018; Mark and Workman, 2007; Naes et al., 2004). The most used indicator is the coefficient of determination R^2 (goodness of fit), describing how well the regression line fits the points in a scatter plot of predicted ($\hat{\mathbf{y}}$) vs. reference ($\mathbf{y}$) data. R^2 is calculated based on the residual sum of squares (RSS) and the total sum of squares (TSS) calculated as follows:

$$\mathrm{RSS} = \sum_{\mathrm{i}=1}^{\mathrm{n}} (\mathrm{y_i} - \hat{\mathrm{y}}_{\mathrm{i}})^2 \quad (29)$$

calculating the difference between the reference and predicted data,

$$\mathrm{TSS} = \sum_{\mathrm{i}=1}^{\mathrm{n}} (\mathrm{y_i} - \bar{\mathrm{y}})^2 \quad (30)$$

and the TSS calculating the difference between the reference value and the average reference value ($\bar{y}$), which leads then to the following equation for R^2

$$\mathrm{R}^2 = 1 - \frac{\mathrm{RSS}}{\mathrm{TSS}} = 1 - \frac{\sum_{\mathrm{i}=1}^{\mathrm{n}} (\mathrm{y_i} - \hat{\mathrm{y}}_{\mathrm{i}})^2}{\sum_{\mathrm{i}=1}^{\mathrm{n}} (\mathrm{y_i} - \bar{\mathrm{y}})^2} \quad (31)$$

But R^2 can only give a coarse overview over the behaviour of the model, and model diagnostics have to utilize the other indicators. The Root Mean Squared Error of Calibration/Validation (RMSE, RMSEC, RMSEP) measures the accuracy of the model. It is calculated as following

$$\mathrm{RMSE} = \sqrt{\frac{\sum_{i=1}^{n}(y_i - \hat{y}_i)^2}{N}} \quad (32)$$

where the RMSEC will be calculated with **y** and **ŷ** resulting from the calibration model whereas the RMSEP will be calculated with **y** and **ŷ** from the validation, with N being the number of objects used.

The BIAS measures the average difference between the predicted and reference set, useful to evaluate if the prediction systematically over-or underestimates the reference values.

$$\mathrm{BIAS} = \frac{\sum_{i=1}^{n}(\hat{y}_i - y_i)}{N} \quad (33)$$

The Standard Error of Prediction (SEP) measures the precision of the prediction including the BIAS:

$$\mathrm{SEP} = \frac{\sum_{i=1}^{n}(\hat{y}_i - y_i - \mathrm{BIAS})^2}{N-1} \quad (34)$$

The relationship of RMSEP, SEP and BIAS can be approximated by

$$\mathrm{RMSEP}^2 \approx \mathrm{SEP}^2 + \mathrm{BIAS}^2 \quad (35)$$

Goal in model diagnostics and model building is, to increase the coefficient of determination, indicating that a big part of the variance in the input data is described by the model, while minimizing the error (RMSE, SEP), keeping the BIAS close to zero and the slope of the regression line close to one. These requirements additionally have to be balanced with the requirement to keep the model parsimonious, meaning using as little LVs as possible, as with the addition of more LVs, the probability to model only noise increases.

When the quality of calibrations or predictions among different studies, instruments or fields needs to be compared, it is not feasible to simply compare RMSE’s as their magnitude is depending on the range of values used for the calibration/prediction. Normalizing the error measurement of the model by some statistic for the spread of the input data is a feasible approach. The Ratio of Performance to InterQuartile distance (RPIQ) is a parameter widely used to normalize the model performance by normalizing the RMSE of the model with the interquartile range (IQR) of the reference data, which makes it an especially useful indicator for datasets which don’t show a normal distribution. The IQR based on the 25% (Q_1)- and 75% percentiles (Q_3) of the data is calculated as follows (Bellon-Maurel et al., 2010)

$$\mathrm{IQR} = Q_3 - Q_1 \quad (36)$$

with which in turn the RPIQ can be calculated with

$$\mathrm{RPIQ} = \frac{\mathrm{IQR}}{\mathrm{RMSE}} \quad (37)$$

To incorporate a confidence interval around the estimated value, similar to regular statistics where $\mu \pm 2\sigma$ is utilized to calculate a 95% confidence interval based on a normal distribution with mean μ and standard deviation σ, in multivariate modelling this can be seen as $\hat{y} \pm 2\mathrm{RMSEP}$ (Esbensen and Swarbrick, 2018). Based on that assumption, a performance indicator utilizing the entire range of the reference dataset was calculated to evaluate the predictive performance, in the case of Paper 1 for each field. This Range Confidence Prediction Indicator (RCPI) is calculated by

$$\mathrm{RCPI} = \frac{\max - \min}{2 * \mathrm{RMSEP}} \quad (38).$$

3.8 Statistical analyses

3.8.1 Generalized linear mixed model (GLIMMIX)

The variation in soil parameters between sample zones was statistically analysed with a generalized linear mixed model (proc GLIMMIX in SAS 9.4) (SAS Institute Inc.) by analysing the difference between the four zones based described in Section 3.2.1. Proc GLIMMIX was run with field and zone as fixed effects. To compare the zones with each other, the least squares means of the four zones are calculated with the LSMEANS statement and the means of the zones are tested for significant differences, with the p values adjusted for multiple comparisons with “adj= simulate” which calculates the adjustment based on a simulated distribution. By slicing the interaction of field and zone, the model is able to deliver a detailed view of the zones in each field separately (Bolker et al., 2009; Davis, 2018; SAS, n.d.; Schabenberger, 2005). In this case, proc GLIMMIX delivers the same results as a two factorial ANOVA, but with the advantage that the setup is simpler and allows easier implementation of the adjustment for multiple comparisons, slicing of the interaction and it delivers residual plots. Through the slicing, single fields can be analysed in the context of the entire model. In the residual plots the distribution of the residuals of the linear model fitted to the data is displayed. Proc GLIMMIX runs under the assumption that the residuals of the model are normally distributed which is tested by inspecting the residual panel output. If the residuals are spread equally around 0 that assumption is justified, if there is a trend in the residuals, the input data has to be transformed (with agricultural data it is often a log-transformation). Proc GLIMMIX was executed for the following soil parameters: P, K, %OM, LR and pH, in SD1 and SD2 for the entire dataset as well as an analysis for the dataset grouped by texture classes in SD1. The input code for LR in SD1 is displayed in the following:

```
proc glimmix data=Km plots=(residualpanel studentpanel);
        title 'LR, all';
        where horizon=1 & field_no not=1;
        class field_no zone rep_no;
        model lr=field_no |zone rep_no;
        lsmeans zone/pdiff adj=simulate;
        lsmeans zone*field_no/pdiff adj=simulate slice=(field_no)
slicediff=field_no lines ;
run;
```

The full results of the analysis can be found in the digital appendix.

3.8.2 Bland-Altman method comparison

The efficiency of different MIR prediction methods was evaluated with the Bland-Altmann method comparison (Altman and Bland, 1983; Bland and Altman, 2010, 2003). This statistic is used to compare the agreement of two different methods to measure the same parameter. It is a tool plotting the difference between the measurements of the two methods (A_i-B_i) against their average ((A_i+B_i)/2). Quantification is given through the bias (mean difference), the total deviation index, the concordance correlation coefficient and the upper and lower limit of agreement (mean difference ± 2 standard deviation) resulting in a 95% agreement interval. For the upper and lower limits of agreement (ULoA and LLoA) themselves, a 95% confidence interval is calculated as well. All calculations and plots comparing the different prediction approaches are done with the “blandr” package in R studio (Datta, 2017)

Chapter 4

Research papers

4.1 Mid-infrared spectroscopy as an alternative to laboratory extraction for the determination of lime requirement in tillage soils

In this paper MIR spectroscopy was used to substitute laboratory extractions for lime requirement analysis with the “Shoemaker-McLean and Pratt” (SMP) buffer method, which requires carcinogenic reagents soon to be abolished under the EU legislation. Samples from the 41 sampled fields (n=655) were used to build a calibration and validation for DRIFTS using partial least squares regression (PLSR). In the model it was shown that the signals of soil constituents having an influence on the LR were picked up in the spectra and were identified in the loading weights of the PLSR. While the error is too high to predict the variability of LR within the field, MIR prediction using field averages provided a viable alternative to current laboratory methods for blanket spreading of lime on tillage fields.

Work for this paper was conducted to 80% by me, including fieldwork, laboratory analyses (partially), data exploration and evaluation, manuscript writing and editing. Field work was done in collaboration with Mark Ward, Teagasc Oak Park. Part of the laboratory analyses were done by the staff of Teagasc, Johnstown Castle.

In the following is the manuscript for the paper as submitted to the journal with the following reference (chapter-, figure- and table- numbering adapted)

Metzger, K., Zhang, C., Ward, M., Daly, K. 2020. Mid-infrared spectroscopy as an alternative to laboratory extraction for the determination of lime requirement in tillage soils. Geoderma, https://doi.org/10.1016/j.geoderma.2020.114171

Mid-infrared spectroscopy as an alternative to laboratory extraction for the determination of lime requirement in tillage soils

Konrad Metzger [a, b], Chaosheng Zhang [b], Mark Ward [c, d], Karen Daly [a]*

[a] *Environment, Soils and Land Use Department, Teagasc, Johnstown Castle Research Centre, Wexford, Y35 TC97, Republic of Ireland*

[b] *International Network for Environment and Health (INEH), School of Geography and Archaeology National University of Ireland, Galway, H91 CF50, Republic of Ireland*

[c] *Teagasc CELUP, Crops Research, Oak Park, Carlow, Republic of Ireland*

[d] *School of Agriculture and Food Science, UCD, Belfield, Dublin 4, Republic of Ireland*

* Corresponding author email: Karen.Daly@teagasc.ie

4.1.1 Abstract

Lime is a crucial soil conditioner to bring agricultural soils to optimum pH values for nutrient availability. Lime recommendations are typically determined in laboratory extractions, the most common being the "Shoemaker-McLean and Pratt" (SMP) buffer method, that requires carcinogenic reagents soon to be abolished under the EU legislation. As an alternative to wet chemistry, mid-infrared (MIR) spectroscopy has shown to be a cost-and time effective method at predicting soil properties. The capability and feasibility of diffuse reflectance infrared spectroscopy (DRIFTS) to predict lime requirement (LR) in tillage fields is examined. Samples from 41 cereal tillage fields (n=655) are used to build a calibration for DRIFTS using partial least squares regression (PLSR). The samples were split into calibration set (31 fields, n=495) and validation set (10 fields, n= 160). After pre-processing with trim, smoothing and standard normal variate, a calibration model using 6 latent variables, provided R^2 of 0.89 and root mean square error of cross-validation (RMSECV) of 1.56 t/ha. Prediction of all fields from the validation set resulted in R^2 of 0.76 and root mean square error of prediction (RMSEP) of 1.68 t/ha. The predictions of the single fields ranged from R^2 values of 0.41 to 0.72, RMSEP of 0.48 to 4.2 t/ha and ratios of performance to inter-quartile distance (RPIQ) of 0.45 to 3.56. It was shown that the signals of soil constituents having an influence on the LR were picked up in the spectra and were identified in the loading weights of the PLSR. While the error is too high to predict the variability of LR within the field, MIR prediction using field averages provided a viable alternative to current laboratory methods for blanket spreading of lime on tillage fields.

Keywords

Soil spectroscopy; Lime requirement; SMP buffer; MIR DRIFTS; Chemometrics.

4.1.2 Introduction

One cornerstone for reaching sustainable soil utilization (FAO, 2009) is improved soil management. To achieve this, soil parameters have to be closely monitored, so that measures to improve soil quality can be put in place where and when needed (FAO, 2017; Karlen et al., 1997).

Lime is a crucial soil conditioner in both tillage and grassland systems. It helps to bring the soil pH ($-\log_{10}[H^+]$) to the optimum level for crop production. In humid climate, soils tend to acidify naturally due to the slight acidity of the rain in equilibrium with the atmospheric CO_2 (McLean, 1982). The acidic water percolates the soil and neutralizes with the basic cations in solution and transports these cations away from plant roots. In addition to the leaching of bases, at lower pH values (below pH 4.7 (Sparks, 2003)), aluminium (Al) adsorbed to clay minerals gets exchanged with the H^+ in the solution. Once the Al ion is in solution, it is coordinated by H_2O molecules, which then, depending on the pH, hydrolyse and release H^+ ions. Below pH 4.7, $Al^{3+}$is the dominant species, which, in comparison to the $Al(OH)_2$ present until pH 6.5, is soluble and toxic to the plant root system (Sparks, 2003).

In productive agricultural systems the most important source of soil acidity is the application of chemical fertilizer based on ammonium N (Goulding, 2016). Added to soil, N-fertilizer is nitrified (Barak et al., 1997; Goulding, 2016), and if the resulting NO_3^- isn´t taken up by the crops, it will get leached, causing acidification (Barak et al., 1997). The soil itself works as a buffer by exchanging the acid forming cations with basic cations which are adsorbed to the surface (clay minerals, organic matter). This buffering capacity is strongly dependant on the type and amount of clay minerals and organic matter (OM), as these factors govern the cation exchange capacity (CEC) (Thomas and Hargrove, 1984). Once this buffer system is exhausted, the pH drops rapidly with additional acidity introduced. With lower pH, nutrients such as P, K, Mg, Ca and S will no longer be available for plant uptake. In addition, the availability of metals such as Fe, Mn, Cu, Zn, Co and Al also increases to toxic levels (Sparks, 2003; The Fertilizer Association of Ireland, 2016).

By applying lime ($CaCO_3$) to the soil, it neutralizes the acidity, and so helps to improve soil structure (and thus drainage),the solubility of nutrients and provides optimum growth conditions for soil microorganisms (Goulding, 2016). The general neutralization reaction of acidity with lime is shown in Eq 1 (Goulding, 2016), which leads to an exchange of the adsorbed H^+ ions with the Ca^{2+} ions.

$$CaCO_3 + 2H^+ \rightarrow Ca^{2+} + CO_2 + H_2O \qquad (39)$$

Or, taking the acidifying effect of Al^{3+} into consideration the overall reaction is described by Eq 2 (Sparks, 2003).

$$2Al\text{-soil} + 3CaCO_3 + 3H_2O \rightarrow 3\ Ca\text{-soil} + 2\ Al(OH)_3 + 2CO_2 \quad (40)$$

As soil acidification is influenced by numerous soil parameters, it is hard to measure with simple laboratory measurements and thus is typically summarized by the soil lime requirement (LR). The LR is expressed as the amount of lime needed to bring the soil to the target pH (in t/ha, usually measured in the top 10 cm of soil. It is a recommendation based on intrinsic soil properties such as CEC, clay mineralogy and OM which govern soil acidity (McLean, 1982). The strong dependence on these intrinsic soil parameters becomes apparent where soils with the same pH value can have different LR, largely because cation exchange mechanisms differ greatly among soil types. The exact LR is measured in time consuming incubation trials, where lime and soil are mixed and left to react and the resulting pH is measured. This test is not used routinely anymore, but is still used to calibrate laboratory methods (McLean, 1982). In commercial soil laboratories, routine methods are deployed that involve titration of the soil solution with a base (soil-base titration) or measuring the resulting pH after mixing the soil with a buffer (soil-buffer equilibration) (McLean, 1970). In the soil-buffer equilibration methods the soil is left to react with a solution made up from different buffers which in combination lead to linear change in pH with neutralized acidity (Sikora, 2006). Prominent buffer methods include the “Adams and Evans” buffer (Adams and Evans, 1962) the “Shoemaker, McLean and Pratt” buffer (SMP) (Shoemaker et al., 1961), the “Sikora” buffer, an alternative to the SMP buffer without hazardous chemicals (Sikora, 2006) and the “Mehlich” buffer which was developed for a soil pH range from 6.6 to 3.8 (Mehlich, 1976). Other methods include the LR determination by titration with calcium hydroxide ($Ca(OH)_2$) (Kissel et al., 2007) and texture and crop dependent models developed from long term trials in the United Kingdom (ROTH lime) (Goulding, 2016) Of the routine laboratory procedures, the “Shoemaker, McLean & Pratt” (SMP) buffer method delivers the most accurate results in the pH and LR ranges usually present in agricultural soils. However, SMP buffer solution contains hazardous substances such as potassium chromate (K_2CrO_4) and 4-nitrophenol, which are a threat to health and safety, making waste disposal an important financial factor. Potassium chromate is designated as a “Substance of Very High Concern’’ (SVHC) and included in the candidate list for authorization within the REACH framework (ECHA (European Chemicals Agency), 2010). As this compound will be phased out, there are several efforts to find an alternative method to determine the LR, with reliable results for agricultural soils (McLean et al., 1966; Tunney et al., 2010).

Soil spectroscopy has emerged as a rapid, non-destructive method to analyse soils for a wide range of parameters, making it a potential alternative for the LR determination by lab extraction. Infrared (IR) spectra of soil samples contain information about the entire ensemble of soil components simultaneously. Using spectroscopy, the whole complex system causing soil acidity will be incorporated in the prediction of LR.

The main soil components which absorb IR radiation are OM (aliphatic, aromatic and amide vibrations), clay minerals (lattice water, O-H, Si-O and Al-O vibrations), sand (quartz, Si-O, lattice vibration), carbonates (X-H vibration) and Fe-oxides (Fe-O/H vibrations) (Janik et al., 1998; Nocita et al., 2015; Soriano-Disla et al., 2014; Stenberg and Viscarra Rossel, 2010; Vohland et al., 2014). Historically, two main regions in the IR are used for spectroscopy: near infrared (NIR, 700 – 2,500 nm [14,000 – 4,000 cm^{-1}]) and mid-infrared (MIR, 4,000 – 400 cm^{-1} [2,500 nm – 25,000 nm]) (Sherman Hsu, 1997). These spectrally active components occur in variable combinations and concentrations in the analysed soil, depending on soil genetics, soil formation and land use interact with each other, creating a complex pattern of fundamental-overtone- and combination absorptions (see figure with raw spectra). While the NIR range is dominated by these broad overtone and combination patterns, the MIR range shows more fundamental absorptions and a clearer peak resolution (Hutengs et al., 2019). And while for some applications it is advantageous that the NIR range is insensitive to quartz, the MIR range is sensitive to quartz and other silicates, which gives it the possibility to also detect inorganic soil fractions(Reeves, 2010; Reeves et al., 2005). Initially, mostly NIR was used for soil spectroscopy, but with the emergence of more accessible Fourier Transform spectroscopy technology and diffuse reflectance scanning, the MIR range has moved into the focus of soil scientists and will be the method of choice in the present work (Janik et al., 1998; Soriano-Disla et al., 2014).

By means of “chemometric modelling” complex spectral patterns are analysed and key information in the spectra can be extracted. Chemometric modelling refers to multivariate models capable of dealing with a high number of variables, where, in the case of soil spectroscopy the whole spectrum is used to predict a soil parameter. The most intuitive and commonly used multivariate methods in soil spectroscopy are partial least squares regression (PLSR) and principal component regression (PCR). Here, the multivariate directions of maximum variance are determined for both the spectra (**X**, predictor variables) and the laboratory data (**Y**, response variables) and used to build a new “coordinate system”. This coordinate system displays the whole dataset with an extremely reduced number of variables (from hundreds of wavelengths to <10 factors (in PCR) or latent variables (LV, in PLSR)). The original data is displayed by scores (position of the samples in the new coordinate system) and loadings (influence of the variables (here: wavenumber) on the calculation of the scores). As a simplistic way of describing the following regression, one can say that those new “coordinate systems” are being rotated until the best fit is reached, which is then described by the regression equation (Esbensen and Swarbrick, 2018; Wold et al., 2001).

Another crucial part in chemometric modelling is the pre-treatment of the spectra. Hereby the goal is to get as much information from the spectra and decrease the influence of random noise and scattering

Common pre-treatment measures are smoothing of the spectra, where several points of the spectrum are averaged to reduce the influence of random noise, using derivatives of the spectra (usually first or second derivative) to enhance the peaks (Savitzky and Golay, 1964), corrections for multiplicative effects on the spectra such as multiplicative scatter correction (MSC) (Geladi et al., 1985) and standard normal variate (SNV) (Barnes et al., 1989), normalization to make the different spectra comparable, and baseline corrections to compensate for an offset in the spectra due to differences during measurement. Trimming the spectra can also improve the information content of the spectra as regions of the spectrum which contain no viable information and only add to the noise can be cut out (Engel et al., 2013; O’Rourke et al., 2016; Rinnan et al., 2009). After successful pre-treatment, the model should have a small number of LVs (be parsimonious), maximize the variance explained by the model (R^2) and minimize the prediction error (root mean square error, RMSE) (Esbensen and Swarbrick, 2018).

Even if the LR isn´t a soil parameter *per se* (there is no molecule indicating LR, much less a spectrally active one), it can still be predicted, as it is strongly dependent on the CEC and hence clay content, clay type and OM (Chang et al., 2001; Janik et al., 1998; Soriano-Disla et al., 2014).

There are previously reported approaches in predicting the LR with IR spectroscopy. Tekin et al. (2013) developed an on-the-go NIR sensor, which was calibrated for pH. From the pH they developed a LR map according to DEFRA fertilizer manual (Department for Environment Food and Rural Affairs, 2010). Demattê et al. (2019) researched the precision of vis-NIR-SWIR spectroscopy (short wave IR) to predict LR based on CEC and base saturation (BS). They found high correlation between laboratory derived LR and spectral LR, proposing a hybrid approach with 20% of the samples analysed in the lab and the remaining 80% analysed spectrally. These approaches derived lime recommendations from proxy soil parameters, the only studies on LR derived from buffer pH were conducted by Viscarra Rossel et al.(2001) and Viscarra Rossel and McBratney (2001). They investigated the LR measured with a Mehlich-buffer response model measured at 122 points in a field in Australia. The MIR calibration resulted in an R^2 of 0.75 and a RMSE of 0.61 t/ha. Merry and Janik (1999) researched the potential of MIR to predict LR in different regions in Australia and could predict the LR on a large scale. A follow-up analysis of this report from 1999, or an indication of actual routine use of MIR for LR in Australia couldn't be found.

In Ireland, agronomic recommendations for LR are derived from the SMP buffer method which will shortly be discontinued due to the reagent composition including a SVHC. The objective of this study was to examine the application of Diffuse Reflectance Infrared Fourier Transform Spectroscopy (DRIFTS) in the MIR range in combination with chemometrics to predict LR and the feasibility of this approach to replace current wet chemical methods with spectral predictions. In productive agricultural systems LR is an agronomic recommendation given in tonne/ha and to our knowledge, no previous studies have predicted this recommendation using MIR calibrations derived from the SMP method directly. Therefore the objective of this study was to examine the ability of MIR to predict LR of cultivated soils and assess the viability of the predictions to substitute lengthy and hazardous laboratory extractions. The application of MIR models in precision agriculture was assessed by examining the predictive power of MIR to predict the variability of LR at field scale. This work focussed on Irish tillage soils at multiple fields in regions where tillage is the predominant agricultural land use.

4.1.3 Materials and Methods

4.1.3.1 Study sites/land use

A total of 655 soil samples were collected and analysed to build the calibration database from 41 tillage fields in the Republic of Ireland (Figure 11). The fields were recently harvested, and the previous two crop rotations were cereals (wheat and barley). The field sizes ranged from 2 to 37 ha with a median size of 8 ha. In each field four zones based on field traffic patterns were sampled (headland, headland tramline, transition zone and main field), in replicate, resulting in 16 samples per field taken at a depth of 5-10 cm in the plough layer, accompanying bulk density samples at the same depth. This sampling pattern is part of a parallel study examining the spatial distribution of soil properties across trafficked and non-trafficked areas in fields.

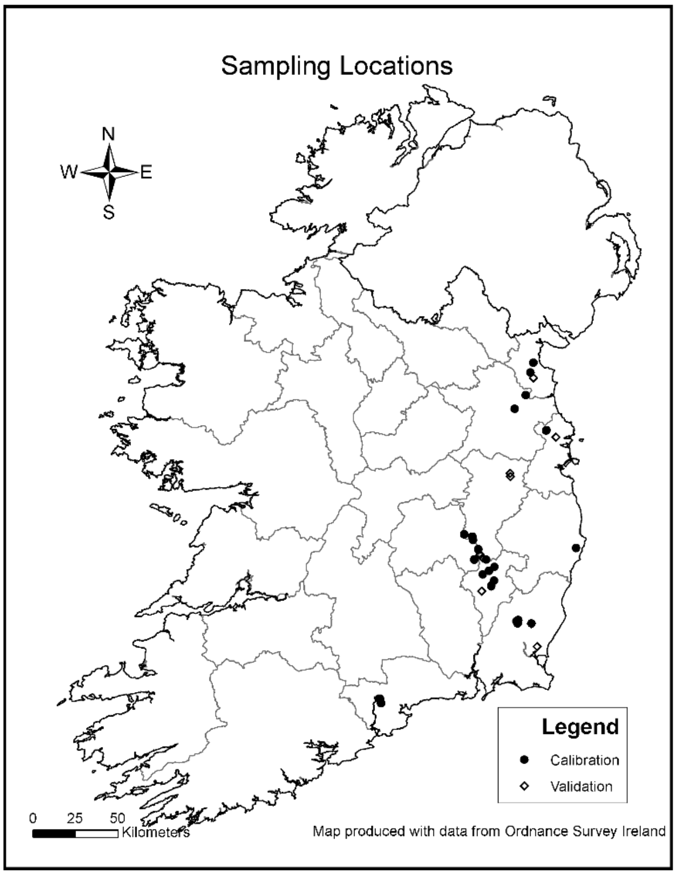

Figure 11 Sites selected for sampling, with calibration (filled) and validation (open) fields indicated

4.1.3.2. Reference data acquisition

The disturbed samples were collected in cardboard sample boxes, brought to the laboratory and dried at 40°C and mechanically sieved to 2 mm prior to analysis.

For pH analysis, 10 cm^3 of soil was mixed with 20 ml of deionized water and analysed with a pH autoanalyser with Mettler Toledo “in lab Routine” pH electrode.

For the determination of LR, 20 ml of SMP buffer solution (pH 7.5, T.E. Laboratories, Tullow, Ireland) was added to 10 cm^3 of dried and sieved (<2 mm) soil and shaken for 30 min on a gyratory shaker at 180 rpm. The solution was filtered through a Whatman no. 2 filter and analysed for pH with a Mettler Toledo “*InLab Routine*” (Mettler Toledo, Columbus, Ohio, USA) pH electrode. Based on the linear behaviour of the buffer pH to the neutralized acidity, the equivalent amount of lime can be calculated. Known values of lime requirement from soil incubation studies were related to the soil buffer pH after extraction. The amount of ground limestone needed to be applied to the soil to reach the crop specific target value can then be looked up in tables based on these experiments (McLean, 1982; Shoemaker et al., 1961).

The percentage OM (w/w) was determined by loss on ignition using 5 g of sample weighed into a crucible and dried at 105°C to remove capillary water. Samples and crucibles were then weighed and put into a furnace at 500 °C for 12 hours and the loss on ignition determined by comparing the weights.

Particle size distribution was determined on a composite sample for each field to describe the texture class at each field. They were analysed with the sieve pipette method using 20 g samples for the USDA particle size classification (Gee and Bauder, 1986; Massey et al., 2007). The organic matter in the sample was removed by oxidizing it with hydrogen peroxide, after which the clay aggregates were dispersed with sodium hexametaphosphate. The dispersed sample was then sieved with a 50 µm sieve to retain the sand fraction. The silt and clay fractions were determined through sedimentation.

4.1.3.3. Spectral data acquisition

A subsample of each of the 655 field samples was ball milled at a frequency of 25/s for three minutes and 1 g of the milled soil was filled into a sample cup (diameter 10 mm) and the surface smoothed with a blade. Spectral samples were prepared in triplicate for each soil. Samples were loaded onto the sample tray using a PIKE Technologies “AutoDiff” auto sampler (PIKE Technologies, Madison, WI, USA). MIR spectra were collected using a Perkin Elmer "Spectrum 400 FT-IR” spectrophotometer (Perkin Elmer, Inc. Waltham, MA, USA) with KBr beam splitter and nitrogen cooled mercury cadmium telluride (MCT) detector in diffuse reflectance mode. The samples were scanned in the MIR range from 4,000 – 450 cm^{-1} in a 2 cm^{-1} sampling interval and are reported smoothed at a resolution of 4 cm^{-1}. 16 scans of each sample cup were made and averaged and the results are displayed in absorbance units ($A=\log_{10}(1/R)$, R=reflectance) (Esbensen and Swarbrick, 2018; Sherman Hsu, 1997). Before every run of 60 samples, the background was calibrated with a silicon carbide reference disk

4.1.3.4. Chemometric calibration and validation

Triplicate spectra of each sample were analysed for their uniformity by calculating the overall standard deviation of the repeats. First the standard deviation in each wavenumber of the triplicates was calculated, then, the standard deviation of the values of all standard deviations was calculated. A threshold value of 0.1 was set differences to establish the criteria for removing spectral reps from the dataset. None of the scanned samples exceeded the threshold criterion and all samples were kept for further processing. Triplicate spectra were then averaged to reduce signal to noise ratio, and averaged spectra brought forward for pre-processing and analysis.

For the spectral calibration, MIR spectra and their corresponding laboratory data were loaded in the UNSCRAMBLER X software. The dataset was split into a calibration set (ca.75% of the data) and validation set (ca. 25% of the data). The random selection was carried out on a field basis, so that samples from 31 fields (495 samples) were assigned to the calibration, and samples from 10 fields (160 samples) were assigned to the validation dataset. The calibration set was then used to research the best pre-treatment options for the LR prediction with PLSR. The calibration set was loaded in the model with 10 LVs to be calculated. To get a better estimate of the model, a 20-fold random cross-validation (bin size: 24 samples) was applied.

Different combinations of pre-treatments including trimming, smoothing, Savitzky-Golay smoothing, mean centring, Savitzky-Golay derivatives, MSC and SNV were applied to the spectra which were then used in a PLSR run. From these runs, the model performance parameters R^2, RMSE and the optimal number of LVs needed was used as a selection criterion for the pre-treatment. The goal hereby was to maximize the R^2, minimize the RMSE and keep the model as parsimonious as possible (minimize number of LVs). Theoretically the R^2 can be increased to reach close to 1 with additional LVs, but very often this leads to an increase in RMSE and model overfitting. set.

The goodness of the prediction was evaluated with the a set of performance indicators: the R^2 value describing the amount of the variance explained by the model, the root mean square error of prediction RMSEP, the bias describing the mean error (Esbensen and Swarbrick, 2018), the ratio of performance to interquartile range IQR (RPIQ), which is calculated as the fraction of the interquartile range of the laboratory data (Q3-Q1, quantifying the spread of the central 50% of the data) and the RMSEP (RPIQ=IQR/RMSEP) (Bellon-Maurel et al., 2010; O'Rourke et al., 2016) and the ratio of performance to deviation RPD, which is calculated as the fraction of the standard deviation of the laboratory data (SD) and the RMSEP (RPD=SD/RMSEP) (Chang et al., 2001). The last two indicators are used in spectroscopic literature to make data more comparable, accounting for the differences in the spread of the data. Their explanatory power to classify the model performance is the same as the R^2 (Minasny and McBratney, 2013), but useful to compare datasets with different spreads of data, with the advantage of the RPIQ being able to handle skewed data (Bellon-Maurel et al., 2010).

4.1.4 Results and Discussion

4.1.4.1. Field/soil description

Five Great Soil Groups from the Irish Soil Information System (Simo et al., 2007) were represented in the data, with Luvisols and Brown Earths recorded at 21 and 12 fields, respectively. These soil types, especially Luvisols are generally favouring tillage operations (Blume et al., 2010). Other Great Soil Groups represented across the fields included Groundwater Gley (1 field), Surface Water Gley (2 fields), Brown Podzolic (2 fields) and Alluvial Soil (1 field).

The summary statistics of the laboratory values (see Table 11) show ranges of OM from 1.9 % to 10.2 %, of pH between 5 and 8.2 and LR from -10.5 to 10 t/ha, with the negative values meaning that the fields do not need lime to bring the pH to favourable levels. Field composites were described by four USDA texture classes: the majority of the fields were described as loam (18 fields) and sandy loam (16 fields), with clay loam being found in six fields and one field recorded as sandy clay loam.

Closer examination of the LR data showed that around 75% of the samples had a LR less than or equal than zero. Examining the pH values, around 60% of the samples had a pH value of 6.5 or higher (target value for cereals in tillage fields (The Fertilizer Association of Ireland, 2016)). In a report from the Professional Agricultural Analysis Group (Professional Agricultural Analysis Group, 2016) about soil analysis data from soil laboratories around the United Kingdom an average pH value for tillage samples (n= 64,000) of 6.73 was found. 40% had a pH value under the target value of 6.5. These values are in line with the findings of the current study. Consulting the database for soil fertility in Ireland in 2018 (Teagasc, 2018) the same behaviour is visible, with 65% of the samples from tillage being above pH 6.5. For liming advice the negative values are simply reported as “no LR”, but in this research the actual values will be used as they are measuring a response to the SMP buffer, and hence it will increase the range of the calibration.

Table 11 Summary statistics for the laboratory values of OM (loss on ignition), pH (water) and LR (SMP) and texture classes by field

	OM [%]	pH	LR [t/ha]	Texture by field		
				USDA texture class	**n (fields)**	**%**
min	2.0	5.0	-10.5			
max	10.2	8.2	10.0	sandy loam	16	39%
average	5.8	6.6	-3.0	loam	18	44%
median	5.6	6.6	-2.5	clay loam	6	15%
range	8.3	3.2	20.5	sandy clay loam	1	2%

4.1.4.2. Calibration

Examples of raw spectra for three fields with maximum, minimum and zero LR are presented in Figure 12 with regions of known absorptions of soil parameters indicated in the graph.

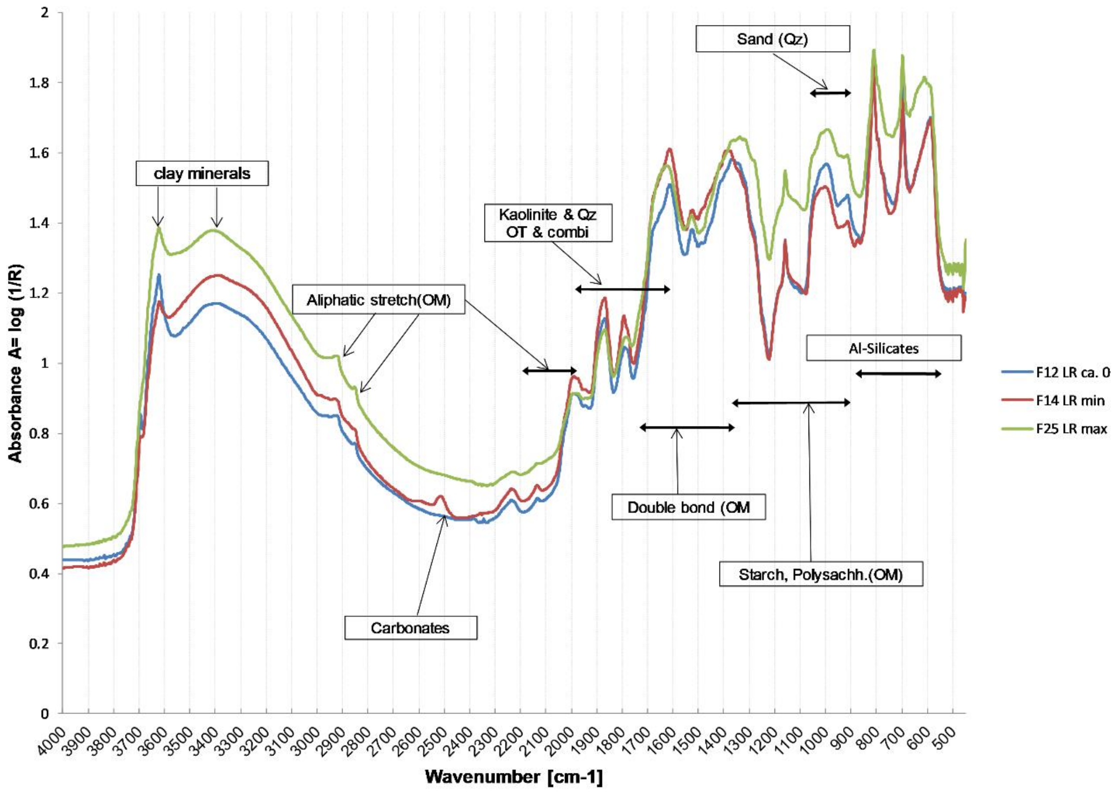

Figure 12 Raw spectra for minimum, maximum and zero lime requirements with regions of known absorption indicated

Spectral pre-treatment for the best calibration consisted of trimming the spectra at 650 cm^{-1}, Savitzky-Golay smoothing (polynomial order: 2, smoothing window: 11 points) and SNV. Using 6 LVs, the model produced an R^2 of 0.87, a root mean squared error of cross validation (RMSECV) of 1.55 t/ha, a bias of 0.01 and a RPIQ of 5.1. No considerable improvement in adding more latent variables after LV6 was achieved, and further addition of LVs would over-fit the model. The pre-treatment of the spectra improved the model performance considerably, R^2 was increased from 0.75 to 0.87 while the RMSECV decreased from >2 to 1.55 t/ha using the same number of LVs. The number of LVs was considerable lower than the eleven described by Viscarra Rossel et al. (2001). In their calibration they could reach an RMSE of 0.6 t/ha which is considerable lower than that in the present study. This can be explained by the fact that they used 122 samples from one field, while our study encompassed 41 fields and only 16 points per field.

In addition to the subdivision of the full dataset into calibration and validation (by field), it was also grouped by texture class, to examine its effect on the model performance. The only sandy clay loam field was re-assigned to the group of sandy loam (n= 271). This decision is justified, as the sandy clay loam sample contains 20.5% clay, which is only 0.5% above the threshold between sandy loam and clay loam.

The other two groups were loam (n=288) and clay loam (n=96). From the sandy loam and the loam datasets, 25% of the samples (in this case randomly selected from the 271 and 288 data points respectively), were held back for validation, while the clay loam dataset was only modeled with cross-validation due to the lower number of samples.

Using the same pre-treatment options, the subsets by texture class didn't show considerable improvements in the model, conversely, the number of LVs increased to 7 for the sandy loam subset, to 8 for the loam subset, and to 10 for the cross-validated clay loam subset. The R^2 was with 0.91 slightly higher for the loam subset, for sandy loam and clay loam they were slightly lower with 0.83 and 0.81 respectively. For the RMSECV, the subsets showed lower values with 1.51 t/ha for the sandy loam subset and 1.26 t/ha for the loam subset. The clay loam subset exhibited with 0.86 t/ha a considerably lower value than the rest. This pattern wasn't displayed in the RPIQs, which were all lower than the value for the entire dataset, ranging from 4.4 for the loam subset to 3.0 for the clay loam subset. The different behaviour of RMSECV and RPIQ shows that more than one statistical measure has to be used to assess the model performance (Hutengs et al., 2019).

Spectral scores and loading weights provided some insight into the drivers behind the calibration model. Figure 13a shows the scores grouped by texture class for LV1 vs. LV2. Here a clear trend in clay content can be seen to be positively correlated with LV1. Taking the loading weight for LV I into consideration (Figure 14), this connection between clay content and LV1 is seen in strong positive peaks in areas where absorptions for clay have been recorded in previous studies (Janik et al., 1998; Nocita et al., 2015; Soriano-Disla et al., 2014; Stenberg and Viscarra Rossel, 2010; Vohland et al., 2014). LV1 describes 46 % of the variance in the laboratory dataset and 69% in the spectra respectively, therefore representing half of the variance in the model compared to LV2 (20% of laboratory variance and 4% of spectral variance explained).

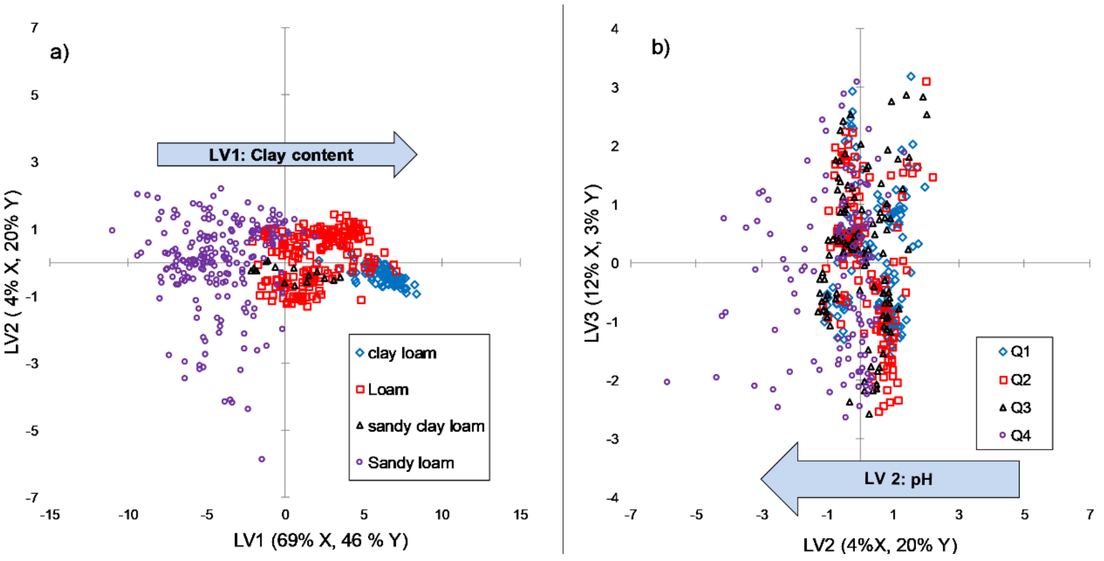

Figure 13 Score plots of a) LV1 vs. LV2, grouped by texture class and b) LV2 vs. LV3 grouped by quartiles of pH

The discrepancy in variance described for LV2 could be also linked to the strong peak in the loading weights for LV2 at 1320 cm^{-1}, a waveband where no distinct absorptions for soils have been reported in the literature. It can be linked to an absorbing feature of carbonates (1295 cm^{-1}) (Bruckman and Wriessnig, 2013) or silica which was distorted by specular reflectance (1360 cm^{-1}) (Reeves et al., 2005)This peak falls into a region where generally complex OM absorbs IR radiation, but inspecting LV2 in the score plot for OM didn´t show clear trends. Interestingly this distinct peak is also visible in Viscarra Rossel et al. (2001), once as negative valley for LV1 and positive peak in LV3. By examining the plot grouped by pH (pH laboratory values split into the four quartiles Q1-Q4, Figure 13b), a slight negative correlation was observed, pointing to the pH value influencing the second LV. The loading weights for LV2 (Figure 15) were described by positive peaks for 2:1 clay minerals associated with higher CEC than kaolinite (Blume et al., 2010) and a negative peak for carbonates

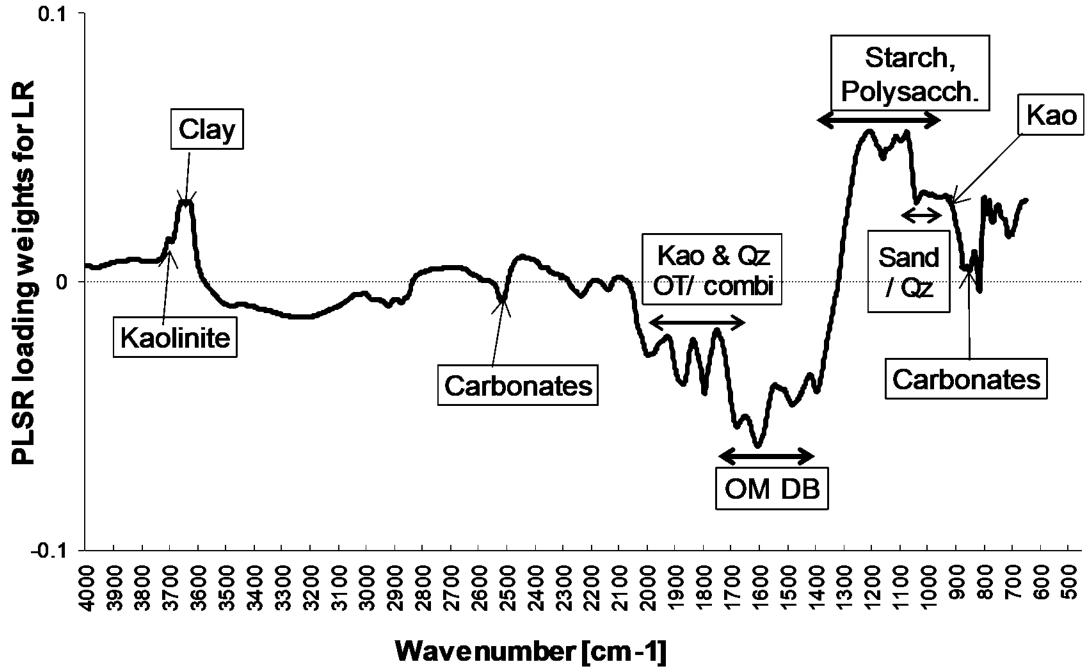

Figure 14 Loading weights for LV1 with peaks for various soil components highlighted (Kao: kaolinite, Qz: quartz, OT: overtones, combi: combination bands, OM DB: organic matter double bonds)

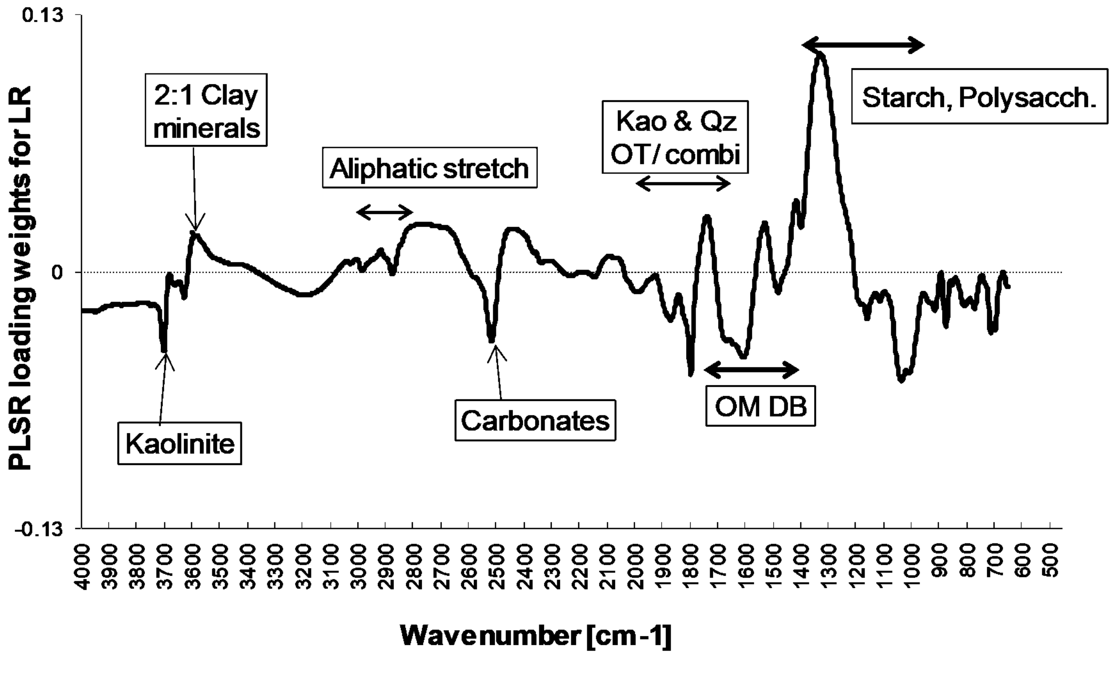

Figure 15 Loading weights for LV2 with peaks for various soil components highlighted (Kao: kaolinite, Qz: quartz, OT: overtones, combi: combination bands, OM DB: organic matter double bonds)

4.1.4.3. Validation - Total dataset and single field prediction

The model was applied to the data retained for validation, which was compiled as a single dataset of 160 samples, and also as a field database using ten fields with 16 samples per field retained for field scale validation. The results of the prediction are displayed in Table 12, with the entire prediction set producing a R^2 of 0.76, an RMSEP of 1.68 t/ha and an RPIQ of 3.58.

The R^2 decreased considerably compared to the result of 0.87 in the calibration set, while the RMSEP didn't increase to the same extent. The values for the predictions of the single fields are in Table SI1 and varied with R^2 between <0.2 to 0.72, RMSEP from 3.22 to 0.74 t/ha LR, and for RPIQ from 0.4 to 3.6. The fields with the best performance were field 5 and field 40, whereas field 8, 21 and 33 have very low R^2 and RPIQ, and very high RMSEP values. The predicted vs. reference plot for all fields of the prediction set is displayed in Figure 16.

Table 12 Summary stats and prediction results with the coefficient of determination (R^2), root mean square error of prediction (RMSEP/CV) or cross-validation, standard error of prediction or cross-validation (SEP/CV) bias, the ratio of performance to IQR (RPIQ=IQR/RMSE), the ratio of performance to deviation RPD (RPD=SD/RMSE), model bias and the number of latent variables used by the model for overall calibration and validation set and calibration and validation grouped by texture class

	Calibration all	Validation all	Sandy Loam cal	Sandy Loam val	Loam cal	Loam val	Clay Loam (Xval)
			Summary statistics (lab)				
n	459	160	203	68	216	72	69
Q1	-7.0	-7.0	-8.3	-8.5	-4.5	-4.5	-1.1
Q3	0.9	-1.0	-2.5	-3.0	1.0	1.0	1.5
min	-10.5	-9.5	-10.5	-10.0	-9.5	-9.0	-4.0
max	10.0	4.0	5.5	1.0	10.0	8.0	4.5
median	-2.0	-3.5	-6.0	-6.0	-1.5	-1.5	0.0
SD	4.3	3.4	3.7	3.3	4.2	3.6	1.9
range	20.5	13.5	16.0	11.0	19.5	17.0	8.5
IQR	7.9	6.0	5.8	5.5	5.5	5.5	2.6
			Model Performances				
R^2	0.87	0.76	0.83	0.86	0.91	0.85	0.81
RMSEP/CV	1.55	1.68	1.51	1.22	1.26	1.40	0.86
SEP/CV	1.56	1.68	1.51	1.22	1.26	1.40	0.86
Bias	0.01	0.05	0.018	0.015	0.015	-0.145	-0.04
LVs	6	6	7	7	8	8	10
RPIQ	5.08	3.58	3.81	4.51	4.37	3.93	3.05
RPD	2.79	2.06	2.46	2.73	3.30	2.56	2.26

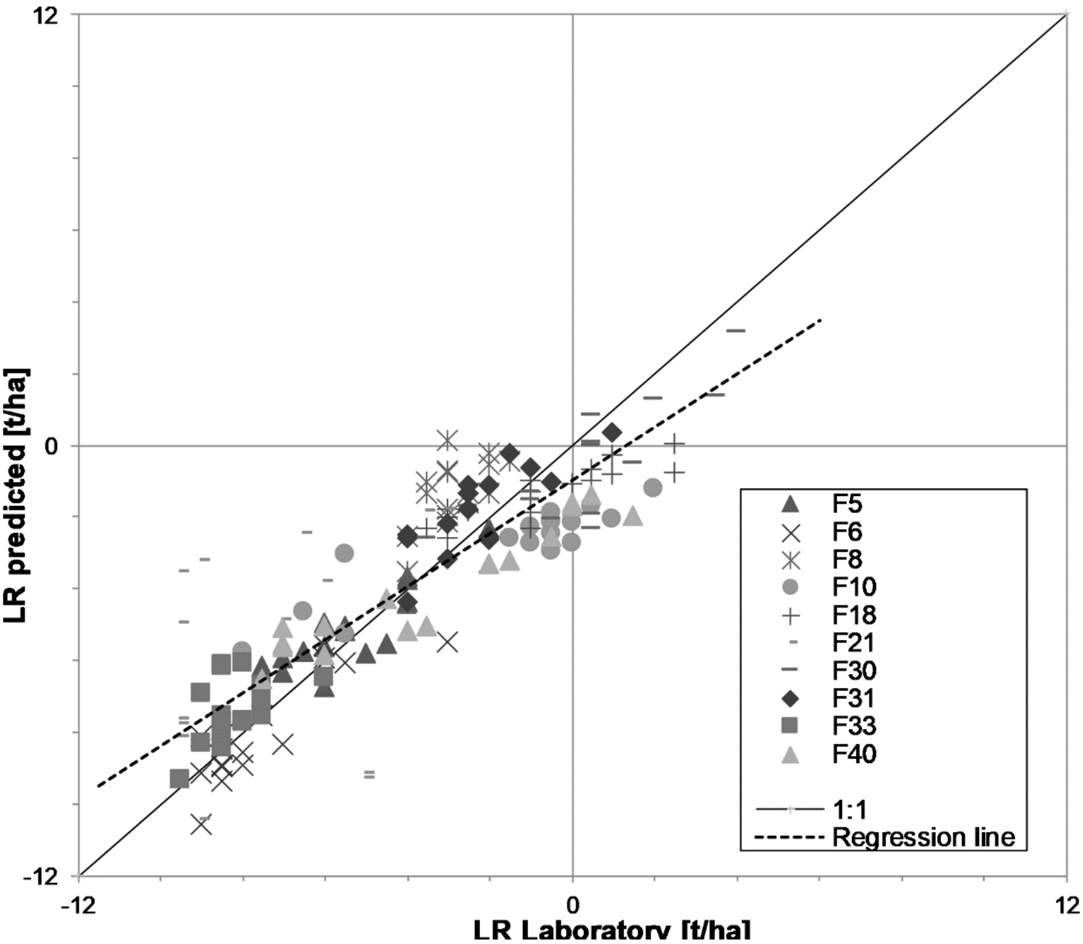

Figure 16 Laboratory LR (SMP) vs. predicted (MIR) values of the prediction set, marked by field and overall R^2 and RMSEP

4.1.4.4. Validation - Prediction for subsets by texture class

The prediction of the validation subsets for sandy loam and loam were better compared to prediction derived from the entire dataset. For the sandy loam subset, the R^2 of 0.86 was higher than in the calibration subset (0.83), for the loam subset it was with 0.85 still higher than the overall prediction R^2 of 0.76. The RMSEs were in the same order of magnitude as in the whole prediction with 1.22 t/ha for the sandy loam and 1.40 for the loam subset respectively. These slightly better performance indicators come at the cost of one and two more LVs, making the model less parsimonious. Regarding the relative model performance indicator RPIQ, the sandy loam subset with RPIQ 4.5 showed a higher value than its calibration set, whereas the loam subset performed slightly worse with 3.9. Compared to the entire validation set both subsets performed better.

The slight improvement of the model parameters when subdividing the dataset by texture class, in conjunction with the increased number of LVs indicates that there would be no significant gain in information by testing the sample for texture class first and applying texture-specific models.

The prediction statistics presented here are in a similar range reported by Janik et al. (1998) and Merry and Janik (1999) for a data set for 180 Australian soils where LR was predicted from land uses and soil types. The soils in our study are all from the same land use, and LR values are typical for tillage soils in Ireland (Teagasc, 2018) and the United Kingdom (Professional Agricultural Analysis Group, 2016).

To investigate the accuracy of the spectral calibrations for use as an alternative to the current laboratory SMP method the predicted values for each field (16 samples per field) were used to calculate a field average. This average was compared to the average of the laboratory values. The results in Table 13 show the difference between MIR predictions and laboratory values from 0.25 t/ha LR in field 5 up to 1.5 t/ha for field 8.

4.1.4.5. Model performance indicators

The RPIQ (as well as the RPD) are widely used in soil spectroscopy and various classifications are applied to categorize model performance into “good” and “bad”. The thresholds for the classes often vary among different authors, and all attempts give arbitrary thresholds (Minasny and McBratney, 2013). However, these parameters are used to describe the relationship between the spread of the data (be it SD or IQR) and the error of prediction. Hence, an RPIQ of 2 describes a prediction, where the error of prediction is half of the spread of 50% of the data around the median. To examine the predictive power of the MIR models at single field scale and to get a better grasp of the desired precision of the model, an additional performance parameter was used. It calculates the ratio of the range of the whole dataset to the error including a 95% confidence interval l(Esbensen and Swarbrick, 2018; Naes et al., 2004) with an equation similar to the RER (RER=range/RMSE) (Fearn, 2002) which results in the following equation

$$(\text{max-min})/2*\text{RMSE}. \qquad (41)$$

This approach quantifies the prediction uncertainty as well as the desired level of accuracy and is useful when a number of samples was taken and their average is formed, as it is the case in the single field predictions. With this parameter it can be evaluated if the predicted value with the confidence interval lies within the spread of the laboratory data. If the value is >1 it indicates, that the spread of the lab dataset is bigger than the prediction interval, justifying the use of predicted values. As displayed in Table 13, the parameter shows that, in the case of the predicted validation fields a spectral prediction is justified.

Table 13 Field averages for laboratory and predicted LR and the difference between the two methods and the range/2*RMSE as a metric for the precision of the prediction

Field #	Average LR lab [t/ha] ± SD	Average LR prediction [t/ha]	Difference Laboratory-prediction (abs)	Range/2*RMSE
5	-5.44 ± 1.4	-5.19	0.25	2.02
6	-7.53 ± 1.6	-8.02	0.49	2.85
8	-2.84 ± 0.7	-1.34	1.50	2.09
10	-1.72 ± 2.9	-2.86	1.14	10.58
18	-0.69 ± 1.9	-1.36	0.67	4.34
21	-7.50 ± 2.3	-6.06	1.44	10.46
30	-0.06 ± 2.2	-0.98	0.92	5.63
31	-2.22 ± 1.3	-1.86	0.36	2.27
33	-8.19 ± 0.8	-7.38	0.81	2.07
40	-3.41 ± 3.0	-4.00	0.60	7.43

4.1.4.6. Implications on current practices of LR determinations

Current practice of lime application on farms, required applications of lime every five years, mostly spread in one blanket application where rates are often based on estimates from crop offtakes and fertilizer application (0.2 t/ha lime per 100 kg nitrogen fertilizer applied, 15 kg lime/ t cereal offtake) (The Fertilizer Association of Ireland, 2016). Taking into consideration the variability of LR in a field (see Table 12) and the current blanket application of lime, the alternative MIR derived LR based on averages is a faster and safer alternative at this level of accuracy to current methods using potassium chromate (SHVC). Figure 17 visualizes the precision of the average on the example of one field.

The SMP buffer LR has been compared with other methods in the USA (Sikora buffer, $Ca(OH)_2$ titration, Mehlich buffer) and the UK (RothLime model), and Tunney et al. (2010) reported R^2 values between SMP LR and similar methods ranging from 0.7 to 0.84. The MIR prediction provided a value for R^2 of 0.76 for the entire prediction set, which lies in the range of values comparing laboratory-based tests, indicating that the MIR model is as good as the laboratory alternatives at replacing the SMP extraction for future LR measurements.

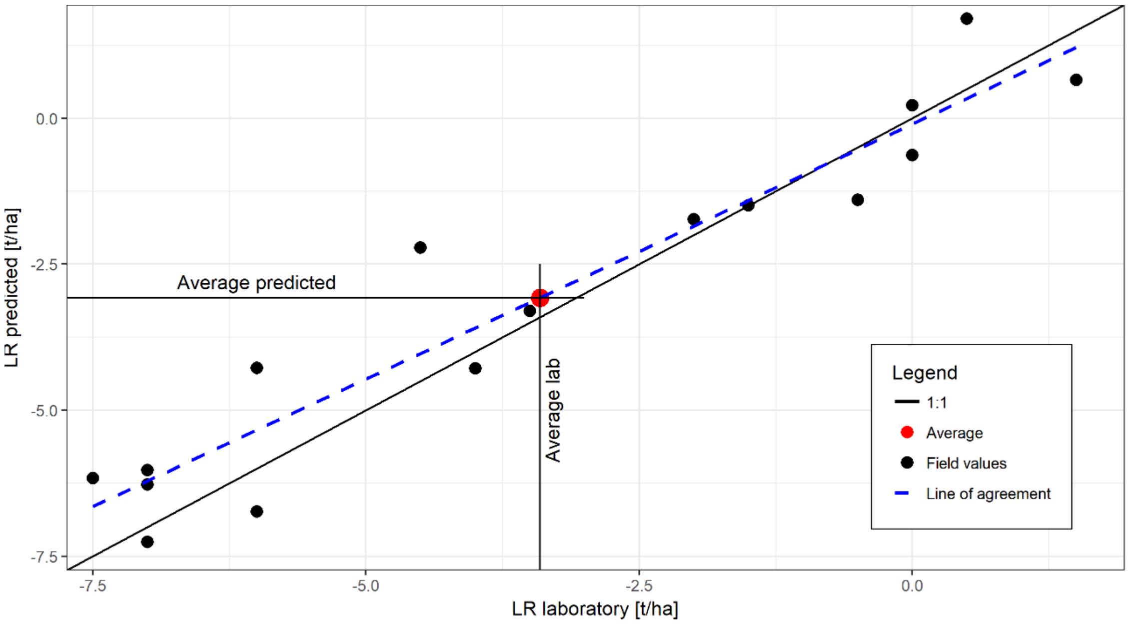

Figure 17 Calculated LR averages from laboratory and MIR predicted values for field 40

Merry et al. (Merry and Janik, 1999) used the predicted LR to derive a LR map of an area of 50 x 50 km. For field sizes of 2-37 ha as in our research, the accuracy of the prediction isn't precise enough (yet). But the potential for predicting other soil parameters (e.g. particle size, OM, pH, CEC) with the same MIR scan offers an opportunity for future applications. As it can be seen in the loading weights (Figures 14&15), there are clear signals for components which are influencing the LR, whih means that the MIR spectrum indeed can be used to predict LR.

4.1.5 Conclusions

Soil samples from tillage fields in Ireland were analysed for LR with the SMP buffer method in the laboratory and a spectral calibration with PLSR was developed from MIR scans of the samples. By examining the loading weights, clear signals for soil parameters influencing the LR could be found as drivers for the model. This shows that MIR spectroscopy is capable of detecting the LR in soils. With an RMSEP of 1.68 t/ha the precision of the PLSR model is not sufficient to predict the spatial variability of LR within the field for most single field predictions. When the prediction values for one field are averaged, the results lie close to the laboratory averages. This indicates that MIR spectroscopy can be used to estimate an average LR as a substitute for the SMP buffer method, and with future research it can be optimized to be used in precision agriculture. This study forms the basis for a fast and cheap substitute for lab analyses of LR, especially as information about other important soil parameters are contained in the same spectrum, which can be predicted simultaneously.

4.1.6 Acknowledgements

This research was funded by the Teagasc Walsh Fellowship Fund (RMIS 6837) and the Department for Agriculture Food and the Marine ICT AGRI ERANET-CTF Optimove project (15/ICTAGRI 2). The authors are grateful for the help of the laboratory staff and summer students in Teagasc Johnstown Castle in processing the samples.

4.1.7 Supplementary Information

SI 1 Summary statistics and model performances for the prediction of the fields (F: field number) selected for validation

	F5	F6	F8	F10	F18	F21	F30	F31	F33	F40
	Summary statistics (lab)									
n	16	16	16	16	16	16	16	16	16	16
Q1	-6.5	-8.5	-3.1	-2.5	-2.6	-9.5	-1.3	-3.0	-8.5	-6.3
Q3	-4.4	-6.8	-2.4	0.0	0.6	-5.8	0.8	-1.9	-7.9	-0.4
min	-7.5	-9.0	-4.0	-8.0	-3.5	-9.5	-4.0	-4.0	-9.5	-7.5
max	-2.0	-3.0	-1.5	2.0	2.5	-3.0	4.0	1.0	-6.0	1.5
median	-5.8	-8.3	-3.0	-0.5	-1.0	-9.0	0.5	-2.3	-8.5	-3.8
SD	1.4	1.6	0.7	2.9	1.9	2.3	2.2	1.3	0.8	3.0
range	5.5	6.0	2.5	10.0	6.0	6.5	8.0	5.0	3.5	9.0
IQR	2.1	1.8	0.8	2.5	3.3	3.8	2.0	1.1	0.6	5.9
	Model performances									
R^2	0.72	0.65	0.34	0.45	0.41	0.11	0.59	0.50	0.18	0.70
RMSEP/CV	0.74	0.95	1.67	2.12	1.45	3.22	1.41	0.91	1.18	1.65
SEP/CV	0.88	0.84	3.19	1.84	1.32	4.20	1.10	1.14	1.90	1.59
Bias	0.25	-0.49	1.50	-1.14	-0.67	1.40	-0.92	0.36	0.81	-0.60
LVs	6	6	6	6	6	6	6	6	6	6
RPIQ	2.89	1.85	0.45	1.18	2.25	1.17	1.42	1.24	0.53	3.56
RPD	1.91	1.69	0.42	1.35	1.30	0.71	1.55	1.42	0.67	1.84

4.1.8 References

Adams, F., Evans, C.E., 1962. A Rapid Method for Measuring Lime Requirement of Red-Yellow Podzolic Soils1. Soil Sci. Soc. Am. J. 26, 355. doi:10.2136/sssaj1962.03615995002600040015x

Barak, P., Jobe, B.O., Krueger, A.R., Peterson, L.A., Laird, D.A., 1997. Effects of long-term soil acidification due to nitrogen fertilizer inputs in Wisconsin. Plant Soil 197, 61–69. doi:10.1023/A:1004297607070

Barnes, R.J., Dhanoa, M.S., Lister, S.J., 1989. Standard normal variate transformation and de-trending of near-infrared diffuse reflectance spectra. Appl. Spectrosc. 43, 772–777. doi:10.1366/0003702894202201

Bellon-Maurel, V., Fernandez-Ahumada, E., Palagos, B., Roger, J.M., McBratney, A.B., 2010. Critical review of chemometric indicators commonly used for assessing the quality of the prediction of soil attributes by NIR spectroscopy. TrAC - Trends Anal. Chem. 29, 1073–1081. doi:10.1016/j.trac.2010.05.006

Blume, H.-P., Brümmer, G.W., Horn, R., Kandeler, E., Kögel-Knabner, I., Kretzschmar, R., Stahr, K., Wilke, B.-M., 2010. Scheffer/Schachtschabel: Lehrbuch der Bodenkunde, 16th ed. Springer-Verlag, Heidelberg.

Bruckman, V.J., Wriessnig, K., 2013. Improved soil carbonate determination by FT-IR and X-ray analysis. Environ. Chem. Lett. 11, 65–70. doi:10.1007/s10311-012-0380-4

Chang, C.-W., Laird, D.A., Mausbach, M.J., Hurburgh, C.R., 2001. Near-Infrared Reflectance Spectroscopy–Principal Components Regression Analyses of Soil Properties. Soil Sci. Soc. Am. J. 65, 480–490. doi:10.2136/sssaj2001.652480x

Demattê, J.A.M., Dotto, A.C., Bedin, L.G., Sayão, V.M., Souza, A.B. e., 2019. Soil analytical quality control by traditional and spectroscopy techniques: Constructing the future of a hybrid laboratory for low environmental impact. Geoderma 337, 111–121. doi:10.1016/j.geoderma.2018.09.010

Department for Environment Food and Rural Affairs, 2010. Fertiliser Manual RB209, 8th ed. The Stationery Office.

ECHA (European Chemicals Agency), 2010. Member state committee support document for identification of potassium chromate as a substance of very high concern because of its cmr properties. SVHC Support Doc. 1–27.

Engel, J., Gerretzen, J., Szymańska, E., Jansen, J.J., Downey, G., Blanchet, L., Buydens, L.M.C., 2013. Breaking with trends in pre-processing? TrAC - Trends Anal. Chem. 50, 96–106. doi:10.1016/j.trac.2013.04.015

Esbensen, K.H., Swarbrick, B., 2018. Multivariate Data Analysis, 6th ed. Camo Software AS, Oslo, Magnolia TX.

FAO, 2017. Voluntary Guidelines for Sustainable Soil Management, 155th session of the FAO Council, Rome, Italy, 5th December 2016. Rome. doi:10.1007/978-3-319-68885-5_3

FAO, 2009. Global agriculture towards 2050. Rome.

Fearn, T., 2002. Assessing calibrations: SEP, RPD, RER and R2. NIR news 13, 12. doi:10.1255/nirn.689

Gee, G.W., Bauder, J.W., 1986. Particle-size Analysis·, in: Klute, A. (Ed.), Methods of Soil Analysis. Part 1. Physical and Mineralogical Methods. pp. 383–411.

Geladi, P., MacDougall, D., Martens, H., 1985. Linearization and Scatter-Correction for Near-Infrared Reflectance Spectra of Meat. Appl. Spectrosc. 39, 491–500. doi:10.1366/0003702854248656

Goulding, K.W.T., 2016. Soil acidification and the importance of liming agricultural soils with particular reference to the United Kingdom. Soil Use Manag. 32, 390–399. doi:10.1111/sum.12270

Hutengs, C., Seidel, M., Oertel, F., Ludwig, B., Vohland, M., 2019. In situ and laboratory soil spectroscopy with portable visible-to-near-infrared and mid-infrared instruments for the assessment of organic carbon in soils. Geoderma 355, 113900. doi:10.1016/j.geoderma.2019.113900

Janik, L.J., Merry, R.H., Skjemstad, J.O., 1998. Can mid infrared diffuse reflectance analysis replace soil extractions? Aust. J. Exp. Agric. 38, 681–696. doi:10.1071/EA97144

Karlen, D.L., Mausbach, M.J., Doran, J.W., Cline, R.G., Harris, R.F., Schumann, G.E., 1997. Soil Quality: A Concept, Definition, and Framework for Evaluation. Soil Sci. Soc. Am. J. 61.

Kissel, D.E., Isaac, R.A., Hitchcock, R., Sonon, L.S., Vendrell, P.F., 2007. Implementation of soil lime requirement by a single-addition titration method. Commun. Soil Sci. Plant Anal. 38, 1341–1352. doi:10.1080/00103620701328735

Massey, P., O'Connor, C., Sills, P., Fenelon, A., Maloney-Finn, L., Stone, D., Reidy, B., Creamer, R., 2007. Irish Soil Information System: Laboratory Standard Operating Procedures. Environmental Protection Agency, Wexford.

McLean, E.O., 1982. Soil pH and lime requirement, in: Methods of Soil Analysis. Part 2. Chemical and Microbiological Properties. American Society of Agronomy, Soil Science Society of America, pp. 199–224.
McLean, E.O., 1970. Lime requirements of soils—inactive toxic substances or favorable pH range? Soil Sci. Soc. Am. J. 34, 363–364.
McLean, E.O., Dumfohd, S.W., Coronel, F., Dumford, S.W., Coronel, F., 1966. A Comparison of Several Methods of Determining Lime Requirements of Soils. Soil Sci. Soc. Am. J. 30, 26–30.
Mehlich, A., 1976. New buffer ph method for rapid estimation of exchangeable acidity and lime requirement of soils. Commun. Soil Sci. Plant Anal. 7, 637–652. doi:10.1080/00103627609366673
Merry, R.H., Janik, L.J., 1999. New Methodology for Lime Requirements. Barton, ACT, Kingston ACT.
Minasny, B., McBratney, A.B., 2013. Why you don ’ t need to use RPD. Pedometron 33, 14–15.
Naes, T., Isaksson, T., Fearn, T., Davies, T., 2004. A User-friendly Guide to Multivariate Calibration and Classification. NIR Publications, Chichester, UK.
Nocita, M., Stevens, A., van Wesemael, B., Aitkenhead, M., Bachmann, M., Barthes, B., Ben Dor, E., Brown, D.J., Clairotte, M., Csorba, A., Dardenne, P., Dematte, J.A.M., Genot, V., Guerrero, C., Knadel, M., Montanarella, L., Noon, C., Ramirez-Lopez, L., Robertson, J., Sakai, H., Soriano-Disla, J.M., Shepherd, K.D., Stenberg, B., Towett, E.K., Vargas, R., Wetterlind, J., 2015. Soil Spectroscopy: An Alternative to Wet Chemistry for Soil Monitoring. Adv. Agron. 132, 139–159. doi:10.1016/bs.agron.2015.02.002
O’Rourke, S.M., Stockmann, U., Holden, N.M., McBratney, A.B., Minasny, B., 2016. An assessment of model averaging to improve predictive power of portable vis-NIR and XRF for the determination of agronomic soil properties. Geoderma 279, 31–44. doi:10.1016/j.geoderma.2016.05.005
Professional Agricultural Analysis Group, 2016. Collation of data from routine soil analysis in the UK.
Reeves, J.B., 2010. Near- versus mid-infrared diffuse reflectance spectroscopy for soil analysis emphasizing carbon and laboratory versus on-site analysis: Where are we and what needs to be done? Geoderma 158, 3–14. doi:10.1016/j.geoderma.2009.04.005
Reeves, J.B., Francis, B.A., Hamilton, S.K., 2005. Specular reflection and diffuse reflectance spectroscopy of soils. Appl. Spectrosc. 59, 39–46. doi:10.1366/0003702052940431
Rinnan, Å., van den Berg, F., Engelsen, S.B., 2009. Review of the most common pre-processing techniques for near-infrared spectra. TrAC - Trends Anal. Chem. 28, 1201–1222. doi:10.1016/j.trac.2009.07.007
Savitzky, A., Golay, M.J.E., 1964. Smoothing and Differentiation of Data by Simplified Least Squares Procedures. Anal. Chem. 36, 1627–1639. doi:10.1021/ac60214a047
Sherman Hsu, C.-P., 1997. Infrared Spectroscopy, in: Settle, F.A. (Ed.), Handbook of Instrumental Techniques for Analytical Chemistry. Prentice Hall PTR, New Jersey, pp. 247–283.
Shoemaker, H.E., McLean, E.O., Pratt, P.F., Peatt, P.F., 1961. Buffer Methods for Determining Lime Requirement of Soils With Appreciable Amounts of Extractable Aluminum. Soil Sci. Soc. Am. J. 25, 274–277. doi:10.2136/sssaj1961.03615995002500040014x
Sikora, F.J., 2006. A buffer that mimics the smp buffer for determining lime requirement of soil. Soil Sci. Soc. Am. J. 70, 474–486. doi:10.2136/sssaj2005.0164

Simo, I., Creamer, R.E., Massey, G., Hamilton, P., Mcdonald, J.A., 2007. EPA STRIVE Programme 2007-2013 Irish Soil Information System Soil Profile Handbook.

Soriano-Disla, J.M., Janik, L.J., Viscarra Rossel, R.A., MacDonald, L.M., McLaughlin, M.J., 2014. The Performance of Visible, Near-, and Mid-Infrared Reflectance Spectroscopy for Prediction of Soil Physical, Chemical, and Biological Properties. Appl. Spectrosc. Rev. 49, 139–186. doi:10.1080/05704928.2013.811081

Sparks, D.L., 2003. 9 - The Chemistry of Soil Acidity, in: Sparks, D.L. (Ed.), Environmental Soil Chemistry (Second Edition). Academic Press, Burlington, pp. 267–283. doi:https://doi.org/10.1016/B978-012656446-4/50009-8

Stenberg, B., Viscarra Rossel, R.A., 2010. Diffuse Reflectance Spectroscopy for High-Resolution Soil Sensing, in: Viscarra Rossel, A.R., McBratney, B.A., Minasny, B. (Eds.), Proximal Soil Sensing. Springer Netherlands, Dordrecht, pp. 29–47. doi:10.1007/978-90-481-8859-8_3

Teagasc, 2018. Teagasc Soil Analysis Status and Trends.

Tekin, Y., Kuang, B., Mouazen, A.M., 2013. Potential of on-line visible and near infrared spectroscopy for measurement of pH for deriving variable rate lime recommendations. Sensors (Switzerland) 13, 10177–10190. doi:10.3390/s130810177

The Fertilizer Association of Ireland, 2016. Soil pH & Lime, Technical Bulletin.

Thomas, G.W., Hargrove, W.L., 1984. The Chemistry of Soil Acidity, in: Adams, F. (Ed.), Soil Acidity and Liming, Agronomy Monograph 12. ASA, CSSA, SSSA, Madison, WI.

Tunney, H., Sikora, F.J., Kissel, D., Wolf, A., Sonon, L., Goulding, K., 2010. A comparison of lime requirements by five methods on grassland mineral soils in Ireland. Soil Use Manag. 26, 126–132. doi:10.1111/j.1475-2743.2010.00263.x

Viscarra Rossel, R.A., McBratney, A.B., 2001. A response-surface calibration model for rapid and versatile site-specific lime-requirement predictions in south-eastern Australia. Aust. J. Soil Res. 39, 185–201. doi:10.1071/SR99131

Viscarra Rossel, R.A., Walvoort, D.J.J., MacBratney, A.B., Janik, L.J., Skjemstad, J.O., 2001. Proximal sensing of soil pH and lime requirement by mid infrared diffuse reflectance spectroscopy, in: Third European Conference on Precision Agriculture (3 Ecpa): Proceedings. pp. 497–502.

Vohland, M., Ludwig, M., Thiele-Bruhn, S., Ludwig, B., 2014. Determination of soil properties with visible to near- and mid-infrared spectroscopy: Effects of spectral variable selection. Geoderma 223–225, 88–96. doi:10.1016/j.geoderma.2014.01.013

Wold, S., Sjostrom, M., Eriksson, L., 2001. PLS-regression: a basic tool of chemometrics. Chemom. Intell. Lab. Syst. 58, 109–130. doi:10.1016/S0169-7439(01)00155-1

4.2 From benchtop to handheld MIR for soil analysis: Predicting lime requirement and organic matter in agricultural soils.

This paper examined the application of handheld MIR for *in situ* sampling and analysis of agricultural soils. Here, a handheld MIR-DRIFTS instrument (Agilent 4300 handheld FTIR) was used to determine primary soil fertility metrics, specifically, lime requirement (LR) and organic matter (%OM) with calibrations derived from benchtop and from handheld spectra. To overcome the adverse effects of moisture on spectral predictions of LR and %OM, moisture correction spectra for seven different moisture classes were applied to soil samples under field conditions. Moisture corrected spectra predicted LR close to the laboratory values but only when corrections were applied to soil with initial moisture contents <15%GMC. Prediction of %OM using moisture correction was effective across all initial moisture categories, beginning with field moist samples, and predicted values came within 1% of laboratory, using field moist spectra. The examination revealed that calibrations created from the same type of spectra result in better predicted values, and that correcting *in situ* spectra delivers better results and offers potential for future refinements.

Work for this paper was conducted to 90% by me, including fieldwork, laboratory analyses (partially), data exploration and evaluation, manuscript writing and editing. Part of the laboratory analyses were done by the staff of Teagasc, Johnstown Castle.

This paper was published with the following reference (chapter-, figure- and table-numbering adapted) :

Metzger, K., Zhang, C., Daly, K., 2021. From benchtop to handheld MIR for soil analysis: Predicting lime requirement and organic matter in agricultural soils. Biosyst. Eng. 204, 257–269. https://doi.org/10.1016/j.biosystemseng.2021.01.025

From benchtop to handheld MIR for soil analysis: Predicting lime requirement and organic matter in agricultural soils.

Konrad Metzger [a, b], Chaosheng Zhang [b], Karen Daly [a*]

[a] Environment, Soils and Land Use Department, Teagasc, Johnstown Castle Research Centre, Wexford, Y35 TC97, Republic of Ireland

[b] International Network for Environment and Health (INEH), School of Geography and Archaeology National University of Ireland, Galway, H91 CF50, Republic of Ireland

* Corresponding author email: Karen.Daly@teagasc.ie

4.2.1 Abstract

Recent development of handheld mid-infrared (MIR) spectrometers holds promising applications for soil analysis. However, problems arise due to water content and other *in situ* characteristics, and compatibility with existing spectral libraries and calibrations developed on benchtop instruments. This study examined the potential of handheld MIR for sampling and analysis of field fresh soils. A handheld MIR-DRIFTS instrument (Agilent 4300 handheld FTIR) was used to determine primary soil fertility metrics, specifically, lime requirement (LR) and organic matter (%OM). LR was predicted from handheld collected spectra using calibration models developed from (1) an existing benchtop spectral library and (2) a newly developed model using handheld spectra. Predictions of handheld spectra from the benchtop model exhibited a bias of 2.14 t/ha, however this was improved (-0.13 t/ha) when calibrating the model from spectra collected from the handheld instrument. To overcome the adverse effects of moisture on spectral predictions of LR and %OM, moisture correction spectra for seven different moisture classes were applied to soil spectra under field conditions. The moisture correction for the prediction of LR under field moist condition was partially successful and could correct for soils with moisture contents below the permanent wilting point. Prediction of %OM using moisture correction was effective across all moisture categories, and predicted values came within 1% of laboratory values. This research highlights the challenges of handheld MIR in the field, such as finding moisture corrections, practices for field spectra acquisition and the use of spectral libraries and serves as a starting point for future research.

Keywords

handheld MIR; DRIFTS; soil spectroscopy; lime requirement; organic matter; moisture correction

4.2.2 Introduction

The growing demand for more sustainable food production is putting pressure on agricultural producers to increase the efficiency of their operations, specifically nutrient use efficiency and soil quality. Traditional soil sampling to monitor chemical and physical properties is not at the resolution (spatial and temporal) required for precision applications and monitoring of soil quality indicators. Particular focus of efficiency improvements lies on the precise application of fertilizer as it is one of the highest direct costs on farms, and applying the correct rate benefits the farmer by optimising yield and protecting the environment by minimising fertilizer losses. The application of precision agriculture requires tailoring field applications to the needs of the soil and crop by moving from a single composite soil sample taken per field towards multiple sample locations across the entire field using proximal soil sensing methodologies (Janik, Soriano-Disla, Forrester, & McLaughlin, 2016; Stenberg, Viscarra Rossel, Mouazen, & Wetterlind, 2010). Recent studies have indicated that dividing arable fields into management zones (Metzger, Zhang, Ward, & Daly, 2020b) allows for improved soil fertility management where spatial differences in soil nutrients were evident. A broad range of technologies for soil sensing using the interaction of soil components with (electromagnetic) radiation is currently being researched. For a comprehensive overview over the technologies the readers are directed to Viscarra Rossel et al. (2011).

Soil spectroscopy was first developed using visible (vis) and near infrared (NIR) light sources (Ben-Dor & Banin, 1995; Dalal & Henry, 1986), but with the development of Fourier transform infrared spectrometers (FTIR), enabling smaller instruments and faster scanning times the mid-infrared (MIR) range has gained recognition for this application (Stuart, 2004). The MIR range (4000 to 400 cm^{-1}) offers advantages over the NIR range, in that, many fundamental absorptions of chemical bonds in soil parameters such as clay (O-H), organic matter (O-C, O=C, C-N) and quartz (Si-O) can be captured, while the NIR range is mainly characterized by broad overtone and combination absorptions which mask weak organic peaks and quartz cannot be picked up in NIR (Janik, Merry, & Skjemstad, 1998). By means of chemometric modelling and multivariate statistics, with partial least squares regression (PLSR) being the most accomplished technique (H. Wold, 1973; S. Wold, Sjostrom, & Eriksson, 2001), the information contained in the spectra can be decoded and related to laboratory values with chemometric models (Esbensen & Swarbrick, 2018; Martens & Næs, 1984). Apart from soil components which absorb in the MIR range, soil parameters which depend on spectrally active components such as particle size distribution (Minasny, McBratney, Tranter, & Murphy, 2008), aggregate size distribution (Madari et al., 2006), phosphorus sorption capacity (Dunne, Holden, O'Rourke, Fenelon, & Daly, 2020), pH and cation exchange capacity (Minasny et al., 2008; Soriano-Disla, Janik, Viscarra Rossel, MacDonald, & McLaughlin, 2014) can be predicted in this manner. Typically soil parameters are predicted from spectra collected with benchtop FTIR spectrometers (Janik et al., 1998; Nocita et al., 2015). Metzger, Zhang, Ward, and Daly (2020a) developed a MIR prediction of lime requirement (LR) as alternative to the Shoemaker- McLean- Pratt (SMP) buffer extraction using benchtop scanned spectra of arable soils. They found the sensitivity of the analysis (RMSE 1.55 t/ha) to be not sufficient for PA applications, however their analysis showed that this technique can be used as green chemistry alternative to the laboratory extractions on a composite sample per field basis. To advance the application of the MIR range in precision agriculture, portable, handheld FTIR spectrometers for *in situ* use together with improved sensitivity of the calibrations would provide high spatial and temporal resolution required for soil quality monitoring.

NIR spectrometers are relatively easy to minimize for use in a portable version as they usually don´t contain interferometers with moving parts, however, handheld MIR spectrometers are not as widely used, are more expensive, and have only recently become available. Their performance to predict dried and ground soil samples has been reviewed for example by Soriano-Disla, Janik, Allen, and McLaughlin (2017) as a comparative study of several portable infrared instruments, and the authors found, that MIR instruments using the full MIR range deliver similar results to the benchtop instrument. Several other studies used small, portable instruments as an alternative to benchtop instruments and found that, despite losses in signal to noise ratio, range and stability, these instruments especially in the MIR range offer a good alternative to benchtop analyses (Hutengs, Ludwig, Jung, Eisele, & Vohland, 2018; Hutengs, Seidel, Oertel, Ludwig, & Vohland, 2019; Martínez-España, Bueno-Crespo, Soto, Janik, & Soriano-Disla, 2019; Soriano-Disla et al., 2019). Calibrations directly based on the field moist spectra collected with a prototype MIR spectrometer with a limited spectral range delivered promising results, but with lower accuracy than the same samples measured dried and ground (Dhawale et al., 2015; Ji et al., 2016).

Another important factor to consider in the development of portable MIR instruments for soil sensing is, that MIR radiation is interacting with the soil moisture and causing distorted spectra due to specular reflectance and broad peaks of water absorption, which overlap weaker features (Janik et al., 2016), making the application of MIR spectroscopy on fresh soil samples more complicated than that of dried soils in the laboratory. The soil moisture, as well as other irregularities on the *in situ* samples in addition to other influences such as weather, lead to considerable distortions in the spectra, which renders it extremely complicated to compare scans from fresh samples with a spectral database usually built from dried and ground samples (Hutengs et al., 2019; Soriano-Disla et al., 2017).

Starting from visible and NIR spectra, where the influence of soil water, even though weaker than in MIR spectra, still caused problems with prediction, methodologies to remove the distorting influence of “*in situ* conditions” (Soriano-Disla et al., 2017) are being developed by several groups. Direct standardization (Ji, Viscarra Rossel, & Shi, 2015), grouping the samples by moisture content to eliminate the moisture contribution to the spectra (Mouazen, Karoui, De Baerdemaeker, & Ramon, 2006) and a truly chemometric approach, the external parameter orthogonalization (EPO) (Minasny et al., 2011; Roger, Chauchard, & Bellon-Maurel, 2003) are among the most used methods for NIR samples.

With the more accessible hardware (handheld FTIR spectrometer) and possible methodologies to tackle the problem of *in situ* conditions, research has started to explore the application of portable MIR soil spectroscopy. The first attempts in using portable MIR directly in the field developed predictions of C and N using different spectrometers and (IR) ranges in addition to three different soil states (field moist, dried and sieved, dried, sieved and finely ground), but they built separate calibrations for each instrument and soil state, which resulted in relatively good predictions of soil C content (Reeves, McCarty, & Hively, 2010). Hutengs et al. (2019) conducted a comparative study with the same handheld MIR spectrometer used in our study (Agilent FTIR 4300) to predict soil organic carbon. They scanned the soil directly in the field, built a calibration from the wet samples and compared the spectral predictions with those derived from dried and sieved samples as well as dried, sieved and finely ground samples. They found that the calibration derived from *in situ* scanned MIR spectra came to the same level of accuracy in terms of R^2 and RMSE as NIR calibrations from dried and dried and ground samples. The MIR calibration from dried and dried and ground samples showed better results, with the dried and ground samples delivering the best results.

In the presented studies for the use of handheld MIR spectrometers, separate calibrations were built for each type of scan. A knowledge gap exists for corrections for moisture and *in situ* characteristics like the ones described for vis-NIR spectra have, which not yet been applied to MIR spectra.

The overarching objective of this work is therefore to assess the application of handheld MIR for spectra collection directly in agricultural soils and the evaluation of methods to make the field spectra comparable to established spectral databases Essential soil parameters for efficient crop production such as lime requirement (LR, the amount of ground limestone needed to bring the pH of an agricultural field back to optimum levels for plant growth (Tunney et al., 2010)) and %organic matter (%OM) were selected in this study to:

1) evaluate the feasibility of benchtop calibrations to predict LR and %OM from spectra collected using a handheld spectrometer
2) evaluate data collection and spectral model calibration of fresh samples in the field

4.2.3 Methodology

To meet the objectives set out above, an existing soil archive alongside newly derived models and additional field sites were used in the study.

4.2.3.1 Overview of archieved samples and field sites used

The two main datasets which were used for this study are described in the following:

1. An archive and database of 160 topsoil samples with corresponding laboratory data and a benchtop-scanned spectral MIR library. The samples were collected on arable farms throughout the Republic of Ireland. The soils belong mostly to the Luvisol and the Brown Earth great groups of the Soil Information System of Ireland (Simo, Creamer, Massey, Hamilton, & Mcdonald, 2007), with 60% of the samples being in the USDA texture class sandy loam, 30% loam and 10% clay loam (NRCS, 2018).
2. Three agricultural field sites representing different soil texture classes, located on a commercial dairy farm in Ireland, used in an exploratory experiment to evaluate an in-field sampling strategy for fresh soil spectra. These sites were also used to develop a moisture correction methodology.

4.2.3.2 Laboratory reference data

For both the archive soils and field sites, laboratory analyses were run for %OM, pH and LR. %OM was determined by loss on ignition, where 5 g of soil were placed in a furnace at 500°C for 12h and the fraction of organic matter being defined as the difference in mass of raw and fired soil. For the pH analysis, 10 ml of soil were mixed with 20 ml of deionized water, after which the pH was analysed with a Mettler-Toledo

In-Lab Routine pH electrode. The LR, defined as the amount of lime needed to bring acidified soil back to a target pH of 6.5 is measured with the “Shoemaker, McLean and Pratt” (SMP) buffer method. For that, 10 ml of soil are extracted with 20 ml of the SMP buffer solution, and after the extraction, the pH of the buffer is measured and the LR is calculated from the difference between initial buffer pH and the pH after the soil extraction (McLean, 1982; Shoemaker, McLean, & Pratt, 1961). The particle size was analysed gravimetrically with the sieve-pipette method (Gee & Bauder, 1986)using composite samples from each farm. Each of the samples for the infield experiment was analysed with the same method.

For the field application dataset, field moist gravimetric water content was measured by taking three subsamples of the fresh soil, weigh them once field moist and once after drying the samples at 105°C for 48 hrs. The difference in mass between wet and dry in relation to the dry samples represents the gravimetric water content in %.

4.2.3.3 Spectral data acquisition

4.2.3.3.1 Archived soil samples

The archive of 160 dried and sieved topsoil samples was used in this study. Benchtop spectra from these samples were previously reported as the independent validation set from Metzger et al. (2020a) that describes a benchtop calibration in MIR for LR. The samples were scanned with a Perkin Elmer “Spectrum 400 FTIR” (Perkin Elmer Inc., Waltham, MA, USA) in diffuse reflectance mode in a range from 4000 cm^{-1} to 450 cm^{-1} with a 2 cm^{-1} resolution. The laboratory database accompanying this archive was used to test the compatibility of handheld and benchtop spectra in this current study. To examine the handheld spectra, we collected spectra from this archive using an “Agilent 4300 FTIR” (Agilent Technologies, Inc., Santa Clara, CA, USA) handheld spectrometer in the benchtop configuration fixed in a stand (Figure 18). Samples were loaded into a 10 mm stainless steel sample cup (part of the PIKE AutoDiff diffuse reflectance accessory of the benchtop instrument), smoothing the surface with a blade. This sample cup was placed under the handheld instrument and scanned with the following settings: full spectral range: 4000-650 cm^{-1}, 32 co-added background scans every 15 min, 32 co-added sample scans with a resolution of 4 cm^{-1} in diffuse reflectance mode (DRIFTS) with Happ-Gentzel apodization. The spectra are reported in Absorbance units (A=log(1/Reflectance)) as it is common in soil spectroscopy (Esbensen & Swarbrick, 2018; Sherman Hsu, 1997). The instrument was lowered onto the sample cup until the tip of the diffuse reflectance accessory was in close contact with the sample surface. Sufficient contact was established when the live view of the spectrum on the connected computer took the expected shape of a MIR soil spectrum. Every sample was scanned in three positions by turning the sample holder by 120°.

Figure 18 Scanning setup for the Agilent 4300 FTIR and the sampling template positioned in the soil pit

4.2.3.3.2 *In situ* scanning of fresh soil

To assess the feasibility of the handheld FTIR under field conditions a field sampling template was deployed to ensure consistent sampling (see Figure 18) to scan surface and sides of a shallow profile of fresh, loose soil, *in situ*.

Initial attempts using this set up were unsuccessful as the instrument failed to start recording. After several more attempts using this approach, we concluded that the soil water content and the roughness of the soil profile absorbed so much of the incident radiation that no reflectance could be detected. Further scoping experiments revealed that the spectrometer had to be fixed in the stand and the surface of the sample had to be smooth to be able to collect samples from field moist soils. This led to a revised sampling strategy described as *ex-situ* scanning.

4.2.3.3.3 *Ex-situ* scanning of fresh soil and moisture correction

Based on attempts to capture spectra in the field, a new sampling strategy for field conditions was devised: three replicate samples were taken from each of the three fields as described above and fresh soil was packed into small petri dishes filled to the surface, smoothed with the bottom of another petri dish. Each petri dish was returned to the lab and was scanned at three points in the dish, using the handheld instrument in the stand (in the benchtop configuration) to collect spectral replicates.

The settings on the handheld spectrometer allowed for 32 co-added scans in diffuse reflectance mode (DRIFTS, 4000-650 cm^{-1}) at a resolution of 4 cm^{-1} at each position in the petri-dish. Background readings were collected by scanning a gold coated reference disk every 15 minutes (deemed sufficient in the stable conditions inside the laboratory) and all spectra collected in absorbance.

To examine the impact of soil water on the spectra, the samples were left to air-dry over several days, and measurements of gravimetric moisture content (GMC) were collected at 14 time-intervals over the drying period. The moisture content was determined by weight and a corresponding spectrum was recorded at each time interval. After 14 intervals, the sample was dried in the oven for 48 hours at 105°C and then cooled in a desiccator and weighed to provide an oven dried reference. The GMC for each time point is then calculated with

$$GMC=100*(wet-dry)/dry \tag{42}$$

To provide an ideal standard, a subsample of the fresh soil was dried at 40°C and sieved through a 2 mm sieve, following which it was ball milled at a frequency of 25/s for three minutes and it was scanned in triplicates in a 1 cm diameter sample cup, as described in 2.2.1.

4.2.3.4 Spectral modelling for method comparison and field-fresh samples

The chemometric model used for the present research is partial least squares regression (PLSR) (H. Wold, 1973; S. Wold et al., 2001), calculating a regression model between the spectra (**X)** and the laboratory data (**y**). In this model, the dimensionality of the spectra is drastically reduced by building a new set of latent variables, describing the variance in **X**, and by directly using the information in the **y** data for the decomposition of **X**, the covariance between **X** and **y** is maximized, building the basis for the regression (Esbensen & Swarbrick, 2018; Mark & Workman, 2007).

4.2.3.4.1 Archived soil samples

The spectra collected from the existing archive of 160 topsoils using the benchtop and the handheld spectrometer were loaded into The UNSCRAMBLER X software (CAMO Software AS, Oslo, Magnolia TX). Handheld spectra which were recorded at a resolution of approximately 4 cm^{-1} had to be re-sampled to a resolution of 2 cm^{-1} using the interpolation feature in The UNSCRAMBLER X, so the spectra would be compatible with the benchtop model. The spectral replicate scans were averaged to produce more stable input spectra. To check the stability of the spectral replicates, for each wavenumber the standard deviation of the triplicates was calculated after which the average standard deviation throughout all wavenumbers was calculated. If the average standard deviation lies under the threshold of 0.1 the spectra are considered stable enough, which was the case for all spectra collected with the handheld instrument.

Based on the findings from previous research in predicting LR (Metzger et al., 2020a), both sets of spectra were pre-treated with a second order derivative Savitzky-Golay smoothing over eleven points, following a standard normal variate (SNV) transformation. The region of the spectra below 750 cm^{-1} was trimmed to reduce noise and to be consistent. The samples were randomly split into a calibration set (n=100) and a validation set (n=60), with the help of a random number generator (random.org). With the respective calibration set, a PLSR model was built from the benchtop and the handheld spectra. The models were then used to predict the validation sets: the benchtop model applied to the benchtop validation set (benchtop), the handheld model to predict the handheld validation set (handheld) and, to test compatibility, the benchtop model to predict the handheld validation set (mixed).

4.2.3.4.2 Field-fresh/*ex-situ* field samples

The spectra recorded from field moist soil stored in petri dishes across the range of moisture contents were transferred into The UNSCRAMBLER X and resampled to a resolution of 2 cm^{-1} through interpolation. Spectral replicates taken at the three positions in the dish were averaged, resulting in three sample replicates per field, which were averaged to one field value. Different pre-treatment steps were applied to the spectra to reduce noise and baseline offset effects caused by the *field-fresh* soil conditions such as soil moisture and sample heterogeneity, including averaging the three spectra of the sample replicates, moving average smoothing over 15 points, Savitzky-Golay smoothing with 2nd order polynomial fitted over eleven points, SNV normalization and cutting off the noisy end from 750-650 cm^{-1}.

From the set of the *ex-situ* spectra at decreasing moisture content, the LR was predicted with the handheld model. In addition, as %OM values were measured in the archive, a PLSR calibration model predicting %OM from the calibration set of the handheld spectra was also developed and the adequate pre-treatments were evaluated based on R^2, root mean square error (RMSE) and the number of latent variables (LV). As only three fields were sampled to predict LR and %OM for them, the evaluation statistics including R^2 and RMSEP couldn´t be applied here, however The UNSCRAMBLER X calculates a parameter to estimate the prediction uncertainty, called deviation (CAMO Software AS, 2014; De Vries & Ter Braak, 1995) that describes how similar unknown spectra are to those used for model calibration, by calculating the uncertainty of the prediction based on the sample leverage and residual X-variance. A large deviation value means that the unknown spectra used to predict a parameter is dissimilar to the dataset used for the development of the calibration, while a small deviation indicates closeness. In The UNSCRAMBLER X, this deviation can be used as a method to calculate a 95% confidence interval (by multiplying it by two) similar to the standard deviation used in normal statistics.

4.2.3.5 Development of moisture correction spectra

To develop correction spectra, the difference between the spectral absorbances at each of the 14 moisture conditions (plus oven dried) and the "ideal" spectrum for the dried and ground sample was calculated, using averaged sample spectra (one difference spectrum per field and per drying step), resulting in 45 difference spectra (15 x 3 fields). For this the absorbance value of the ideal spectrum was subtracted from the moist spectrum through each wavenumber. Seven different moisture groups were identified in the difference spectra, and each difference spectrum belonging to the same moisture class was used to calculate one average correction spectrum for each moisture class.

The correction spectra were calculated for two different pre-treatments to evaluate at which point the correction would be most effective. In the first instance, spectra were smoothed with a moving average smoothing over 15 points (Correction 1) and in the second instance, spectra were smoothed with 15 points moving average, Savitzky-Golay smoothing (2nd order polynomial over eleven points) and SNV normalization (Correction 2). To correct the spectra for moisture before prediction, the correction spectrum for the according moisture class was subtracted from the raw spectrum.

4.2.3.6 Bland-Altmann method comparison

To evaluate the feasibility of using models developed on benchtop scanned spectra to predict spectra collected with another instrument (in this case the handheld FTIR), the predicted results were compared using the Bland-Altmann method comparison (Altman & Bland, 1983; Bland & Altman, 2003). This statistic is used to compare the agreement of two different methods used to measure the same parameter, usually involving one established method and a new one (Daly & Fenelon, 2017). It calculates how close the two methods are to perfect agreement (all points are on the 1:1 line in a scatter plot) by calculating the bias (mean error) and the upper and lower limit of agreement (mean difference ± 2 standard deviation) between the two methods.

Predicted values derived from the benchtop and handheld MIR models using the archive of 160 soils were each compared with the laboratory values. The analysis was executed in R (R Core Team, 2019) with the "blandr" package (Datta, 2017).

4.2.4 Results and Discussion

4.2.4.1 Laboratory results

4.2.4.1.1 Archived soil samples

Summary statistics of the soil parameters measured in the archived soils (n=160) with their median values and ranges are as following: 5.6% (2.8% to 10.2%) for %OM, -3.5 t/ha (-9.5 t/ha to 4.0 t/ha) for the LR and 6.8 (5.0-8.0) for pH. For the calibration and the validation subset, the summary statistics are displayed in Table 14. The values of the validation set are within the range of the calibration set, with the medians for sand, silt, clay, %OM, pH and LR being similar to the corresponding values in the calibration set. These values fall within the range of values to be expected for arable fields in the republic of Ireland (Creamer et al., 2016).

Table 14 ***Summary statistics for the archive of 160 topsoil samples used for model calibration and validation. Minimum (Min), 1st Quartile (Q1), Median, 3rd Quartile (Q3) and Maximum (Max) values for Sand, Silt and Clay, percentage organic matter (%OM) pH and lime requirement (LR)***

	Sand [%]	**Silt [%]**	**Clay [%]**	**% OM**	**pH**	**LR [t/ha]**
	Calibration n=100					
Min	28.7	15.4	10.6	2.8	5.0	-9.5
Q1	39.5	24.5	17.0	4.9	6.5	-7.0
Median	47.3	32.2	20.5	5.8	6.8	-3.5
Q3	57.4	37.5	22.6	7.3	7.4	-1.5
Max	74.1	40.8	32.8	10.2	8.0	4.0
	Validation n=60					
Min	28.7	15.4	10.6	3.2	5.5	-9.5
Q1	35.3	24.5	18.1	4.4	6.2	-7.5
Median	42.5	35.4	22.0	5.4	6.8	-3.5
Q3	57.4	38.9	24.0	7.7	7.5	-0.5
Max	74.1	40.8	32.8	10.2	8.0	2.5

4.2.4.1.2 Field sites and soil samples for *ex-situ* analysis

Soil characteristics of the three field sites are presented in Table 15. The laboratory values were used to evaluate the model performance by comparing them with the predicted values. The characteristics of the test fields for the infield scanning are within the range of the calibration and validation sets from the spectral library. Field B has a slightly increased clay content (35% vs. the maximum of 32.8%) in respect to the library, %OM is within the range in the upper 50% of the library, and field A and B are in the fourth quartile, while field C with 6.5 t/ha is outside the range of the calibration dataset.

Table 15 ***Soil parameters of the three selected fields***

Field	Texture Class	Sand [%]	Silt [%]	Clay [%]	Field Moisture [% w/w]	% OM	LR [t/ha]	pH
Field A	Sandy loam	62.3	15.3	22.3	38.3	7.5	1.5	6.2
Field B	Loam	47.3	17.7	35.0	22.4	6.2	0.5	6.3
Field C	Sandy loam	55.0	15.9	29.1	54.7	9.2	6.5	5.5

4.2.4.2 Method comparison

4.2.4.2.1 Spectral modelling

The PLSR models and the validation statistics for LR and %OM are displayed in Table 16. The models for LR used 7 latent variables and the model for %OM used five with Savitzky-Golay smoothing only, always using the spectra trimmed at 750 cm^{-1}. As benchmark, for the normal use of benchtop spectra, the benchtop model showed a R^2_{cal} of 0.78 and a RMSE of 1.57 t/ha, this aligns with previously reported MIR models to predict LR from a larger archive of 459 soils with R^2_{cal} of 0.87 and a RMSE of 1.55 t/ha (Metzger et al., 2020a). In this present study, calibration using handheld spectra resulted in a R^2_{cal} of 0.85 and a RMSE of 1.29 t/ha. When the models were applied to the validation sets, results improved when both calibration and validation spectra were collected from the same instrument. For example, R^2_{val} of 0.87, RMESP of 1.31 t/ha using benchtop instrument and R^2_{val} 0.91, RMSEP 1.11 t/ha using handheld were significantly better than validation statistics derived from the benchtop model using handheld validation set (R^2_{val} of 0.36 and RMSEP of 2.92 t/ha). The performance of the mixed prediction could be improved by incorporating a bias correction of 2 t/ha in the prediction model, but yet the other model parameters showed poorer performances (R^2_{val} 0.70, RMSEP 1.99t/ha, RPIQ 3.5). The RMSE values from the benchtop and the handheld predictions are within the range of the values from the previous study (Metzger et al., 2020a) where results with a RMSE of 1.55 t/ha were found to be useful as an alternative to lab based field averages. Better performance of validations with the same instrument was also evident in the ratio of performance to interquartile distance (RPIQ). The RPIQ makes different model performances comparable by standardizing the spread of the dataset (in the form of the interquartile range with Q3- Q1) to the model error RMSE (Bellon-Maurel, Fernandez-Ahumada, Palagos, Roger, & McBratney, 2010) with:

$$RPIQ= (Q3-Q1)/RMSE. \tag{43}$$

RPIQ for the validations with the same instrument was 5.3 and 6.3 for benchtop and handheld validations respectively, while it was 2.4 for the mixed validation. Even if there is no threshold of 'good' and 'poor' RPIQ, the higher the RPIQ, the better, and the results show that the use of spectra of different origin in prediction is not recommended without further processing. To align the spectral databases, an internal soil standard (ISS) approach widely discussed in the soil spectroscopy community (Kopačková & Ben-Dor, 2016; Romero et al., 2018), could be used in future experiments to improve the alignment.

Table 16 ***Model performances and validation results for LR and %OM with the performance statistics R^2, root mean squared error (RMSE), the number of latent variables needed to describe the model, the mean error (bias) and the ratio of performance to interquartile distance (RPIQ= Q3-Q1/RMSE)***

Name	Explanation	R^2	RMSE	LV	Bias	RPIQ
	Calibration, n=100					
Benchtop	Benchtop model for LR	0.78	1.57	7	-0.03	3.5
Handheld	Handheld model for LR	0.85	1.29	7	-0.001	4.3
OM	Handheld model for %OM	0.90	0.49	5	-0.003	11.2
	Validation, n=60					
Benchtop	LR predicted from benchtop spectra with benchtop model	0.87	1.31	7	-0.1	5.3
Handheld	LR predicted from handheld spectra with handheld model	0.91	1.11	7	-0.13	6.3
Mixed	LR predicted from handheld spectra with benchtop model	0.36	2.92	7	2.14	2.4
Mixed-bias	Bias-corrected mixed prediction (bias used for correction: 2.0)	0.70	1.99	7	0.14	3.5
OM	%OM predicted from handheld spectra with handheld model	0.91	0.56	5	-0.06	12.5

4.2.4.2.2 Bland-Altman method comparison

The different predictions of LR values (benchtop, handheld and mixed) were compared to the laboratory reference values using the Bland-Altman method comparison. The results of the comparisons are provided in Table 17 and show, that using spectra recorded on the same instrument reported closer agreement than transferring them. The agreement between the methods was evaluated by their bias and by the range of the limits of agreement. The benchtop validation and the handheld validation exhibited similar values compared to laboratory values, with a bias of 0.1 t/ha and 0.13 t/ha for benchtop and handheld, respectively, with according ranges between upper and lower levels of agreement of 5.16 and 4.35 t/ha. Here, the benchtop model showed a slightly lower bias, but the handheld model showed a smaller range between the limits, indicating a smaller deviation from the 1:1 line. Comparison of the lab values against the mixed validation showed poor results with an (average) underestimation of more than 2 t/ha (bias -2.14), which is almost the double of the RMSEP of the handheld validation. Also, this is an indication that calibrations and validations developed using the same instrument performed better and are preferrable to mixed predictions.

Table 17 ***Bland-Altman comparison of the laboratory reference values (Lab) and the predictions from the benchtop calibration (Benchtop), the handheld calibration (Handheld) and the handheld spectra predicted with the benchtop calibration (Mixed) for lime requirement (LR [t/ha]] with bias, upper (ULoA) and lower (LLoA) limit of acceptance and the range between upper and lower limits***

	Lab vs. Benchtop	*Lab vs. Handheld*	Lab vs. Mixed
Bias	*0.10*	*0.13*	-2.14
ULoA	*2.68*	*2.31*	1.77
LLoA	*-2.48*	*-2,04*	-6.06
Range	*5.16*	*4.35*	7.83

Figure 19 shows the Bland-Altman plot for the comparison of the laboratory reference LR values with the handheld predicted values. The bias of 0.13 t/ha is clearly visibly indicated as the blue line in the centre of the points, with the limits of agreement enclosing 95% of the data.

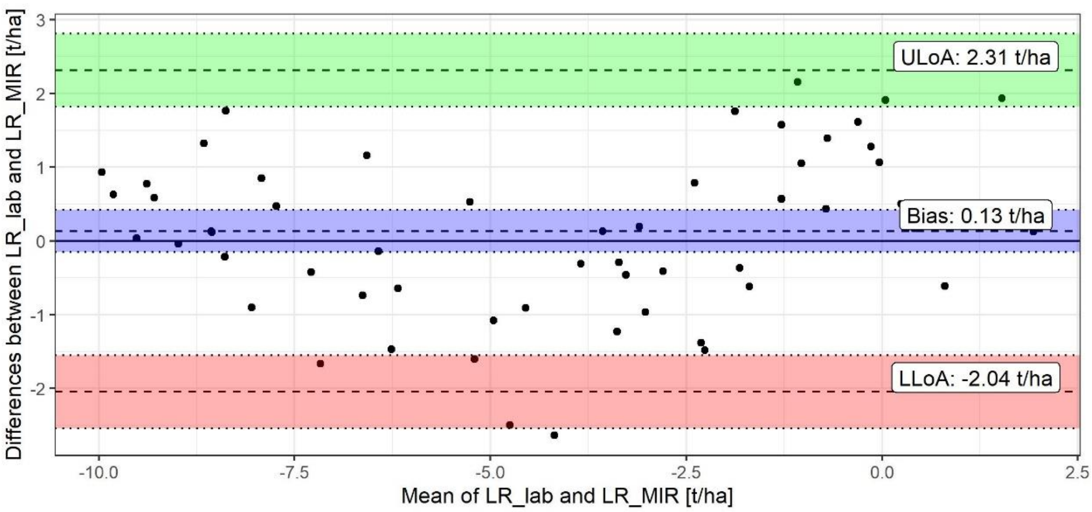

Figure 19 Bland-Altman method comparison for lab vs. handheld predicted datasets for LR with the additional 95% confidence intervals around the limits of agreement (LoA) marked in green (upper, ULoA) and red (lower, LLoA) and the bias (blue)

4.2.4.3 Ex-situ spectra of field moist soil

4.2.4.3.1 Moisture content

The water content of the samples for the three field sites over the 14 time intervals of drying from field moist to air-dried (step 15 and 16 are oven dried and are defined as having a water content of zero) is displayed in Figure 20. Field C was sampled several days after the other fields, following a rainfall event which explains the higher moisture content. As water capacity parameters couldn't be measured in the laboratory, the values from research conducted on the same farm (Bacher, Schmidt, Bondi, & Fenton, 2020) and estimations based on the German soil classification handbook (Eckelmann et al., 2006) were used to approximate the field capacity (FC), which ranged between 39% and 44% moisture content and the permanent wilting point (PWP) between 18% and 23%.

Figure 21 shows the individual spectra for each field, collected at each time interval (or run) from 1 to 14 with decreasing gravimetric water content (dark to light hue), dried and dried and ground (averaged to field level and smoothed with moving average over 15 points). The first series of spectra with high water content depicted a distinctively different pattern to the later spectra as soils were dried out, close to the ideal sample.

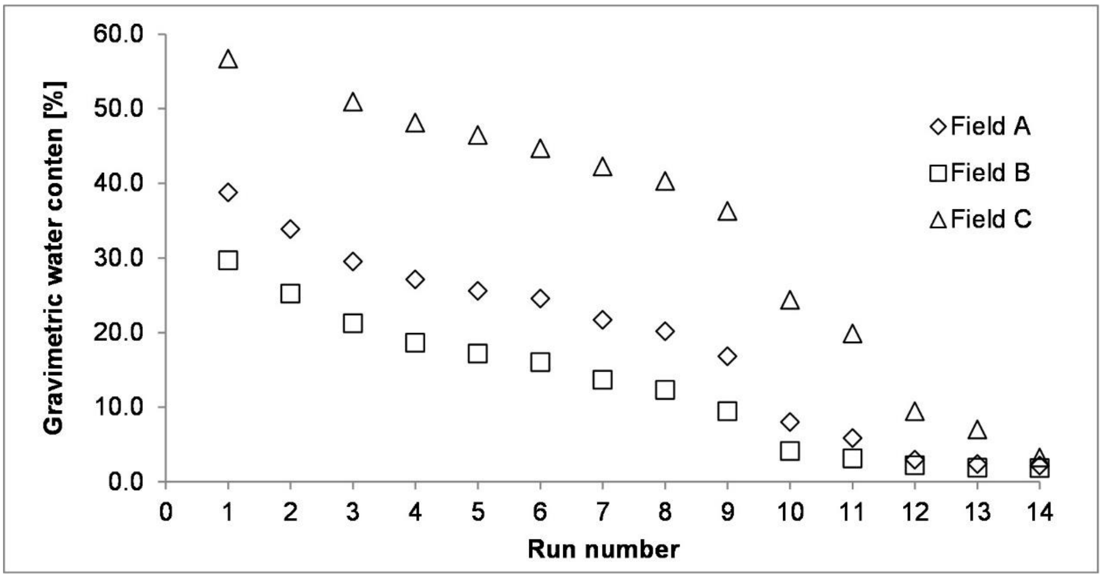

Figure 20 gravimetric water content for the three test fields throughout the scans

Also, the noisiness of the spectra decreased with decreasing water content. Overall, the increased water content increased the absorbance, which is clearly visible in the offset of the wet spectra (spectra 1-9) from 4000 cm^{-1} onwards, as well as in the constantly high absorbances between 3000 and 2000 cm^{-1}. This behaviour was also found by Hutengs et al. (2019): they described overall lower reflectance (i.e. higher absorbance) in similar positions to the present findings, attributing that change to soil moisture and sample heterogeneity. Generally lower albedo (i.e. higher absorbance) was also described for NIR spectra by Ge, Morgan, and Ackerson (2014), where they also found that the water content has a higher influence than soil intactness, which appears to be the case for the samples analysed here, as the differences between the dried and dried and ground ideal spectra were small. Absorption peaks around

3600, 3000, between 2000 and 1800 and between 1700 and 1200 cm^{-1} were less pronounced in the wet samples and became more pronounced with decreasing water content, showing that the higher absorbance caused by the soil moisture covers finer structures in the spectra (Janik et al., 2016).Visual inspection of the spectra in Figure 21 led to grouping spectra by moisture content. Seven categories of moisture content were created, as illustrated in Table 18.

Table 18 ***Moisture content range for correction spectra***

Moisture range [g/g]	Number of spectra used
>45	4
35-45	5
25-35	6
15-25	10
5-15	7
0-5	9
Airdry	3

4.2.4.3.2 Correction spectra

To correct for the influence of the water content as evident in Figure 21, correction spectra were calculated across the seven different moisture groups (see Table 18). This was realized by calculating the average difference between each moist spectrum belonging to one class and the "ideal" spectrum for the ground and dried sample. Correction spectra were calculated for two steps in pre-processing: once for only averaged and smoothed (moving average smoothing over 15 points, Correction 1), and once for the final Savitzky-Golay and SNV corrected spectra (Correction 2). Correction spectra for Correction 1 are shown in Figure 22.

Analysis of the correction spectra identified regions of the spectrum more susceptible to water content than others, including one region where clay minerals are known to absorb (4000-3600 cm^{-1}) easily detectable in MIR due to their ability to absorb water (Janik et al., 2016), one large peak centred around 2500 cm^{-1} and smaller fluctuations below 2000 cm^{-1} and in the fingerprint region below 1600 cm^{-1}. The two peaks at the beginning of the spectra were especially pronounced in the moisture groups above 15% whereas the fluctuations below 1600 cm^{-1} were prevalent in all moisture groups, notably as well in the airdry correction spectra. The fact, that in the region below 1600 cm^{-1} there was no significant improvement with decreasing water content could be an indicator, that this region of the spectrum is more susceptible to structural effects, while in the region from 4000 to 1600 cm^{-1} effects of changing moisture contents are dominating. The two correction spectra for the highest moisture content (>45% and

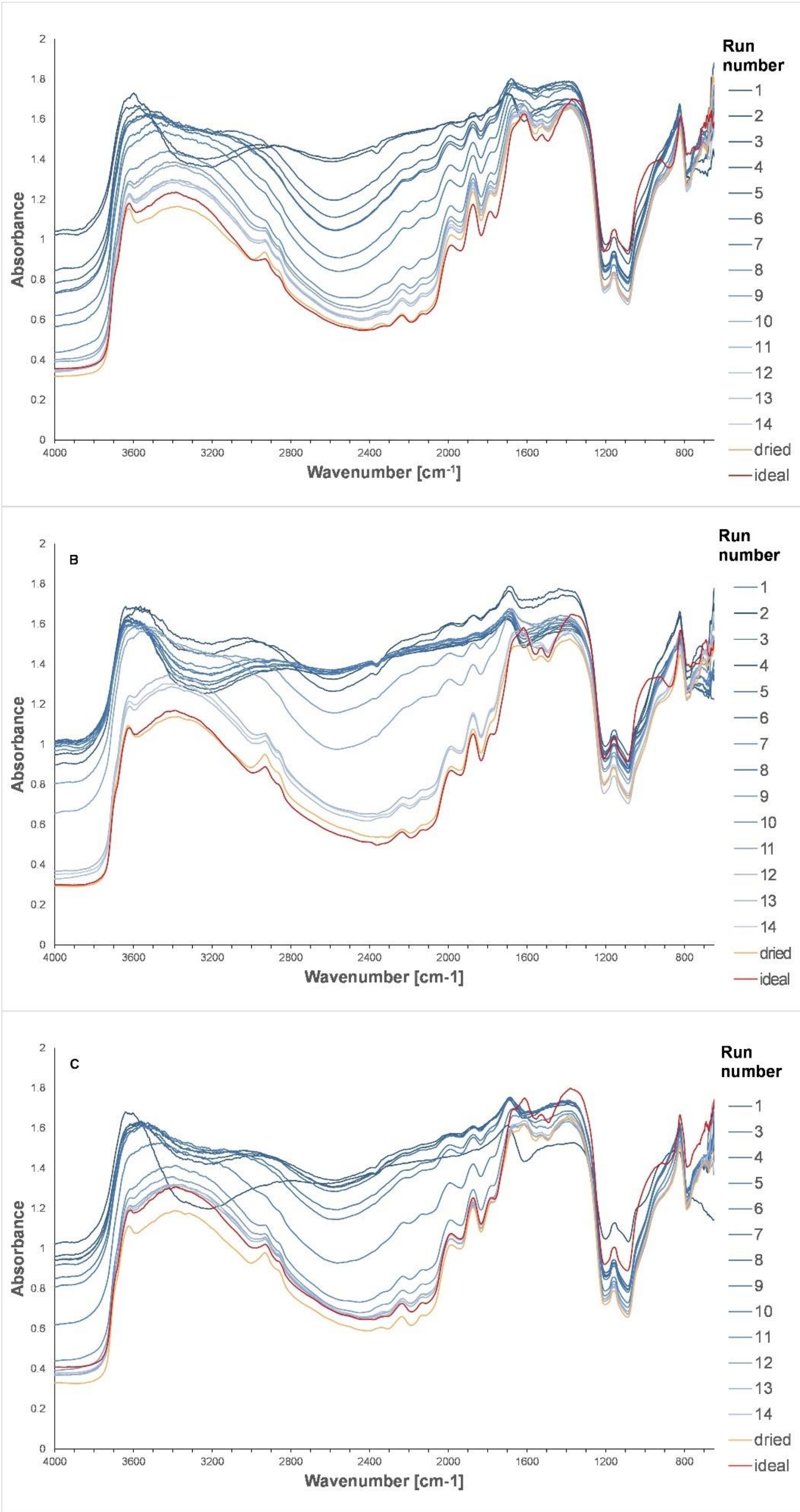

Figure 21 Spectra with decreasing water content (run 1-14) plus dry and ideal (dried and ground) samples for Field A, B and C

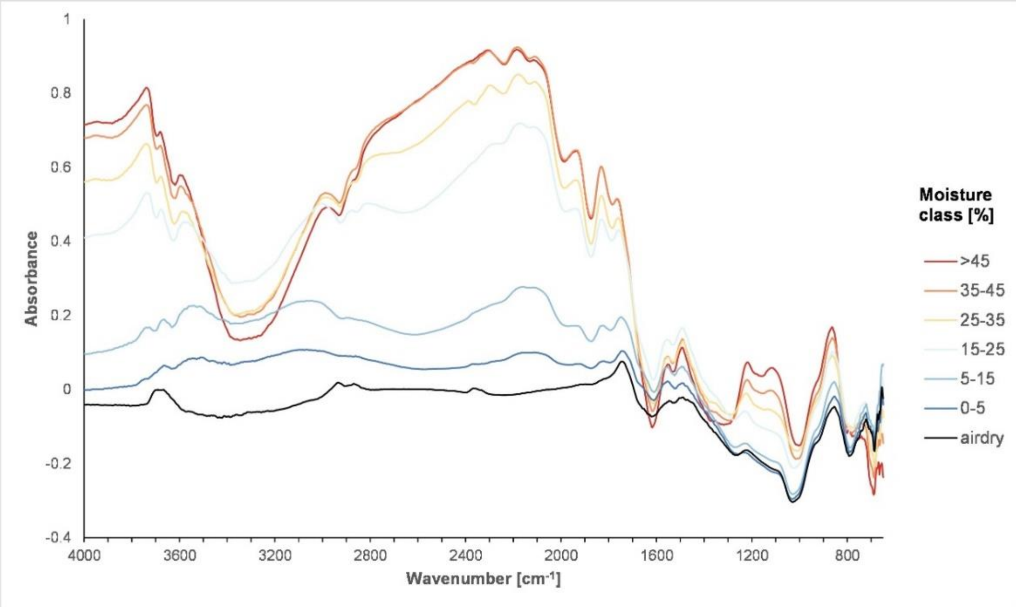

Figure 22 Correction spectra Correction 1 for the seven moisture classes developed from the smoothed (moving average, 15 points) handheld spectra for all fields.

35-45%, values close to saturation) followed a similar shape, the spectra for the following groups gradually approached the “ideal” spectrum with decreasing differences.

Correction 1 applied on the handheld spectra is displayed in Figure 23. The corrections offered a substantial improvement in the spectra which now provide the shape one would expect from soil MIR spectra.

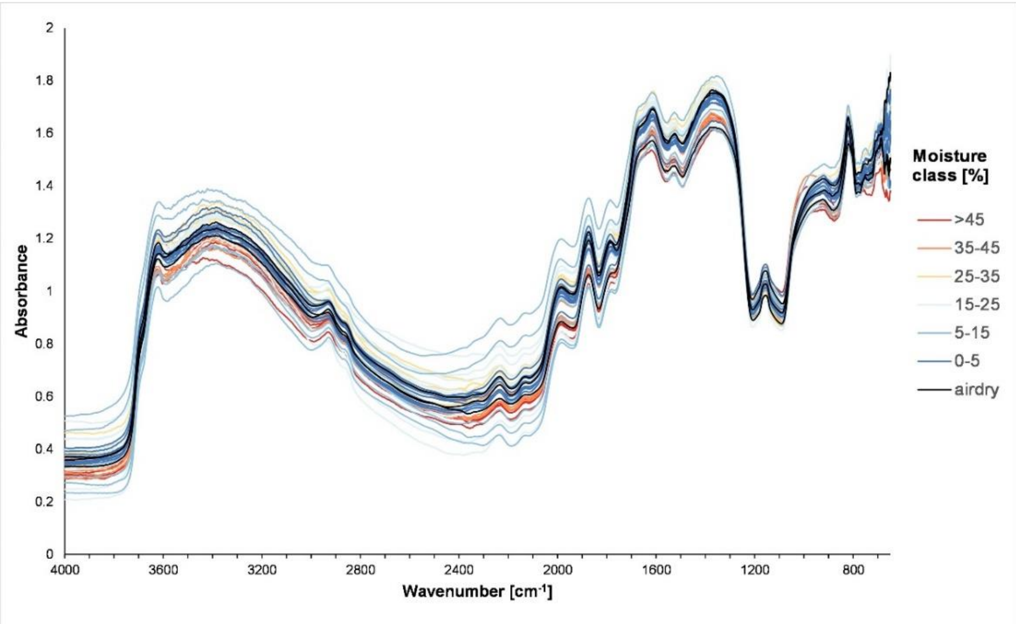

Figure 23 Result for the correction of the raw spectra (Figure 21) with the correction spectra (Figure 22)

4.2.4.3.3 Using moisture correction to predict LR from field moist soils

The spectral dataset obtained from the field sites under different moisture conditions was used to predict LR: a) without correction for moisture as baseline value and, b) with correction through Correction 1 based on the set which was only smoothed, and c) correction with Correction 2 based on the set which was smoothed (moving average, Savitzky-Golay) and normalized (SNV). The correction spectra based on the smoothed only spectra (Correction 1) delivered results closer to the laboratory values compared to corrections based on the normalized spectra (Correction 2). One explanation for that is, that through the normalization, offset effects are reduced, which makes the correction spectra less specific to correct the offset introduced through soil moisture.

Values of LR predicted from uncorrected field moist spectra (38.8%, 29.7% and 56,7% GMC respectively for field A, B and C) ranged from 29-70 t/ha, far in excess of laboratory values (1.5, 0.5 and 6.5 t/ha for field A, B and C respectively).

Correcting field moist spectra for moisture reduced the difference between predicted and laboratory values from >30 t/ha (54.3 t/ha for field A, 29.5 t/ha field B and 67.4 t/ha for field C) to < 12t/ha (11.4, 4.9 and 10.5 t/ha for field A, B and C respectively), showing an improvement but still far from laboratory values. For spectra collected from soils with moisture contents below the estimated PWP the differences between laboratory and predicted LR were below 10 t/ha for the uncorrected spectra and below 5 t/ha with Correction 1 (-0.6, -5.9 and -3.8 t/ha difference for field A, B and C respectively), bringing LR somewhat closer to lab values. The predictions from the corrected spectra reached a similar accuracy as the prediction from ideal samples (dried, ground) (i.e. the difference between laboratory values of 4.0, 0.5 and 2.9 t/ha for fields A, B and C respectively). This shows that a correction for the prediction of LR becomes effective if the soils are below PWP. A possible reason for that behaviour is that the moisture effect occurs strongly in regions which have strong influence on the calculation of the LR model (Metzger et al., 2020a), but if the moisture content reaches the PWP, the differences decrease which enables a better correction of the spectra. These results hint at the possibility to correct for moisture in LR predictions, however, in order to reach sensitivities as in the calibration model for LR developed from laboratory samples (1.11 t/ha) a deeper analysis and more elaborate correction methods are required. Future analyses require a refinement of the correction methods, which could be realized by using different texture classes and perhaps a different classification of the moisture groups based on water capacity parameters such as PWP.

The prediction results for LR of field moist, moisture below PWP and ball milled and dried samples with and without correction are displayed in Figure 24.

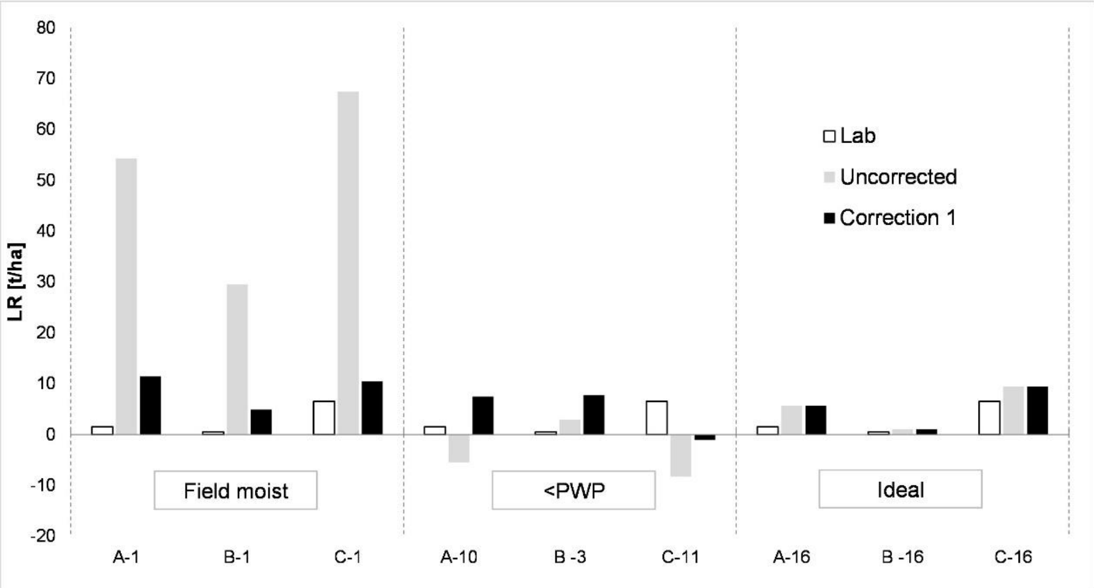

Figure 24 LR laboratory (hollow) and predicted results from uncorrected (grey) and corrected (Correction 1, black) spectra for samples in field moist, below PWP, and ideal (ball milled and dried) water contents.

4.2.4.3.4 Using moisture correction to Predict %OM in field-moist soils

The moisture correction was effective at corrected spectra for %OM prediction consistently across all moisture contents: beginning with field moist scans, where predicted values were close to the laboratory reference.

Predictions of %OM were obtained from uncorrected spectra as well as from the spectra corrected with Correction 1. The uncorrected spectra grossly underestimated the reference laboratory value in the scans with moisture above the PWP, leading to the occurrence of negative predicted %OM values. In samples below the PWP, the underestimation of the laboratory determined %OM decreased to <3.6%OM (2.6, 3.6 and 3.6%OM underestimation for field A, B and C respectively). Correction 1 for %OM was effective also for the field moist samples, predicting %OM for the field moist samples within 1%OM of the laboratory values for field A and B and 3%OM for field C. The bigger difference for field C is likely to be rooted in the higher water content at the time of sampling and the generally high %OM content, which is close to the maximum of the calibration set and thus it is not so well described by the model as samples with lower %OM content.

4.2.5 Conclusions

This study examined the feasibility of using a handheld FTIR for soil analysis. The findings from this study indicated that the application of handheld FTIR spectrometers for precision agriculture are not without their challenges in terms of collection of stable spectra in the handheld configuration, deploying existing chemometric models and developing moisture correction factors for predicting multiple parameters.

When the handheld MIR instrument is used directly on field fresh soils with high moisture contents and an irregular sample surface, the returning signal was too weak to result in meaningful spectra. However, with simple sample pre-processing, such as smoothing the surface and mounting the instrument in a stable position was sufficient to be able to record spectra at high moisture contents. When a meaningful correction for high moisture contents is available those spectra can then be used for predictions.

As a recommendation from this study, handheld MIR for soil analysis should include the development of calibration models derived from the same instrument, as opposed to deploying benchtop calibrations to predict parameters derived from handheld spectra. The results from this study showed that the errors introduced by using spectra from different instruments are substantial and calibrations from the same instrument are preferable and reduced the bias in LR predictions from 2.4 t/ha to -0.13 t/ha and model RMSEP from 2.92 t/ha to 1.11 t/ha.

Spectral data collected at different moisture contents were used to create correction spectra applied to MIR predictions of LR and %OM. Moisture corrected spectra predicted LR close to the laboratory values only at moisture contents below the PWP. Prediction of %OM using moisture correction was effective across all initial moisture categories, beginning with field moist samples, and predicted values came within 1%OM of laboratory values from field moist spectra. These preliminary findings highlighted the effect of water content on soil spectra for LR predictions, even at low levels below the PWP large peaks rendered the detection of small variations difficult. In contrast to LR, correction for %OM was effective across all moisture classes, which could be rooted in the fact, that the spectra are sensitive to %OM in regions which are not so adversely influenced by the presence of water.

To improve the predictions in future research, moisture correction factors need to be standardized across a range of texture classes, by relating moisture contents to fixed points in the drying curve, such as saturation, FC or PWP. Additionally, calibrations for the water content need to be developed to be able to automatically determine the appropriate correction.

4.2.6 Acknowledgements

This research was funded by the Teagasc Walsh Scholarship Fund (RMIS 6837) and the Department for Agriculture Food and the Marine ICT AGRI ERANET-CTF Optimove project (15/ICTAGRI 2). The authors are grateful for the help of the laboratory staff and summer students in Teagasc Johnstown Castle in processing the samples. Special thanks are due to Maame Croffie for sharing the texture results for the three test fields and to Joseph McCurley from Camo Analytics for providing individual access to The Unscrambler X software during COVID-19 restrictions.

4.2.7 References

Altman, D. G., & Bland, J. M. (1983). Measurement in Medicine : The Analysis of Method Comparison. The Statistician, 32(3), 307–317. https://doi.org/https://www.jstor.org/stable/2987937

Bacher, M. G., Schmidt, O., Bondi, G., & Fenton, O. (2020). Influence of dung pats on soil physical quality mediated by earthworms: From dung deposition to decay and beyond. Soil Research. https://doi.org/10.1071/SR19319

Bellon-Maurel, V., Fernandez-Ahumada, E., Palagos, B., Roger, J. M., & McBratney, A. B. (2010). Critical review of chemometric indicators commonly used for assessing the quality of the prediction of soil attributes by NIR spectroscopy. TrAC - Trends in Analytical Chemistry, 29(9), 1073–1081. https://doi.org/10.1016/j.trac.2010.05.006

Ben-Dor, E., & Banin, A. (1995). Near-Infrared Analysis as a Rapid Method to Simultaneously Evaluate Several Soil Properties. Soil Science Society of America Journal, 59(2), 364–372. https://doi.org/10.2136/sssaj1995.03615995005900020014x

Bland, J. M., & Altman, D. G. (2003). Applying the right statistics: Analyses of measurement studies. Ultrasound in Obstetrics and Gynecology, 22(1), 85–93. https://doi.org/10.1002/uog.122

CAMO Software AS. (2014). The Unscrambler X v10. 3 User Manual, (47), 1370.

Creamer, R. E., Simo, I., Sullivan, L. O., Reidy, B., Schulte, R. P. O., & Fealy, R. M. (2016). Irish Soil Information System: Soil Property Maps. Wexford, Ireland.

Dalal, R. C., & Henry, R. J. (1986). Simultaneous determination of moisture, organic carbon, and total nitrogen by near infrared reflectance spectrophotometry. Soil Science Society of America Journal, 50(1), 120–123. Retrieved from http://www.scopus.com/inward/record.url?eid=2-s2.0-0022928032&partnerID=tZOtx3y1

Daly, K., & Fenelon, A. (2017). A rapid and multi-element method for the analysis of major nutrients in grass (Lolium perenne) using energy-dispersive X-ray fluorescence spectroscopy. Irish Journal of Agricultural and Food Research, 56(1), 1–11. https://doi.org/10.1515/ijafr-2017-0001

Datta, D. (2017). blandr: a Bland-Altman Method Comparison package for R. https://doi.org/10.5281/zenodo.824514

De Vries, S., & Ter Braak, C. J. F. (1995). Prediction error in partial least squares regression : a critique on the deviation used in The Unscrambler. Chemometrics and Intelligent Laboratory Systems, 30, 239–245.

Dhawale, N. M., Adamchuk, V. I., Prasher, S. O., Viscarra Rossel, R. A., Ismail, A. A., & Kaur, J. (2015). Proximal soil sensing of soil texture and organic matter with a prototype portable mid-infrared spectrometer. European Journal of Soil Science, 66(4), 661–669. https://doi.org/10.1111/ejss.12265

Dunne, K. S., Holden, N. M., O'Rourke, S. M., Fenelon, A., & Daly, K. (2020). Prediction of phosphorus sorption indices and isotherm parameters in agricultural soils using mid-infrared spectroscopy. Geoderma, 358(October 2019), 113981. https://doi.org/10.1016/j.geoderma.2019.113981

Eckelmann, W., Sponagel, H., Grottenthaler, W., Hartmann, K.-J., Hartwich, R., Janetzko, P., … Traidl, R. (2006). Bodenkundliche Kartieranleitung. KA5. Schweizerbart'sche Verlagsbuchhandlung. Retrieved from http://www.schweizerbart.de/publications/detail/isbn/9783510959204

Esbensen, K. H., & Swarbrick, B. (2018). Multivariate Data Analysis (6th ed.). Oslo, Magnolia TX: Camo Software AS.

Ge, Y., Morgan, C. L. S., & Ackerson, J. P. (2014). VisNIR spectra of dried ground soils predict properties of soils scanned moist and intact. Geoderma, 221–222, 61–69. https://doi.org/10.1016/j.geoderma.2014.01.011

Gee, G. W., & Bauder, J. W. (1986). Particle-size Analysis·. In A. Klute (Ed.), Methods of soil analysis. Part 1. Physical and mineralogical methods (2nd ed., Vol. 5, pp. 383–411).

Hutengs, C., Ludwig, B., Jung, A., Eisele, A., & Vohland, M. (2018). Comparison of portable and bench-top spectrometers for mid-infrared diffuse reflectance measurements of soils. Sensors (Switzerland), 18(4). https://doi.org/10.3390/s18040993

Hutengs, C., Seidel, M., Oertel, F., Ludwig, B., & Vohland, M. (2019). In situ and laboratory soil spectroscopy with portable visible-to-near-infrared and mid-infrared instruments for the assessment of organic carbon in soils. Geoderma, 355(April), 113900. https://doi.org/10.1016/j.geoderma.2019.113900

Janik, L. J., Merry, R. H., & Skjemstad, J. O. O. (1998). Can mid infrared diffuse reflectance analysis replace soil extractions? Australian Journal of Experimental Agriculture, 38(7), 681–696. https://doi.org/10.1071/EA97144

Janik, L. J., Soriano-Disla, J. M., Forrester, S. T., & McLaughlin, M. J. (2016). Moisture effects on diffuse reflection infrared spectra of contrasting minerals and soils: A mechanistic interpretation. Vibrational Spectroscopy, 86, 244–252. https://doi.org/10.1016/j.vibspec.2016.07.005

Ji, W., Adamchuk, V. I., Biswas, A., Dhawale, N. M., Sudarsan, B., Zhang, Y., … Shi, Z. (2016). Assessment of soil properties in situ using a prototype portable MIR spectrometer in two agricultural fields. Biosystems Engineering, 152(July), 14–27. https://doi.org/10.1016/j.biosystemseng.2016.06.005

Ji, W., Viscarra Rossel, R. A., & Shi, Z. (2015). Accounting for the effects of water and the environment on proximally sensed vis-NIR soil spectra and their calibrations. European Journal of Soil Science, 66(3), 555–565. https://doi.org/10.1111/ejss.12239

Kopačková, V., & Ben-Dor, E. (2016). Normalizing reflectance from different spectrometers and protocols with an internal soil standard. International Journal of Remote Sensing, 37(6), 1276–1290. https://doi.org/10.1080/01431161.2016.1148291

Madari, B. E., Reeves, J. B., Machado, P. L. O. A., Guimarães, C. M., Torres, E., & McCarty, G. W. (2006). Mid- and near-infrared spectroscopic assessment of soil compositional parameters and structural indices in two Ferralsols. Geoderma, 136(1–2), 245–259. https://doi.org/10.1016/j.geoderma.2006.03.026

Mark, H., & Workman, J. (2007). Chemometrics in Spectroscopy. Chemometrics in Spectroscopy (1st ed.). London, Amsterdam: Academic Press. https://doi.org/10.1016/b978-012374024-3/50076-3

Martens, H., & Næs, T. (1984). Multivariate calibration. I. Concepts and distinctions. Trends in Analytical Chemistry, 3(8), 204–210. https://doi.org/10.1016/0165-9936(84)85008-6

Martínez-España, R., Bueno-Crespo, A., Soto, J., Janik, L. J., & Soriano-Disla, J. M. (2019). Developing an intelligent system for the prediction of soil properties with a portable mid-infrared instrument. Biosystems Engineering, 177, 101–108. https://doi.org/10.1016/j.biosystemseng.2018.09.013

McLean, E. O. (1982). Soil pH and lime requirement. In Methods of soil analysis. Part 2. Chemical and microbiological properties (Vol. 9, pp. 199–224). American Society of Agronomy, Soil Science Society of America.

Metzger, K., Zhang, C., Ward, M., & Daly, K. (2020a). Mid-infrared spectroscopy as an alternative to laboratory extraction for the determination of lime requirement in tillage soils. Geoderma, 364, 114171. https://doi.org/10.1016/j.geoderma.2020.114171

Metzger, K., Zhang, C., Ward, M., & Daly, K. (2020b). Variability in Soil Chemical Quality in Traffic-dependent Zones within Headlands in Small Tillage Fields. Communications in Soil Science and Plant Analysis, under revi.

Minasny, B., McBratney, A. B., Bellon-Maurel, V., Roger, J. M., Gobrecht, A., Ferrand, L., & Joalland, S. (2011). Removing the effect of soil moisture from NIR diffuse reflectance spectra for the prediction of soil organic carbon. Geoderma, 167–168, 118–124. https://doi.org/10.1016/j.geoderma.2011.09.008

Minasny, B., McBratney, A. B., Tranter, G., & Murphy, B. W. (2008). Using soil knowledge for the evaluation of mid-infrared diffuse reflectance spectroscopy for predicting soil physical and mechanical properties. European Journal of Soil Science, 59(5), 960–971. https://doi.org/10.1111/j.1365-2389.2008.01058.x

Mouazen, A. M., Karoui, R., De Baerdemaeker, J., & Ramon, H. (2006). Characterization of soil water content using measured visible and near infrared spectra. Soil Science Society of America Journal, 70(4), 1295–1302. https://doi.org/10.2136/sssaj2005.0297

Nocita, M., Stevens, A., van Wesemael, B., Aitkenhead, M., Bachmann, M., Barthes, B., … Wetterlind, J. (2015). Soil Spectroscopy: An Alternative to Wet Chemistry for Soil Monitoring. Advances in Agronomy, 132(March), 139–159. https://doi.org/10.1016/bs.agron.2015.02.002

NRCS. (2018). Soil Texture Calculator | NRCS Soils. Retrieved March 26, 2018, from https://www.nrcs.usda.gov/wps/portal/nrcs/detail/soils/survey/?cid=nrcs142p2_054167

R Core Team. (2019). R: A language and environment for statistical computing. R Foundation for Statistical Computing. Vienna, Austria. Retrieved from https://www.r-project.org/

Reeves, J. B., McCarty, G. W., & Hively, W. D. (2010). Mid- Versus Near-Infrared Spectroscopy for On-Site Analysis of Soil. In A. R. Viscarra Rossel, B. A. McBratney, & B. Minasny (Eds.), Proximal Soil Sensing (pp. 133–142). Dordrecht: Springer Netherlands. https://doi.org/10.1007/978-90-481-8859-8_11

Roger, J. M., Chauchard, F., & Bellon-Maurel, V. (2003). EPO-PLS external parameter orthogonalisation of PLS application to temperature-independent measurement of sugar content of intact fruits. Chemometrics and Intelligent Laboratory Systems, 66(2), 191–204. https://doi.org/10.1016/S0169-7439(03)00051-0

Romero, D. J., Ben-Dor, E., Demattê, J. A. M., Souza, A. B. e., Vicente, L. E., Tavares, T. R., … Eitelwein, M. T. (2018). Internal soil standard method for the Brazilian soil spectral library: Performance and proximate analysis. Geoderma, 312(November 2016), 95–103. https://doi.org/10.1016/j.geoderma.2017.09.014

Sherman Hsu, C.-P. (1997). Infrared Spectroscopy. In F. A. Settle (Ed.), Handbook of Instrumental Techniques for Analytical Chemistry (pp. 247–283). New Jersey:

Prentice Hall PTR. Retrieved from https://pubs.acs.org/doi/10.1021/a1999908r

Shoemaker, H. E., McLean, E. O., & Pratt, P. F. (1961). Buffer Methods for Determining Lime Requirement of Soils With Appreciable Amounts of Extractable Aluminum. Soil Science Society of America Journal, 25(4), 274–277. https://doi.org/10.2136/sssaj1961.03615995002500040014x

Simo, I., Creamer, R. E., Massey, G., Hamilton, P., & Mcdonald, J. A. (2007). EPA STRIVE Programme 2007-2013 Irish Soil Information System Soil Profile Handbook. Retrieved from www.epa.ie

Soriano-Disla, J. M., Janik, L. J., Allen, D. J., & McLaughlin, M. J. (2017). Evaluation of the performance of portable visible-infrared instruments for the prediction of soil properties. Biosystems Engineering, 161, 24–36. https://doi.org/10.1016/j.biosystemseng.2017.06.017

Soriano-Disla, J. M., Janik, L. J., Forrester, S. T., Grocke, S. F., Fitzpatrick, R. W., & McLaughlin, M. J. (2019). The use of mid-infrared diffuse reflectance spectroscopy for acid sulfate soil analysis. Science of the Total Environment, 646, 1489–1502. https://doi.org/10.1016/j.scitotenv.2018.07.383

Soriano-Disla, J. M., Janik, L. J., Viscarra Rossel, R. A., MacDonald, L. M., & McLaughlin, M. J. (2014). The Performance of Visible, Near-, and Mid-Infrared Reflectance Spectroscopy for Prediction of Soil Physical, Chemical, and Biological Properties. Applied Spectroscopy Reviews, 49(2), 139–186. https://doi.org/10.1080/05704928.2013.811081

Stenberg, B., Viscarra Rossel, R. A., Mouazen, A. M., & Wetterlind, J. (2010). Visible and Near Infrared Spectroscopy in Soil Science. In Advances in Agronomy (Vol. 107, pp. 163–215). https://doi.org/10.1016/S0065-2113(10)07005-7

Stuart, B. (2004). Infrared Spectroscopy: Fundamentals and applications. Journal of Chemical Information and Modeling (Vol. 53). JohnWiley & Sons, Ltd.

Tunney, H., Sikora, F. J., Kissel, D., Wolf, A., Sonon, L., & Goulding, K. W. T. (2010). A comparison of lime requirements by five methods on grassland mineral soils in Ireland. Soil Use and Management, 26(2), 126–132. https://doi.org/10.1111/j.1475-2743.2010.00263.x

Viscarra Rossel, R. A., Adamchuk, V. I., Sudduth, K. A., McKenzie, N. J., & Lobsey, C. R. (2011). Proximal Soil Sensing. An Effective Approach for Soil Measurements in Space and Time. Advances in Agronomy (1st ed., Vol. 113). Elsevier Inc. https://doi.org/10.1016/B978-0-12-386473-4.00010-5

Wold, H. (1973). Nonlinear Iterative Partial Least Squares (NIPALS) Modelling: Some Current Developments. Multivariate Analysis–III. ACADEMIC PRESS, INC. https://doi.org/10.1016/b978-0-12-426653-7.50032-6

Wold, S., Sjostrom, M., & Eriksson, L. (2001). PLS-regression: a basic tool of chemometrics. Chemometrics and Intelligent Laboratory Systems, 58, 109–130. https://doi.org/10.1016/S0169-7439(01)00155-1

4.3 Variability in Soil Chemical Quality in Traffic-dependent Zones within Field Headlands

The objective of this paper was to examine the variability in soil chemical quality within the headland zones and assess the application of mid-infrared (MIR) spectroscopy to reproduce the results in the sampling zones as a screening tool. From the data of the 41 tillage fields, soil sampling zones were delineated within headlands based on typical field traffic patterns. With a generalized linear mixed model, soil chemical quality parameters, specifically, phosphorus (P), potassium (K), lime requirement (LR) soil pH and organic matter (%OM) were analysed. Elevated values of major nutrients (P, K) were recorded around the main headland tramline and the linear mixed model resulted in statistically significant differences in P, K, LR and pH between headland zones, whereas %OM values were non-significant. MIR predicted similar patterns in %OM and LR with comparable statistical significance, which highlights the potential of proximal soil sensing to determine soil parameters in traffic dependent headland zones.

Work for this paper was conducted to 75% by me, including fieldwork, laboratory analyses (partially), data exploration and evaluation, manuscript writing and editing. Field work was done in collaboration with Mark Ward, Teagasc Oak Park. Part of the lab work was done by the staff of Teagasc, Johnstown Castle and Jim Grant, Statistician of Teagasc, Johnstown Castle helped with the setup of the generalized linear mixed model.

This paper was published with the following reference (chapter-, figure- and table-numbering adapted)

Metzger, K., Zhang, C., Ward, M., Daly, K. 2021. Variability in Soil Chemical Quality in Traffic-dependent Zones within Field Headlands. *Communications in Soil Science and Plant Analysis.*

https://doi.org/10.1080/00103624.2021.1921191

Variability in Soil Chemical Quality in Traffic-dependent Zones within Field Headlands

Konrad Metzger [a, b], Chaosheng Zhang [b], Mark Ward [c, d], Karen Daly [a]*

[a] *Environment, Soils and Land Use Department, Teagasc, Johnstown Castle Research Centre, Wexford, Y35 TC97, Republic of Ireland*

[b] *International Network for Environment and Health (INEH), School of Geography and Archaeology National University of Ireland, Galway, H91 CF50, Republic of Ireland*

[c] *Teagasc CELUP, Crops Research, Oak Park, Carlow, Republic of Ireland*

[d] *School of Agriculture and Food Science, UCD, Belfield, Dublin 4, Republic of Ireland*

* Corresponding author email: Karen.Daly@teagasc.ie

4.3.1 Abstract

There is increased stress on soil and crop quality caused by machinery traffic during field operations in tillage systems, especially the area where the machinery turns, known as the headlands. While the influence of traffic on soil physical quality is understood, the impact on soil chemical quality and soil fertility is less so. Furthermore, correcting soil fertility and chemical quality in fields under cereal tillage requires strategic sampling due spatial variability, specifically in headlands. Using a simplified sampling strategy, the objective of this study was to examine the variability in soil chemical quality within traffic-dependent zones in the headland. In a case-study in Ireland, 41 fields under tillage were surveyed, and soil sampling zones delineated within headlands based on typical field traffic patterns. Soil phosphorus (P), potassium (K), lime requirement (LR), pH and organic matter (%OM) were measured at two depths. Elevated values of major nutrients (P, K) were recorded around the main headland tramline. Using a generalized linear mixed model, significant differences in P, K, LR and pH were found between headland zones, whereas %OM values did not vary significantly. In addition to laboratory analyses, predictions from mid-infrared spectroscopy (MIR) models resulted in similar patterns in %OM and LR with comparable statistical significance, which highlights the potential of MIR as an alternative to lab analysis of soil in traffic dependent headland zones. Sampling headland zones to determine soil chemical quality coupled with the application of MIR for rapid soil analysis will improve decision support for soil management in tillage systems.

Keywords: headland, soil chemical quality, spectroscopy, tillage, management

4.3.2 Introduction

Soil degradation in tillage systems can be caused by field traffic and heavy machinery (National Research Council 1993; Pierce et al. 1983; Soane and van Ouwerkerk 1994a). While the impact of field traffic on soil physical quality has been the focus of many studies (Emmet-Booth et al. 2020; Koch et al. 2008; Soane and van Ouwerkerk 1995), the impact on soil chemical quality specifically, fertilizer status, acidity and trace elements (Idowu et al. 2008) hasn't received much attention as of now.

In tillage systems, the field area which receives the most traffic caused by machinery turning operations is called the turning headland and is typically situated at the shorter sides of a field (Sparkes et al. 1998). In field operations such as seedbed preparation, sowing, spreading of fertilizer and pesticides, and harvest, the tractor travels along defined lines in the field (tramlines) to minimize compaction, but in the headland area, turning maneuvers are executed to reach the next tramline. In the Irish tillage system with small field sizes, the area used for turning is being used for crop production and typically is worked after operations in the main field are completed. The turning headland closest to the field gate typically receives highest loads, as all traffic into the field has to go through that headland tramline (Alakukku 1999; Ward, Forristal, and McDonnell 2020). Increased traffic, especially in the headland close to the field gate, can negatively impact soil quality due to compaction from frequent wheeling (Koch et al. 2008; Sparkes et al. 1998; Withers et al. 2006) having a negative influence on crop growth and yields due to reduced pore space and water infiltration (Antille et al. 2019; Batey 2009; Hamza and Anderson 2005; Soane and van Ouwerkerk 1994b; Soane and van Ouwerkerk 1995). Sparkes et al. (1998) found that in addition to yield reduction and plant destruction from headland traffic, the influence of hedges and trees at field boundaries decreased yields through shading and competition for water. Furthermore, the irregular application of fertilizer caused by the turning patterns also reduces crop yields and although headland settings exist for most fertilizer spreaders, the precision of application can be poor (Gyldengren et al. 2020). These factors either in isolation or combination can compromise soil fertility and quality, specifically nutrient status, (Karlen, Ditzler, and Andrews 2003) soil acidity (lime requirement and pH) and organic matter content. Sometimes farmers try to compensate for this irregularity by applying additional fertilizer in the headland, often on areas of compacted soil making fertilizer utilization inefficient (Soane and van Ouwerkerk 1995). In tillage systems comprising small fields, yield losses can be significant as headland areas can represent a significant proportion of the field area relative to the overall field size. In Ireland, the average size of tillage farms is 58 ha (Central

Statistics Office 2016) with more than 75% of Irish farms under 100 ha of utilized agricultural area (UAA) (Eurostat 2016). The national average lies well below the average in the European Union where <50% of the farms are smaller than 100 ha. Irish agricultural landscapes are characterized by field boundaries and there is a high cultural and environmental value given to field borders such as hedgerows and ditches (Department of Agriculture Food & the Marine 2015), as they provide valuable habitats and enhance farm biodiversity and carbon storage. Thus, relatively small farm sizes with natural environmental features have limited the development of large field systems in Ireland (Deverell, McDonnell, and Devlin 2009).

Large field systems have benefitted from the advances in precision agriculture (PA) to reduce the problems caused by irregular fertilizer application and frequent field traffic (Earl et al. 2003; Håkansson and Lipiec 2000; Hamza and Anderson 2005; Sørensen and Dalsgaard 2005; Vermeulen, Tullberg, and Chamen 2020). The use of PA to target applications in specific areas of fields, can optimize crop yields by improving efficiency and utilization of soil functions (Ortega and Santibáñez 2007). This is achieved through the increased use of information technology, especially GPS aided navigation systems for large field operations. However, in systems with small field sizes GPS navigation systems may not be traditionally used or financially viable, however, improvement to soil quality could be achieved through simplified targeted sampling and monitoring of field areas based on traffic. Delineating zones within a headland would build the basis of a simplified sampling strategy in headland areas to guide soil management decisions.

Sampling zones based on traffic patterns offers an alternative to composite field sampling or sampling based on yields (S.A. Clay et al. 2017; Bölenius, Stenberg, and Arvidsson 2017; Franzen 2018) for managing soil in these areas. Portable applications in soil spectroscopy for rapid soil analysis using established field zones could capture soil information at higher temporal and spatial resolutions than current methods allow.

Mid-infrared spectroscopy (MIR) calibrations for soil parameters such as texture, pH and lime requirement have been developed for soil sensing applications using spectroscopy (Geladi 2003; Hutengs et al. 2019; Janik, Merry, and Skjemstad 1998; Nocita et al. 2015; Sherman Hsu 1997 Soriano-Disla et al. 2014; Viscarra Rossel et al. 2006). For Irish tillage soils mid-infrared (MIR) has been used to predict lime requirement and organic matter in both benchtop and portable instrumentation (Metzger et al. 2020; Metzger, Zhang, and Daly 2021) applicable at field scale.

The objective of this study was to assess the variability in soil chemical quality in tilled fields by adopting a headland zone-based approach to sampling and analysis for specific parameters, namely, Phosphorus (P), Potassium (K), percentage organic matter (%OM), lime requirement (LR) and soil pH. To evaluate the sensitivity of proximal soil sensing (sensor close to sample surface (Ji et al. 2018)) as cheaper and faster alternative to laboratory analyses, existing MIR models were used to predict %OM and LR in field zones to compare the accuracy with standard laboratory values.

4.3.3 Material and Methods

4.3.3.1 Field Sampling

41 tilled fields in the Republic of Ireland were selected with the help from local farming advisors as case-study sites. The selection criterion was that the fields were under conventional tillage (moldboard plough), cropped only with cereals (barley and wheat) in the last three years and were located throughout the tillage regions in Ireland along the eastern and southern parts of the island. The fields were divided into four sampling zones running parallel to the main headland tramline. The size of the zones was defined by the machinery used by the farmer (especially seeding machine and boom sprayer) to reflect areas affected by more or less turning irregularities. In this design, Zone A represents an area of the field affected by turning traffic with possible influences from the hedgerow and irregular field operations. Zone B represents an area around the headland tramline where all field traffic occurs and the most severe impacts on soil quality are expected. Zone C represents the transition area between the heavily trafficked headland tramline and the main field, and finally, Zone D, characterizes the main field excluded from the influence of field traffic with the sampling point placed in the undisturbed field. Sample points were located at four points per zone as replicates. These were located along a transect through the zones, resulting in four sampling points in each zone, and 16 sampling points per field. The area used for the sampling was determined by the traffic patterns and covered an area of ca. 100 m (4x 24 m tramline in the replicates) by 30-40 m (field edge to location of sampling point in the main field), as displayed in Figure 25. Every point was sampled at two depths determined by field operations: sampling depth 1 (SD1) in 5-10 cm depth which is within the part of the soil being loosened and turned regularly by ploughing operations (plough layer) and sampling depth 2 (SD2) in 25-30 cm depth which is not turned regularly (subsoil, below ploughing depth).

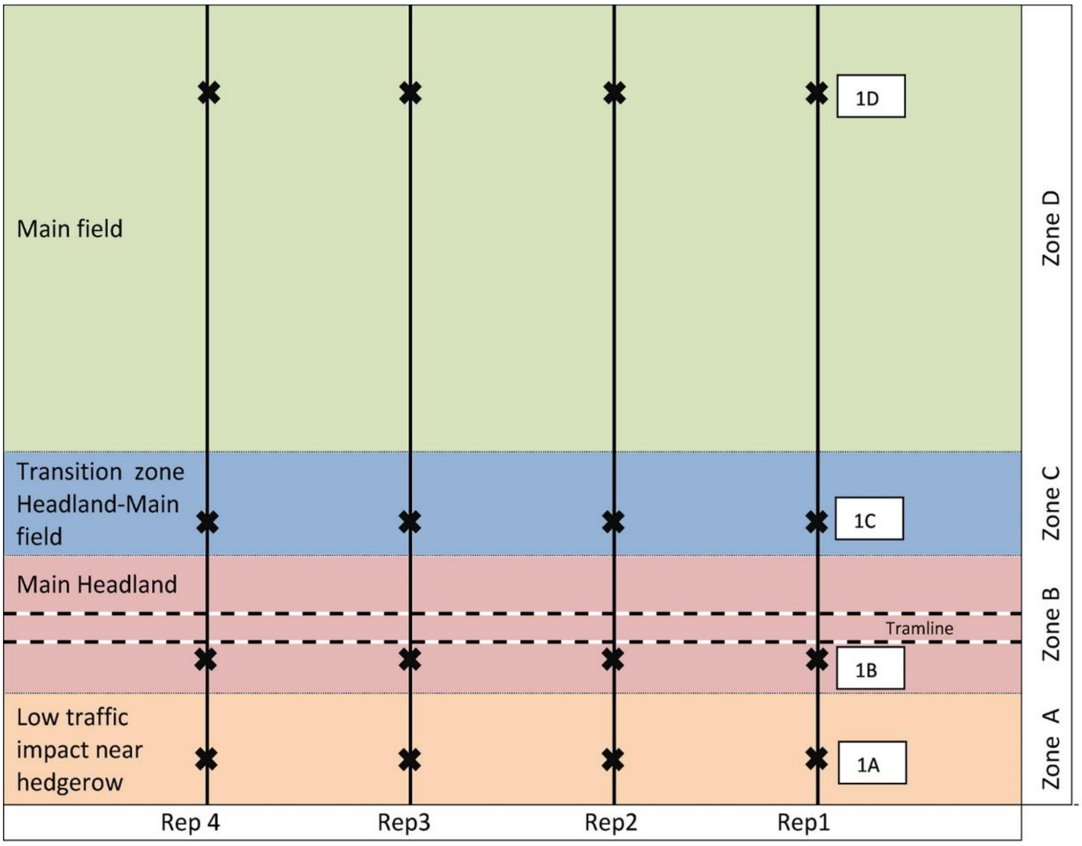

Figure 25 Sampling pattern based on headland traffic for tillage fields with four zones (A-D) and four sample replicates (Rep1-Rep4)

At each sampling depth an undisturbed sample was taken in a 100 cm^3 stainless steel cylinder with an auger and the cylinder wrapped in tinfoil and sealed in a plastic bag. A disturbed sample around that cylinder for chemical analyses was collected into a plastic bag and taken to the laboratory.

Field size ranged from 2 ha to 37 ha, with a median size of 8 ha. In addition to the size of the entire field, the area around the main headland tramline which was mainly influenced by irregular traffic (only zones A, B and C) was measured for the five smallest, five median sized and five biggest fields and their fraction of the entire area of the field was calculated.

4.3.3.2.Laboratory Analyses

Soil samples were dried and sieved to 2 mm and stored in boxes prior to analysis. Particle size distribution was determined using one composite per field and SD with the sieve-pipette method to obtain the USDA texture class. For this method, the organic matter of a 20 g subsample was oxidized with hydrogen peroxide and the clay aggregates dispersed with sodium hexametaphosphate. The sand fraction (50-2000 µm) was retained in a 50 µm sieve while the silt (2-50 µm) and clay (<2 µm) fractions were determined through sedimentation based on Stoke's law. (Gee and Bauder

1986; Massey et al. 2007). Percentage organic matter was determined by loss on ignition, as the difference in weight after heating the dried soil sample to 500°C for 12 h. Soil pH was measured on 10 ml soil mixed with 20 ml deionized water and pH measured with a Mettler Toledo “in Lab Routine” pH electrode and LR was determined by extracting 10 ml of soil in 20 ml “Shoemaker McLean and Pratt” (SMP) buffer solution consisting of para-nitrophenol, potassium chromate, triethanolamine and calcium acetate (McLean 1982; Shoemaker, McLean, and Pratt 1961), with the difference of the measured buffer pH to the initial buffer pH being related to the amount of lime needed to bring the soil pH back to optimum values (pH 6.5 for cereals). Plant available major nutrients P, K, Mg were measured with Morgan’s extraction; 3 ml of soil were extracted with 15 ml of Morgan’s solution (sodium acetate buffered at pH 4.8) and analysed colorimetrically (P and Mg) or with flame photometry (K) (Morgan 1941; Wall and Plunkett 2016)). For nutrient advice, an agronomic index system for P, K and Mg places soil test values for these nutrients into bands (indices), that describe fertilizer requirement based on nutrient status and desired crop. Four categories describe nutrient status as deficient (Index 1), low (Index 2), optimum (Index 3) and excessive (Index 4) and these are presented in Table 19. For P, the index system facilitates knowledge transfer to farmers and guides environmentally sustainable fertilizer applications based on soil test P levels. Optimum growth conditions for the desired crop occur, when the nutrient level is at Index 3, however, soils in P Index 4 represent an excessive amount posing a risk of losses to water, thereby increasing the source pressure on surrounding waterbodies (Bragina et al. 2019).

Table 19 Irish soil index system for major nutrients according to the current national fertilizer recommendations (Wall and Plunkett 2016) with P: Phosphorus [mg/l], K: Potassium [mg/l], Mg: Magnesium [mgl]

Soil index	Description	Response to fertilizer	P [mg/l]	K [mg/l]	Mg [mg/l]
1	Very low	Definite	0.0-3.0	0-50	0-25
2	Low	Likely	3.1-6.0	51-100	26-50
3	Medium/adequate	Unlikely	6.1-10	101-150	51-100
4	High	None	>10	>150	>100

In the laboratory of Teagasc Oak Park, the undisturbed samples in the cylinders were analysed for bulk density and water content by weighing the wet and the dried (105°C) sample.

In Ireland, standard soil testing includes soil pH, lime requirement, organic matter and major nutrients P, K and Mg. There is no suitable test for N in Irish soils and crop N demand is typically estimated from land use and stocking rates (Wall and Plunkett, 2016). For that reason, assessing N at field zone scale was not considered in the present research.

4.3.3.3 Statistical analysis

The variation in soil parameters between sample zones was statistically analysed with a generalized linear mixed model (proc GLIMMIX in SAS 9.4) by analysing the difference between the four zones. Proc GLIMMIX was run with “field” and “zone” as fixed effects with the four replicates within each zone pooled together. To compare the zones with each other, the least squares means of the four zones are calculated from the replicates with the LSMEANS statement and the means of the zones are tested for significant differences. The p values are adjusted for multiple comparisons with “adj=simulate” which calculates the adjustment based on a simulated distribution. By slicing the interaction of field and zone, the model is able to analyse the simple effects (in this case “zone”) in each field separately and removes the effect of “field” (Bolker et al. 2009; Davis 2018; SAS 2020). Proc GLIMMIX runs under the assumption that the residuals of the model are normally distributed which is tested by inspecting the residual panel output. If the residuals are spread equally around 0 that assumption is justified, if there is a trend in the residuals, the input data has to be transformed (with agricultural data it is often a log-transformation).

For the further statistical analysis, data from the first field sampled was left out, as the spatial distribution of the sampling points deviated from the following 40 fields. The procedure was run for all fields together (all) for SD1 and SD2, and for the fields grouped by texture class (sandy loam, loam, clay loam) for SD1. The procedure was run for the following soil parameters: phosphorus (P), potassium (K), organic matter (%OM), pH and lime requirement (LR).

Boxplots of P, K, OM, pH and LR for SD1 and SD2, once for all 40 fields and once grouped by texture class were produced with the ggplot2 package in R studio (Wickham 2016). For the grouped boxplots of SD2, the same texture class as in SD1 was assumed to be able to compare the same fields in each group.

4.3.3.4 Spectral Prediction of Lime Requirement and Percentage Organic Matter across Sample Zones

Lime requirement and %OM predicted with spectral models were used to test if significant differences between the zones of the headland area could be reproduced with the predicted values from MIR spectra. Spectral MIR calibrations for %OM and LR were developed with a partial least squares regression model (PLSR), from a spectral library of samples collected in the fields and the laboratory reference data generated from the chemical analysis. In PLSR the dimensionality within both spectral and laboratory dataset is reduced and the new system consisting of scores and loadings is used to build a regression model. Ball milled samples were scanned in triplicates with a Perkin Elmer Spectrum 400 bench top MIR spectrometer with a PIKE Autodiff sampling accessory in diffuse reflectance mode from 4000 cm^{-1} to 400 cm^{-1}. The triplicate spectra were averaged to give a smoother result and loaded into the chemometric software UNSCRAMBLER X (CAMO Software AS 2013). The dataset was split into a calibration set (data from 31 fields, randomly selected) and an independent validation set (data from 10 fields). The part of the spectra below 650 cm^{-1} was cut off to reduce noise in the model and combinations of various pre-treatments were tested by running the PLSR with a 20 bin cross validation. Model performance was evaluated through the model performance parameters R^2, the root mean squared error RMSE and the number of latent variables for the calibration set. MIR predicted %OM values are denoted as %OM_pr, LR values as LR_pred. This procedure is based on the findings published in Metzger et al (2020), and the readers are referred to there for more details.

4.3.4 Results and Discussion

4.3.4.1 Field Size

For the smallest fields, the proportion of impacted field ranged from 2-12%, for the median fields from 3-11% and for the largest fields from 1-4% respectively. This area represents the headland around the main headland tramline which receives all traffic due to its proximity to the field gate. The headland on the opposite side of the field, while not receiving all the additional traffic, still experiences irregular inputs, if that area were taken into account, up to 20% of the field in the worst case are affected by negative impacts of turning.

4.3.4.2 Laboratory Results

In Figure 26, the USDA texture class was assigned to each field based on percentages of sand, silt and clay and plotted in the texture triangles for both SDs (NRCS, 2018). Given the small size of the sampled area (usually less than 100 x 40 m), the composite sample particle size analysis was deemed sufficient. At the surface depth, SD1, 16 fields fell into the sandy loam texture class, 18 fields in loam, six fields in clay loam and one field in sandy clay loam. The one sandy clay loam field was assigned to the sandy loam group, as the sample's clay content of 20.5% was only 0.5% above the threshold for sandy loam. At SD2, 15 fields were assigned to the sandy loam texture class, 18 to loam, five to clay loam and three to sandy clay loam.

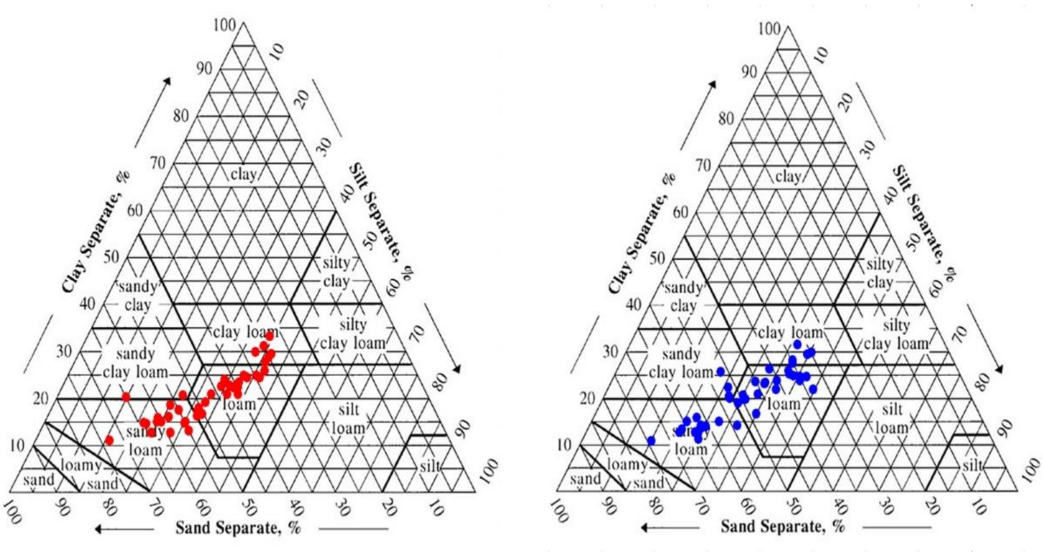

Figure 26 Soil texture classes at sample depth 5-10 cm, SD1 (red), deeper sample depth 25-30 cm SD2 (blue) plotted in the NRCS texture triangle (NRCS, 2018)

Table 20 presents the summary statistics for the laboratory values for all 41 analysed fields together and for the subgroups by texture. In 39% of the samples, soil test P values were >10 mg/l, placing them in P Index 4 and above agronomic and environmentally optimum values (see Table 19). Based on a census of tilled soils, the national average of fields at P Index 4 is 21% (Teagasc 2018). For K, 20% of fields were at the optimum value (K Index 3) and 18% were above the optimum (K Index 4) whereas national averages for K reported 38% and 20% of soils sampled in K Index 3 and 4, respectively. The pH values were similar to the national values. Around 75% of the samples had no lime requirement (LR <0), in line with national values that recorded 75% of samples with optimum pH above 6.2 (Professional Agricultural Analysis Group 2016; Teagasc 2018; The Fertilizer Association of Ireland 2016).

Table 20 summary statistics for laboratory values for all fields and both SDs as well as grouped by texture class with the number of fields in each texture class with P: Phosphorus [mg/l], K: Potassium [mg/l], Mg: Magnesium [mg/l] OM: % Organic Matter [%], OM_pr: MIR predicted OM [%], pH, LR: Lime Requirement [t/ha], LR_pr: MIR predicted LR [t/ha], BD: bulk density [g/cm³]

	P [mg/l]	K [mg/l]	Mg [mg/l]	OM [%]	OM_pr [%]	pH [-]	LR [t/ha]	LR_pr [t/ha]	BD [g/cm³]
All fields (n=41)									
Min.	0.2	0.0	0.0	0.8	2.6	5.0	-11.0	-12.5	0.9
Median	4.7	68.0	106.0	4.9	5.6	6.8	-3.5	-2.3	1.4
Mean	7.4	83.4	129.6	5.0	5.8	6.9	-3.7	-2.9	1.4
Max.	64.0	490.0	421.0	10.2	9.4	8.6	10.0	10.4	1.9
Clay loam (n=6)									
Min.	0.2	6.4	0.0	2.4	6.5	5.9	-6.5	-3.5	1.0
Median	1.5	71.9	189.0	6.9	8.0	6.6	-1.5	-0.2	1.3
Mean	2.4	103.3	196.0	6.7	8.0	6.6	-1.4	-0.1	1.3
Max.	11.8	490.0	413.0	10.1	9.3	7.3	4.5	3.7	1.8
Loam (n=18)									
Min.	0.3	0.0	29.9	0.9	3.2	5.0	-11.0	-10.6	0.9
Median	5.5	76.6	96.6	5.0	5.5	6.5	-2.0	-1.8	1.4
Mean	7.8	89.4	109.6	5.0	5.6	6.6	-2.5	-1.7	1.4
Max.	49.5	410.0	368.0	10.2	9.4	8.6	10.0	10.4	1.8
Sandy loam (n=17)									
Min.	0.2	0.0	20.3	0.8	2.6	5.0	-10.5	-12.5	1.1
Median	6.0	59.7	101.0	4.3	5.3	7.4	-7.0	-5.6	1.5
Mean	9.0	69.2	127.1	4.3	5.3	7.2	-6.0	-5.3	1.5
Max.	64.0	337.0	421.0	8.1	8.0	8.6	5.5	5.0	1.9

4.3.4.3 Statistical Analysis overall

The results of the linear mixed model are reported for P, K, OM, LR and pH. For P and K, the input data were log-transformed to guarantee a normal distribution of residuals. Overall, there was a statistically significant ($p<0.01$) effect of both field and zone, as well as for the interaction of field and zone, except for OM where the effect of zone was only significant at the $p < 0.05$ level. While it has been known for many years, that there is a difference between the main field and the headland zones (Håkansson, 2005), these results show, that even within the headland, there are statistically significant differences between zones with strong links to traffic patterns. With the simple effects available from the slicing command, the impact of the zones could be analysed in each field separately.

Overall, for all five parameters, 28 fields showed at least one significant difference ($p<0.05$) between zones for at least one parameter, with K being the parameter having significant differences between zones in 15 fields, and with one field (Field 40) being the only field having significant differences between the zones in all parameters.

Statistical results for soil fertility parameters are presented for each parameter by comparing the values for the four zones. Results are visualized using boxplots, and statistical differences are based on the least squares means output of the generalized linear mixed model, comparing the zones with the significance adjusted for multiple comparisons (adj. p <0.05). The results of the least squares means comparison for the differences between the zones in SD1 for all parameters of interest are displayed in Table 21, once analysed for all fields together, and analysed by texture class subgroups.

Table 21 Least squares means comparison between the zones for all fields together and grouped by texture class with * indicating statistically significant (adj. p<0.05) difference and with SL: sandy loam, L: loam, CL: clay loam, P: Phosphorus [mg/l], K: Potassium [mg/l], OM: % Organic Matter [%], LR: Lime Requirement [t/ha], pH [-]

	P [mg/l]				K [mg/l]				OM [%]				LR [t/ha]				pH [-]			
	All	SL	L	CL	All	SL	L	CL	All	SL	L	CL	All	SL	L	CL	All	SL	L	CL
A-B	*	*	*	-	*	-	-	-	-	-	-	-	-	-	-	*	-	-	-	*
A-C	-	-	-	-	-	-	*	-	-	-	*	-	*	*	-	-	*	*	-	*
A-D	*	-	*	-	-	-	*	*	-	-	*	-	*	*	*	-	*	*	*	-
B-C	*	-	*	-	*	-	*	-	-	-	*	-	*	*	*	-	*	*	*	-
B-D	*	*	*	-	*	*	*	-	-	-	*	-	*	*	*	*	*	*	*	*
C-D	*	-	-	-	*	*	*	-	-	-	-	-	*	-	*	*	*	-	*	*

For SD2, all fields were analysed together, and the results are shown in Table 22. The patterns of statistically significant differences for P, K, OM and LR are considerably different from the ones in SD1.

Table 22 Results of the generalized linear mixed model for Phosphorus (P [mg/l]), Potassium (K [mg/l]), Percentage Organic Matter (OM [%]), Lime Requirement (LR [t/ha]) and pH for SD1 [_1] and SD2 [_2] for all fields, significant differences (p < 0.05) between zones are denoted with [*], non-significant differences with [-]

	P_1	P_2	K_1	K_2	OM_1	OM_2	LR_1	LR_2	pH_1	pH_2
A-B	*	-	*	-	-	*	-	-	-	-
A-C	-	*	-	*	-	*	*	-	*	-
A-D	*	*	-	*	-	*	*	-	*	*
B-C	*	*	*	*	-	*	*	-	*	*
B-D	*	*	*	*	-	*	*	*	*	*
C-D	*	-	*	-	-	-	*	*	*	*

4.3.4.4 Phosphorous

Figure 27 shows the distribution of plant available soil test P (STP) across all fields. More than 50% of the samples were in P Index 3 (6-10 mg/l P) or above at surface sample depth SD 1, with the highest values in Zone B, where nearly 50% of samples recorded excessive STP values at index 4 (>10 mg/l P). Given that Zone B represents headland tramline, receiving more traffic and potentially compaction, compared to other zones, there is a greater risk of nutrient loss, either through overland flow, or being carried out onto roads on machinery tires where it can easily be washed into adjacent water bodies (Silgram et al. 2010; Withers et al. 2006). This pattern in P values is most likely a management effect, where fertilizer applications on potentially compacted areas of soil in the headland turning Zone B (and also C) and the decreased uptake of P from plants due to sub-optimal soil quality has resulted in excessive STP values. A visual analysis of soil structure by Ward et al. (2021) confirmed the trend of zone B being worst affected by field traffic. In SD 2, poor uptake and assimilation of P in the turning area due to decreased soil physical quality leads to a displacement of fertilizer into the subsoil area. While Zone A experiences irregular fertilizer application rates and decreased yield also due to possible shading and water competition, the traffic is much lower compared to B and C allowing for better infiltration and hence transport of P into lower depths (Sparkes et al. 1998) causing the highest median value for SD2 to be in Zone A.

Across all fields, there was a significant difference in STP between each zone except between A and C. Zone B, as shown in the boxplots, recorded the highest median P values (9.1 mg/l) and is significantly different to all the other zones. This highlights the potential of a traffic-based zoning approach in the headland for better management guidance.

When texture class was considered, lowest STP was recorded in clay loam (median STP 3.7 mg/l) and highest in sandy loam (median STP 10.8 mg/l). Extremely high values in almost 50% of the P Index 4 samples were recorded in the sandy loam and loam subsets compared to the suboptimal values of P index 2 in the clay loam.

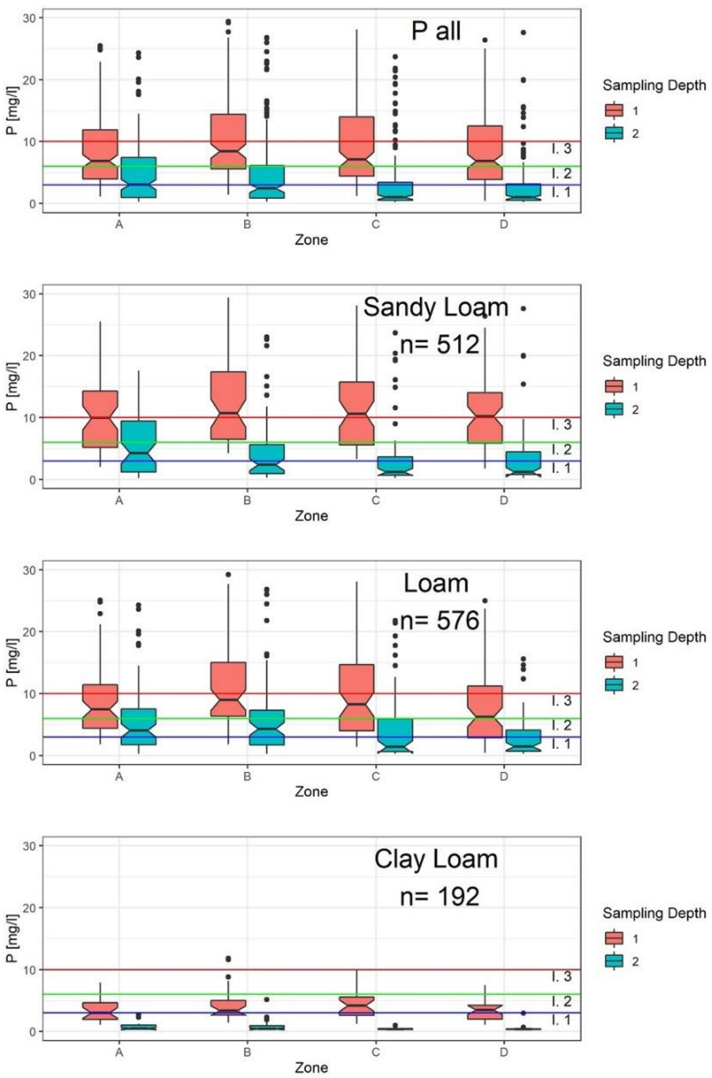

Figure 27 The distribution of P [mg/l] throughout zones A-D for all fields and grouped by texture class with the boundary values for P Index 2 (3.1-6 [mg/l]), P Index 3 (6.1-10 [mg/l]) and P Index 4 (> 10[mg/l]) included as blue, green and red lines, respectively in SD1 (red) and SD2 (blue).

4.3.4.5 Potassium

Potassium followed a similar pattern to P at SD1, with the highest values in Zone B (overall median 98 mg/l, see SI 1). Values for K were in a lower index class compared to P, with the median values being in the optimum index 3. When the values are grouped by texture class, the median values are highest in the loam (90.1 mg/l) and lowest in the sandy loam (72.8 mg/l). The noticeably wider range of values in the clay loam field SD1 compared to the P samples is probably due to a recent application of K fertilizer in one of the fields which is more pronounced due to the limited number of fields with clay loam available for the analysis.

In the statistical analysis of the overall fields (Table 21), there was a significant difference between A and B as well as between B-C, B-D and C-D, reflecting the high value of K in B.

4.3.4.6 Organic Matter

At SD1 the values of %OM ranged from 2.7% to 10.2%, while in SD2 they ranged from 0.8% to 9%. In SD1, the values stayed at similar levels throughout the zones with a median value around 6 %OM, in SD2 the values are generally lower than in the topsoil, and the median values are decreasing from around 4.5 %OM in Zone A to around 3 %OM in Zone D (see SI 2).

The relatively uniform distribution of % OM through the zones in SD1 is very likely a long term management effect, arising from regular offtakes of organic matter, which overrides finer differences, while the decreasing trend from A to D in SD2 could be a mix of management (heavy traffic leading to decreased subsoil quality in the headland area causing less mineralization) and semi-natural effects (water stress and shading from the hedgerow (De Neve and Hoffmann 2000, Sparkes et al. 1998; Ward, Forristal, and McDonnell 2020), which is also accounted for in the lack of statistically significant differences of %OM between the zones in SD1 (see Table 21).

4.3.4.7 Lime Requirement

Overall, the lime requirement across all fields ranged from -11 to 10 t/ha with more than 50% of the fields needing no additional liming. Across all fields, the lowest median value was recorded in Zone B (-3.3 t/ha), whilst zone D showed the highest median (-1.5 t/ha) (see SI 3). This low value in Zone B could be caused by generally lower productivity in that zone, but it doesn´t coincide with the highest values of P if we assume that fertilizer compounds including N are spread, which is known to introduce acidity into the soils and thus increases the LR (Metzger et al. 2020), but could also be due to irregular and overlapping spreading of lime. This pattern is repeated at SD2. Examining the fields by texture class indicated that the heaviest soils (clay loam) recorded the highest LR and the lightest soils (sandy loam) the lowest LR. The increasing LR towards the main field is likely to stem from the higher productivity and thus acidifying rood extrudates and possibly higher acidifying fertilizer turnover due to limited traffic and regular, optimum fertilizer application.

The variability of the LR values could be due to different years of lime application, as the current recommendation for lime is to spread it every three to five years (Wall and Plunkett 2016) so the fields are in different stages of lime reception. The sub-optimal pH indicated by the positive LR could also be the reason for the unusually low P values in the clay loam subset, as the P-availability and solubility is highly dependent on the pH (Sparks 2003: The Fertilizer Association of Ireland 2016).

4.3.4.8 MIR predicted Values for Lime Requirement and Organic Matter

Chemometric modelling followed the approach described for LR in Metzger et al. (2020), with the predicted values being used for the statistical analysis here. For LR, the pre-treatment options of the spectra included trimming (removing the noisy part below a wavenumber of 650 cm $^{-1}$), smoothing with Savitzky-Golay 2nd order polynomial smoothing over 11 points and normalizing with standard normal variate (SNV). With seven latent variables (LV) the model delivered the best description of the dataset. The most efficient pre-treatment options for predicting %OM were tested and resulted in the same as for LR: trimming at 650 cm^{-1}, Savitzky-Golay smoothing 2nd order over 11 points and SNV. The model performance indicators for LR and for %OM developed for this analysis are displayed in Table 23.

Table 23 Model performances of the calibration models for LR [t/ha] and OM [%] developed with PLSR

	LR [t/ha] (Metzger et al)	**%OM**
	Calibration (n= 459)	
LV	7	7
R^2	0.87	0.87
RMSE	1.55 t/ha	0.54 %
	Validation/prediction (n=160)	
R^2	0.76	0.54
RMSE	1.68 t/ha	0.81 %

Figure 28 and Figure 29 show the boxplots of both lab and spectrally (MIR) predicted values. Considering all fields together, the median LR were similar throughout the zones, with differences between 0 t/ha in Zone A and 0.5 t/ha lower values in zone D, while values in Zone B and C were 0.2 and 0.4 t/ha respectively higher. The ranges (max-min) of values were greater for the predicted values (1.2 t/ha in zone D to 4 t/ha in Zone A), due to the associated prediction error. The boxplots show a narrower interquartile range (3rd -1st quartile), probably attributed to the tendency of chemometric models like PLSR to tend to regress towards the mean of the reference values (Bellon-Maurel et al. 2010). As evident in the boxplots, especially Lime requirement values for the first quartile were higher in the MIR predictions compared to laboratory reference values, for zones A and B, however the 3rd quartile values for both were equal. This is probably an effect of the model and has to be examined closer in the further development of the sampling and modelling approach. The results of the generalized linear mixed model on the level of the entire dataset are displayed in Table 24. They show the same significant differences between the zones for the laboratory- and the predicted dataset, except for a missing statistically significant difference between zones C and D in the predicted set. This is due to the prediction median for the two zones being with -2.1 and -2 t/ha resp. exactly in the middle of the reference values (-2.5 and -1.5 resp.) and thus not resulting in a statistically significant difference.

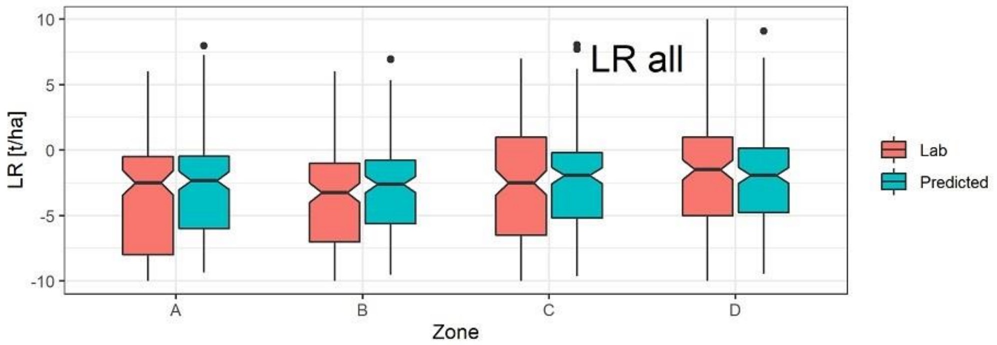

Figure 28 Boxplot of the distribution of the laboratory (red) and the MIR predicted (blue) values of LR [t/ha] throughout the zones (A-D) for all fields.

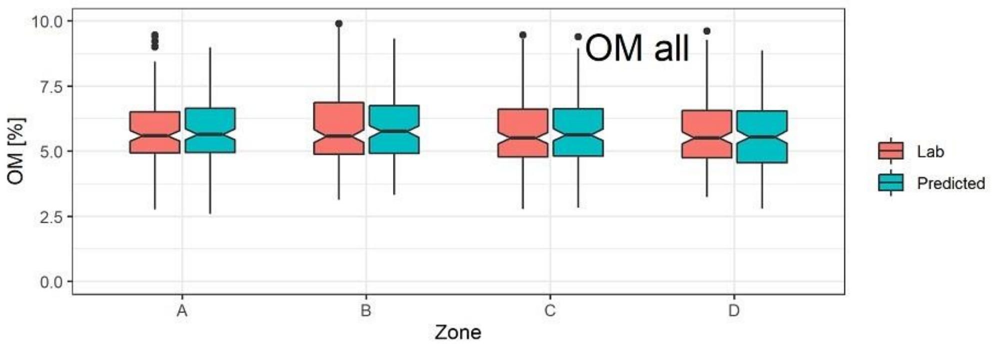

Figure 29 Boxplot of the distribution of the laboratory (red) and the MIR predicted (blue) values of OM [%] throughout the zones (A-D) for all fields.

For %OM predictions, the median %OM values as well as 1st and 3rd quartile values are almost identical for reference and predicted values, with no clear trends visible as in the case of the LR. The occurrence of a statistically significant difference is likely due to a narrower range for the predicted values due to prediction errors.

The statistical analysis of the zones as well as the analysis of the summary statistics showed that proximal sensing techniques, in this case MIR spectroscopy, can be used successfully as a screening tool in a traffic pattern guided headland sampling approach. Also, in the predicted values, associated with a prediction uncertainty, statistically significant differences between the zones were detected. These results lay the groundwork for a simple sampling strategy to improve the soil chemical quality management in headland areas, in which the headland can be divided into different zones guided by traffic patterns, and with a small number of samples areas of different soil chemical quality can be managed according to their needs. This approach is valid for both lab- and MIR derived data.

Table 24 Least squares means comparison of zones for lab and MIR predicted values of LR [t/ha] and OM [%] for SD1

	LR	LR_pr	OM	OM_pr
A-B	-	-	-	-
A-C	*	*	-	-
A-D	*	*	-	-
B-C	*	*	-	-
B-D	*	*	-	*
C-D	*	-	-	-

4.3.5 Conclusions

This study described the variability in soil chemical quality in the main headland area in tillage systems through a zone-based approach to sampling. The study determined a range of parameters such as P, K, %OM, pH and LR in 41 tilled fields in Ireland sampled on a field traffic dependent zone basis at two sample depths. The application of MIR spectroscopy to predict field patterns in %OM and LR was used to examine the sensitivity of proximal sensing technologies for this strategy.

Generalized linear mixed modelling found statistically significant differences between the headland sampling zones in the upper layer of the soil, SD1, across all parameters except %OM. Using a combination of statistical analysis and evaluation of the summary statistics we could show that the highest values of P and K were found in Zone B, the zone with the highest field traffic. The high values in Zone B are due to the lower uptake of fertilizer caused by reduced crop yield as well as possible overlay during fertilizer spreading. This simplified sampling approach for headlands demonstrated statistically significant differences in key soil fertility parameters thereby improving our knowledge of soil chemical variability in these areas of tilled fields. With this information, the field traffic and fertilizing practices can be amended to obtain optimal soil fertility in each of the zones.

For LR, headland zoning can guide management decisions, while the distribution of %OM did not vary, indicating that a less detailed sampling strategy might be sufficient in this case.

The establishment of statistically significant differences between the headland zones provides a sampling strategy to evaluate the sensitivity of proximal sensing technologies, in this case MIR spectroscopy, as a rapid screening method of soil analysis. Significant difference in LR values obtained from spectrally predicted values between zones shows the potential of MIR as a screening tool for soil chemical quality parameters in a headland sampling strategy based on traffic zones.

Based on the findings of this study, we recommend moving towards a headland sampling strategy based on field traffic. With that, fertilizer over-application around the main headland tramline can be detected and adjusted accordingly, resulting in reduced costs of fertilizer and a lower environmental impact. This approach is valid for both lab- and spectrally derived data.

4.3.6 Acknowledgements

This research was funded by the Teagasc Walsh Scholarship Fund (RMIS 6837) and the Department for Agriculture Food and the Marine ICT AGRI ERANET-CTF Optimove project (15/ICTAGRI 2). The authors are grateful for the help of the laboratory staff and summer students in Teagasc Johnstown Castle in processing the samples. Special thanks are due to Jim Grant for the valuable expertise with the statistical analysis.

4.3.7 Supplementary Information

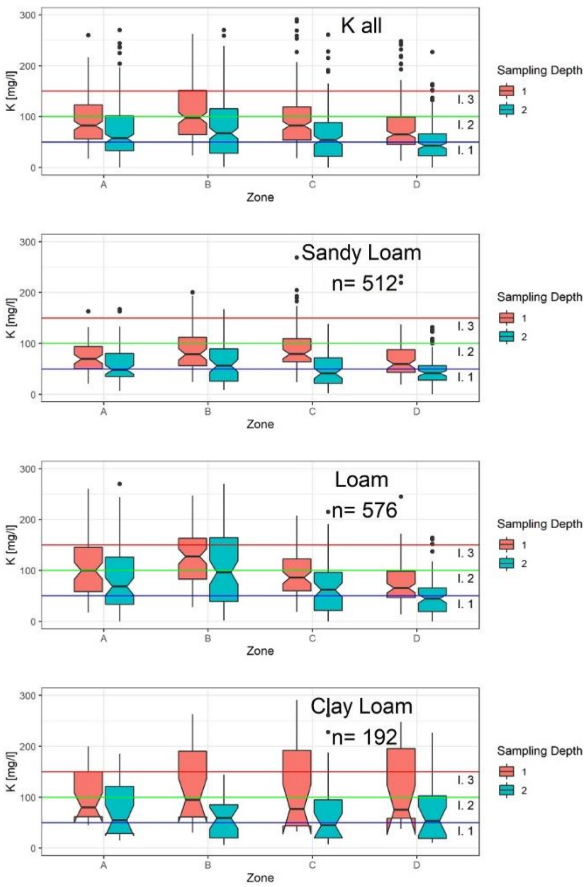

SI1 Boxplot of the distribution of K [mg/l] throughout the zones for all fields and grouped by texture class. Boundary values for the K Index system are included for K Index 2(51-100), K Index 3 (51-100) and K Index 4 (>150) as blue, green and red lines, respectively.

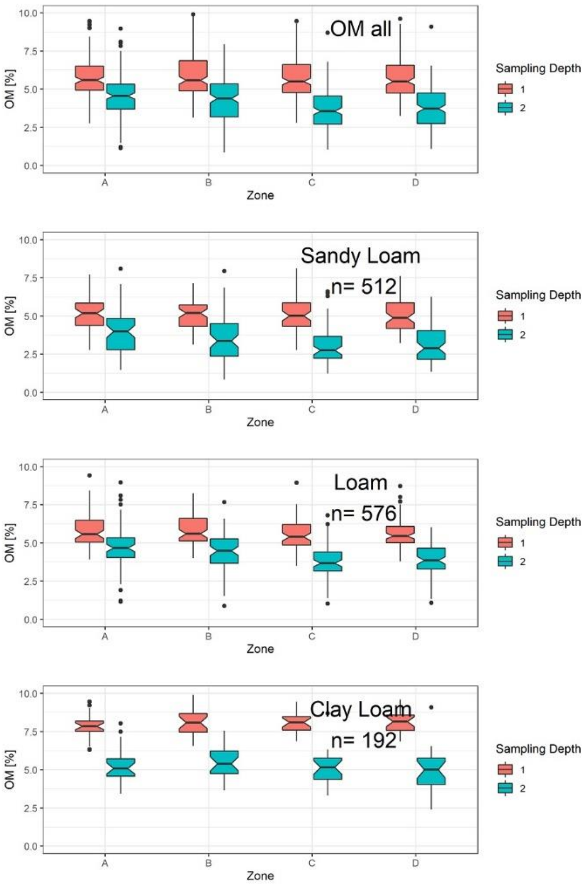

SI2 Boxplot of the distribution of %OM throughout the zones for all fields and grouped by soil texture class

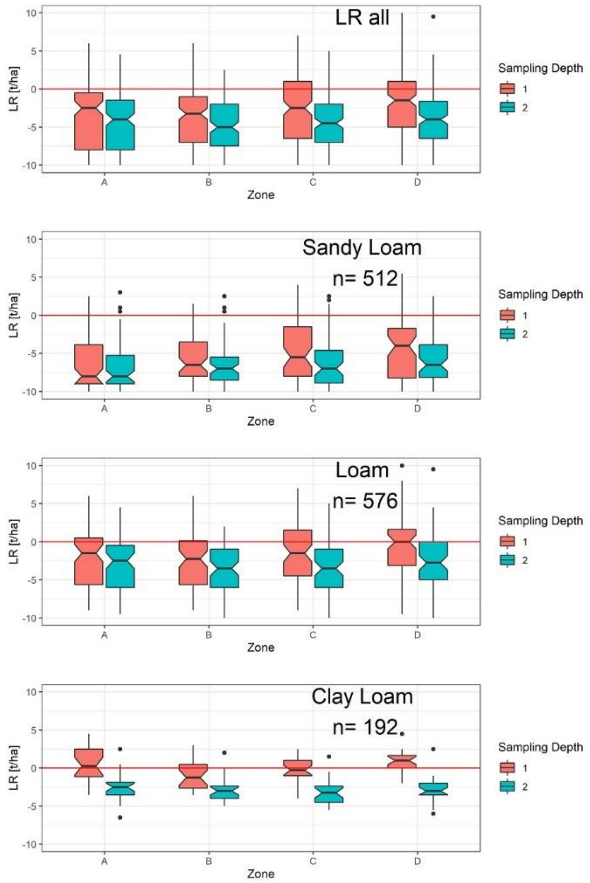

SI3 Boxplot of the distribution of LR [t/ha] throughout the zones for all fields and grouped by texture class, with a LR of zero marked in red.

4.3.8 References

Alakukku, Laura. 1999. "Subsoil Compaction Due to Wheel Traffic." Agricultural and Food Science in Finland 8 (June): 333–351. http://www.mtt.fi/afs/pdf/afsf8_333.pdf.

Antille, D. L., S. Peets, J. Galambošová, G. F. Botta, V. Rataj, M. Macak, J. N. Tullberg, et al. 2019. "Review: Soil Compaction and Controlled Traffic Farming in Arable and Grass Cropping Systems." Agronomy Research 17 (3): 653–682. doi:10.15159/AR.19.133.

Batey, T. 2009. "Soil Compaction and Soil Management - A Review." Soil Use and Management 25 (4): 335–345. doi:10.1111/j.1475-2743.2009.00236.x.

Bellon-Maurel, Véronique, Elvira Fernandez-Ahumada, Bernard Palagos, Jean Michel Roger, and Alex B. McBratney. 2010. "Critical Review of Chemometric Indicators Commonly Used for Assessing the Quality of the Prediction of Soil Attributes by NIR Spectroscopy." TrAC - Trends in Analytical Chemistry 29 (9). Elsevier Ltd: 1073–1081. doi:10.1016/j.trac.2010.05.006.

Bölenius, Elisabeth, Bo Stenberg, and Johan Arvidsson. 2017. "Within Field Cereal Yield Variability as Affected by Soil Physical Properties and Weather Variations – A Case Study in East Central Sweden." Geoderma Regional 11 (November). Elsevier: 96–103. doi:10.1016/j.geodrs.2017.11.001.

Bolker, Benjamin M., Mollie E. Brooks, Connie J. Clark, Shane W. Geange, John R. Poulsen, M. Henry H. Stevens, and Jada Simone S. White. 2009. "Generalized

Linear Mixed Models: A Practical Guide for Ecology and Evolution." Trends in Ecology and Evolution 24 (3): 127–135. doi:10.1016/j.tree.2008.10.008.

Bragina, Lyubov, Evgenia Micha, William M. Roberts, Kay O'Connell, Cathal O'Donoghue, Mary Ryan, and Karen Daly. 2019. "Spatial and Temporal Variability in Costs and Effectiveness in Phosphorus Loss Mitigation at Farm Scale: A Scenario Analysis." Journal of Environmental Management. doi:10.1016/j.jenvman.2019.05.080.

CAMO Software AS. 2013. "The Unscrambler X." Oslo.

Central Statistics Office. 2016. "Farm Structure Survey 2016." https://www.cso.ie/en/releasesandpublications/ep/p-fss/farmstructuresurvey2016/da/fs/.

Clay, Sharon A., Stephanie A. Bruggeman, Newell R. Kitchen, David E. Clay, Stephanie Bruggeman, and Emmanuel Byamukama. 2017. "Calculations Supporting Management Zones." In Practical Mathematics for Precision Farming, edited by David E. Clay, Sharon A. Clay, and Stephanie A. Bruggeman, 122–135. Madison, WI: American Society of Agronomy, Crop Science Society of America and Soil Science Society of America. doi:10.2134/practicalmath2017.0024.

Davis, Jerry W. 2018. Introduction to Generalized Linear Mixed Models A Count Data Example. https://site.caes.uga.edu/expstatgrif/files/2018/07/CountsGLMMfin1.pdf.

De Neve, Stefaan, and Georges Hofman. 2000. "Influence of Soil Compaction on Carbon and Nitrogen Mineralization of Soil Organic Matter and Crop Residues." Biology and Fertility of Soils 30 (5–6): 544–549. doi:10.1007/s003740050034.

Department of Agriculture Food & the Marine. 2015. "Landscape Features - Department of Agriculture, Food & the Marine." Department of Agriculture, Food & the Marine, Ireland.

Deverell, Rory, Kevin McDonnell, and Ger Devlin. 2009. "The Impact of Field Size on the Environment and Energy Crop Production Efficiency for a Sustainable Indigenous Bioenergy Supply Chain in the Republic of Ireland." Sustainability 1 (4): 994–1011. doi:10.3390/su1040994.

Earl, R., J. C. Taylor, G. A. Wood, I. Bradley, I. T. James, T. Waine, J. P. Welsh, R. J. Godwin, and S. M. Knight. 2003. "Soil Factors and Their Influence on Within-Field Crop Variability, Part I: Field Observation of Soil Variation." Biosystems Engineering 84 (4): 425–440. doi:10.1016/S1537-5110(03)00004-7.

Emmet-Booth, J. P., N. M. Holden, O. Fenton, G. Bondi, and P. D. Forristal. 2020. "Exploring the Sensitivity of Visual Soil Evaluation to Traffic-Induced Soil Compaction." Geoderma Regional 20. Elsevier B.V.: e00243. doi:10.1016/j.geodrs.2019.e00243.

Eurostat. 2016. "Share of Total Utilised Agricultural Area by Physical Size of Farm." https://ec.europa.eu/eurostat/statistics-explained/images/4/4b/Share_of_total_utilised_agricultural_area%2C_by_physical_size_of_farm%2C_2013_%28%25_of_total%29.png.

Franzen, D.W. 2018. "Soil Variability and Fertility Management." In Precision Agriculture Basics, edited by D.K. Shannon, David E. Clay, and Newell R. Kitchen, 79–92. American Society of Agronomy, Crop Science Society of America, and Soil Science Society of America. doi:10.2134/precisionagbasics.2016.0091.

Gee, Glendon W, and J W Bauder. 1986. "Particle-Size Analysis·." In Methods of Soil Analysis. Part 1. Physical and Mineralogical Methods, edited by Arnold Klute, 2nd ed., 5:383–411.

Geladi, Paul. 2003. "Chemometrics in Spectroscopy. Part 1. Classical Chemometrics." Spectrochimica Acta - Part B Atomic Spectroscopy 58 (5): 767–782. doi:10.1016/S0584-8547(03)00037-5.

Gyldengren, Jacob, Mette Balslev Greve, Nick Skou-Nielsen, Jørgen E. Olesen, and René Gislum. 2020. “Field Scale Agronomic and Environmental Consequences of Overlapping N Fertilizer Application by Disc Spreaders.” Field Crops Research 255 (June). Elsevier: 107901. doi:10.1016/j.fcr.2020.107901.

Håkansson, Inge, and Jerzy Lipiec. 2000. “A Review of the Usefulness of Relative Bulk Density Values in Studies of Soil Structure and Compaction.” Soil and Tillage Research 53 (2): 71–85. doi:10.1016/S0167-1987(99)00095-1.

Håkansson, Inge. 2005. “Machinery-Induced Compaction of Arable Soil. Incidence-Consequences-Counter Measures.,” no. 109: 1–158. http://pub.epsilon.slu.se/5517/1/hakansson_i_101206.pdf.

Hamza, M. A., and W. K. Anderson. 2005. “Soil Compaction in Cropping Systems: A Review of the Nature, Causes and Possible Solutions.” Soil and Tillage Research 82 (2): 121–145. doi:10.1016/j.still.2004.08.009.

Hutengs, Christopher, Michael Seidel, Felix Oertel, Bernard Ludwig, and Michael Vohland. 2019. “In Situ and Laboratory Soil Spectroscopy with Portable Visible-to-near-Infrared and Mid-Infrared Instruments for the Assessment of Organic Carbon in Soils.” Geoderma 355 (April). Elsevier: 113900. doi:10.1016/j.geoderma.2019.113900.

Idowu, Omololu J., Harold M. van Es, George S. Abawi, David W. Wolfe, Judith I. Ball, Beth K. Gugino, Bianca N. Moebius, Robert R. Schindelbeck, and Ali V. Bilgili. 2008. “Farmer-Oriented Assessment of Soil Quality Using Field, Laboratory, and VNIR Spectroscopy Methods.” Plant and Soil 307 (1–2): 243–253. doi:10.1007/s11104-007-9521-0.

Janik, L. J., R. H. Merry, and J. O. Skjemstad. 1998. “Can Mid Infrared Diffuse Reflectance Analysis Replace Soil Extractions?” Australian Journal of Experimental Agriculture 38 (7). C S I R O PUBLISHING, 150 OXFORD ST, PO BOX 1139, COLLINGWOOD, VICTORIA 3066, AUSTRALIA: 681–696. doi:10.1071/EA97144.

Ji, Wenjun, Raphael Viscarra Rossel, D.E. Clay, Viacheslav I. Adamchuk, Robin Gebbers, Nicolas Tremblay, Newell R. Kitchen, and D.K. Shannon. 2018. “Proximal Soil and Plant Sensing.” In Precision Agriculture Basics, edited by D.K. Shannon, David E. Clay, and Newell R. Kitchen. Madison, WI: American Society of Agronomy, Crop Science Society of America and Soil Science Society of America. doi:10.2134/precisionagbasics.2016.0093.

Kalivas, John H. 2005. “Multivariate Calibration, an Overview.” Analytical Letters 38 (14): 2259–2279. doi:10.1080/00032710500315904.

Karlen, Douglas L., Craig A. Ditzler, and Susan S. Andrews. 2003. “Soil Quality: Why and How?” Geoderma 114 (3–4): 145–156. doi:10.1016/S0016-7061(03)00039-9.

Koch, Heinz Josef, Henning Heuer, Olga Tomanová, and Bernward Märländer. 2008. “Cumulative Effect of Annually Repeated Passes of Heavy Agricultural Machinery on Soil Structural Properties and Sugar Beet Yield under Two Tillage Systems.” Soil and Tillage Research 101 (1–2): 69–77. doi:10.1016/j.still.2008.07.008.

Massey, P, C O’Connor, P Sills, A Fenelon, L Maloney-Finn, D Stone, B Reidy, and R Creamer. 2007. Irish Soil Information System: Laboratory Standard Operating Procedures. Wexford: Environmental Protection Agency.

McLean, E O. 1982. “Soil PH and Lime Requirement.” In Methods of Soil Analysis. Part 2. Chemical and Microbiological Properties, 9:199–224. American Society of Agronomy, Soil Science Society of America.

Metzger, Konrad, C. Zhang, M. Ward, and K. Daly. 2020. “Mid-Infrared Spectroscopy as an Alternative to Laboratory Extraction for the Determination of Lime Requirement in Tillage Soils.” Geoderma 364. Elsevier. doi:10.1016/j.geoderma.2020.114171.

Metzger, Konrad, Chaosheng Zhang, and Karen Daly. 2021. “From Benchtop to Handheld MIR for Soil Analysis : Predicting Lime Requirement and Organic Matter in Agricultural Soils.” Biosystems Engineering 204. Elsevier Ltd: 257–269. doi:10.1016/j.biosystemseng.2021.01.025.Morgan, M F. 1941. “Chemical Soil Diagnosis by the Universal Soil Testing System.” CT Agric. Exp. Stn. Bull. 450, 579–643.

National Research Council. 1993. Soil and Water Quality: An Agenda for Agriculture. Washington, D.C.: National Academy Press. doi:10.17226/2132.

Nocita, Marco, Antoine Stevens, Bas van Wesemael, Matt Aitkenhead, Martin Bachmann, Bernard Barthes, Eyal Ben Dor, et al. 2015. “Soil Spectroscopy: An Alternative to Wet Chemistry for Soil Monitoring.” Advances in Agronomy 132 (March): 139–159. doi:10.1016/bs.agron.2015.02.002.

NRCS. 2018. “Soil Texture Calculator | NRCS Soils.” https://www.nrcs.usda.gov/wps/portal/nrcs/detail/soils/survey/?cid=nrcs142p2_054167.

Ortega, Rodrigo A., and Oscar A. Santibáñez. 2007. “Determination of Management Zones in Corn (Zea Mays L.) Based on Soil Fertility.” Computers and Electronics in Agriculture 58 (1): 49–59. doi:10.1016/j.compag.2006.12.011.

Pierce, F. J., W. E. Larson, R. H. Dowdy, and W. A. P. Graham. 1983. “Productivity of Soils: Assessing Long-Term Changes Due to Erosion.” Journal of Soil and Water Conservation 38 (1): 39–44. http://www.jswconline.org/content/38/1/39.short.

Professional Agricultural Analysis Group. 2016. Collation of Data from Routine Soil Analysis in the UK. www.nutrientmanagement.org.

SAS. 2020. “PROC GLIMMIX: Syntax :: SAS/STAT(R) 9.3 User’s Guide.” Accessed January 29. https://support.sas.com/documentation/cdl/en/statug/63962/HTML/default/viewer.htm#glimmix_toc.htm.

Sherman Hsu, C.-P. 1997. “Infrared Spectroscopy.” In Handbook of Instrumental Techniques for Analytical Chemistry, edited by Frank A. Settle, 247–283. New Jersey: Prentice Hall PTR. https://pubs.acs.org/doi/10.1021/a1999908r.

Shoemaker, H E, E O McLean, and P F Pratt. 1961. “Buffer Methods for Determining Lime Requirement of Soils With Appreciable Amounts of Extractable Aluminum.” Soil Science Society of America Journal 25. Madison, WI: Soil Science Society of America: 274–277. doi:10.2136/sssaj1961.03615995002500040014x.

Silgram, Martyn, D. R. Jackson, Alison Bailey, John Quinton, and Carly Stevens. 2010. “Hillslope Scale Surface Runoff, Sediment and Nutrient Losses Associated with Tramline Wheelings.” Earth Surface Processes and Landforms 35 (6): 699–706. doi:10.1002/esp.1894.

Soane, B. D., and C. van Ouwerkerk. 1994a. “Soil Compaction Problems in World Agriculture.” Soil Compaction in Crop Production 11. Elsevier Science Publishers, B.V.: 1–21. http://www.cabdirect.org/abstracts/19941909182.html;jsessionid=20D741ACD88E983765607B88509CC23A?freeview=true.

Soane, B. D., and C. van Ouwerkerk. 1994b. “Soil Compaction in Crop Production.” Elsevier Science Publishers, B.V. http://www.cabdirect.org/abstracts/19941909181.html?freeview=true.

Soane, B. D., and C. van Ouwerkerk. 1995. “Implications of Soil Compaction in Crop Production for the Quality of the Environment.” Soil and Tillage Research 35 (1–2): 5–22. doi:10.1016/0167-1987(95)00475-8.

Sørensen, L. K., and S. Dalsgaard. 2005. “Determination of Clay and Other Soil Properties by Near Infrared Spectroscopy.” Soil Science Society of America Journal 69 (1): 159. doi:10.2136/sssaj2005.0159.

Soriano-Disla, José M., L. J. Janik, Raphael A. Viscarra Rossel, Lynne M MacDonald, and Michael J McLaughlin. 2014. “The Performance of Visible, Near-, and Mid-Infrared Reflectance Spectroscopy for Prediction of Soil Physical, Chemical, and Biological Properties.” Applied Spectroscopy Reviews 49 (2): 139–186. doi:10.1080/05704928.2013.811081.

Sparkes, D. L., K. W. Jaggard, S. J. Ramsden, and R. K. Scott. 1998. “The Effect of Field Margins on the Yield of Sugar Beet and Cereal Crops.” Annals of Applied Biology 132 (1): 129–142. doi:10.1111/j.1744-7348.1998.tb05190.x.

Sparks, Donald L. 2003. “9 - The Chemistry of Soil Acidity.” In Environmental Soil Chemistry (Second Edition), edited by Donald L Sparks, Second Edi, 267–283. Burlington: Academic Press. doi:https://doi.org/10.1016/B978-012656446-4/50009-8.

Teagasc. 2018. “Teagasc Soil Analysis Status and Trends.” Wexford, Ireland. https://www.teagasc.ie/media/website/environment/soil/All-Soil-Results-and-Enterprises-2018.pdf.

The Fertilizer Association of Ireland. 2016. Soil PH & Lime, Technical Bulletin.

Vermeulen, G.D., J. N. Tullberg, and W. C.T. Chamen. 2020. “Controlled Traffic Farming.” In Soil Engineering, edited by A Dedousis and T Bartzanas, 101–120. Berlin, Heidelberg: Springer Berlin Heidelberg.

Viscarra Rossel, Raphael A., D. J J Walvoort, Alex B. McBratney, L. J. Janik, and J. O. Skjemstad. 2006. “Visible, near Infrared, Mid Infrared or Combined Diffuse Reflectance Spectroscopy for Simultaneous Assessment of Various Soil Properties.” Geoderma 131 (1–2): 59–75. doi:10.1016/j.geoderma.2005.03.007.

Wall, David, and Mark Plunkett, eds. 2016. Major & Micro Nutrient Advice for Productive Agricultural Crops. 4th ed. Teagasc.

Ward, Mark, P.D. Forristal, and Kevin McDonnell. 2020. “Impact of Field Headlands on Wheat and Barley Performance in a Cool Atlantic Climate as Assessed in 40 Irish Tillage Fields.” Irish Journal of Agricultural and Food Research 59 (1). doi:10.15212/ijafr-2020-0113.

Ward, Mark, Kevin McDonnell, Konrad Metzger, and Patrick Dermot Forristal. 2021. “The Effect of Machine Traffic Zones Associated with Field Headlands on Soil Structure in a Survey of 41 Tilled Fields in a Temperate Maritime Climate.” Soil and Tillage Research 210 (December 2019). Elsevier B.V.: 104938. doi:10.1016/j.still.2021.104938.

Wickham, Hadley. 2016. Ggplot2: Elegant Graphics for Data Analysis. Springer.

Withers, P. J.A., R. A. Hodgkinson, A. Bates, and C. M. Withers. 2006. “Some Effects of Tramlines on Surface Runoff, Sediment and Phosphorus Mobilization on an Erosion-Prone Soil.” Soil Use and Management. doi:10.1111/j.1475-2743.2006.00034.x.

Chapter 5

Discussion

5.1 Overview over the research

The overarching topic of the research done for this thesis was to examine methodologies to detect the distribution of soil quality parameters in agricultural fields with the goal to use the information of their distribution to guide management decisions for a productive, sustainable agriculture. Special focus was on the area around the main headland tramline in cereal tillage systems, where management practices such as increased field traffic and irregular fertilizer applications through turning operations lead to significant changes in the distribution of some soil quality parameters. The findings shall then be used to feed into future PA strategies where the conditions in the field are monitored closely with a high spatial and temporal resolution and sustainable management will be enabled. The research is intended to shed light on the challenges of detecting changes in soil quality from three perspectives: from the perspective of using an alternative, faster method (MIR spectroscopy) to examine soil quality parameters (here LR as an example, Paper 1), from the perspective of using MIR spectroscopy with a handheld instrument to determine soil quality indicators *in situ* (Paper 2), and from the perspective of determining the distribution of soil quality parameters by using zones to describe the variability of the parameters around the headland and the main headland tramline (Paper 3) .Fully developed, this approach will enable the handling of numerous samples (i.e. satisfying the need for high spatial resolution) in a short time (i.e. satisfying the need for high temporal resolution) (Ji et al., 2018; Shannon et al., 2018) for sustainable farming practices.

5.1.1 Use of MIR for soil chemical quality, specifically lime requirement

The successful development of a PLSR model for the prediction of LR from MIR spectra highlighted the potential of using MIR spectroscopy as an alternative to wet-chemical laboratory analyses. The analysis of the loading weights which define the influence of each wavenumber on the model construction shows clear correlation with regions of the MIR spectrum in which contributing soil parameters such a clay, organic matter and carbonates absorb light. When the Pearson correlation coefficient between LR and the contributing soil parameters is examined, the above-mentioned correlation is statistically significant and clearly visible (Figure 30). Naturally, the (negative) correlation with the pH is the strongest (-0.96), followed by the clay content (0.59) and the organic matter (0.3). The analysis of the latent variables in Figure 31 strengthens the interpretation in Paper 1 (see Figure 13) where LV1 is mostly associated with change in clay content (Pearson correlation 0.83) and LV2 with pH (Pearson correlation -0.5). This gives a physical basis to the chemometric (statistical and mathematical) model, highlighting that the spectra are able to identify relevant signals from the soil, which justifies the future use of spectra in more sophisticated “black box” (machine learning such as artificial neural networks (ANN), Cubist, Random Forest etc.) models as it was already performed for several other soil parameters. An advanced model possibly improves the prediction error, as the RMSE of 1.5 t/ha determined in this study is not sufficient yet to accurately predict the variability within one field. When the predicted values are averaged in the zones, the values are close to the averaged laboratory values, and when the results are fed into the generalized linear mixed model as described in Paper 3, statistically significant differences similar to those from the laboratory values are detected.

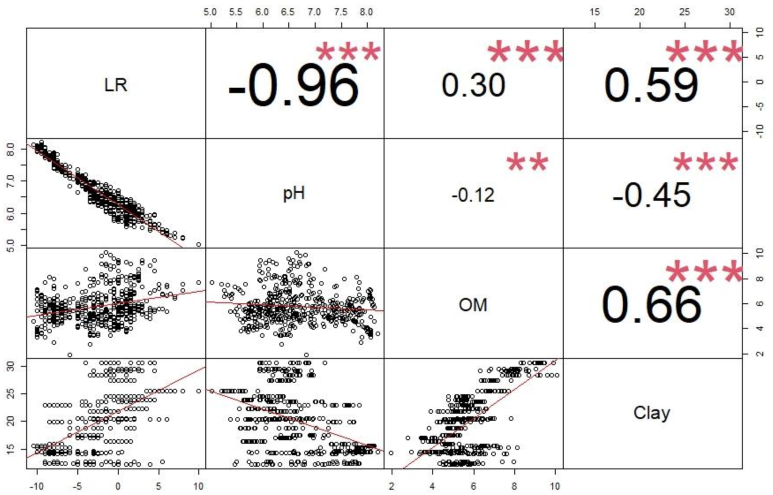

Figure 30 Pearson correlation between LR and influential laboratory parameters (pH, %OM, %Clay)

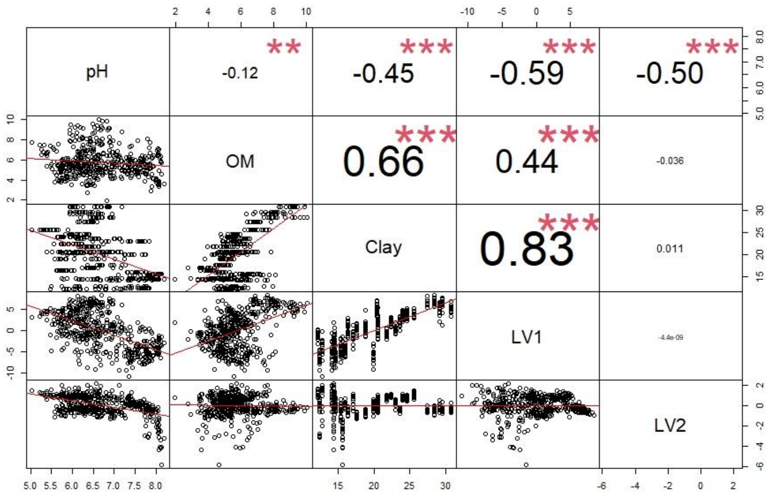

Figure 31 Pearson correlation between influential laboratory parameters (pH, %OM, %Clay) and the first two PCA latent variables (LV1, LV2) of the dataset

As an alternative to the current SMP buffer extraction performed in the soil analysis laboratory of Teagasc, the MIR method shows potential, especially if the practice of collecting composite samples in the field and analysing them in the lab is considered: when replicates of the samples are scanned and averaged, the results are very close to the laboratory values.

The approach of splitting the dataset into calibration and validation set by fields provides an advantage over randomly selecting 160 samples (i.e. 25%) from the set, in that it simulates the real-world situation of predicting values from a completely unknown sample and it provides the opportunity to examine the spatial variability of values within the field. Conversely, including spectra from all fields could improve the calibration performance, especially when specialized sample section algorithms for spectra such as Kennard-Stone or conditioned latin hypercube sampling are applied. In these sample selection approaches, a representative subsample for calibration is selected based on the multivariate sample distribution with the aim to cover all variability to be expected (Hedley et al., 2015; Ji et al., 2015; Wadoux et al., 2021). These approaches are especially valid if a big spectral library is already available and a subset of spectra has to be selected to build an optimal calibration model, which will be the case when the technology will be applied in routine laboratory analyses and when the existing spectra are used to build calibrations for other parameters.

Work done in Germany predicting LR determined according to the German guidelines (VDLUFA, calculated based on SOM, clay content and pH) with MIR (Leenen et al., 2019) from MIR predicted SOM, clay and pH as well as directly from the spectra resulted in similar predictions and underlines the interest and the potential of using MIR for LR and soil chemical quality predictions.

5.1.2 Use of a handheld MIR spectrometer for an application *in situ*

New, handheld spectrometers enable the scanning of samples *in situ* with great potential to be used for soil spectroscopy. However, there are some obstacles to be overcome, mainly problems arising from the presence of water which absorbs MIR radiation and leads to distortions. Together with soil structural (pores, coarse material) and atmospheric (lighting, humidity) influences, these *in situ* characteristics complicate the prediction from spectra collected in this manner. One approach of a simple and fast solution, i.e. subtracting the “error” introduced by the *in situ* characteristics of the soil by calculating difference spectra between wet and ideal (dried and ground) samples was examined in Paper 2. These correction spectra, developed for different moisture contents, improved the predicted values greatly. This research was a feasibility study based on three soils from one region, which has to be expanded for more varying soil types and further examination of the thresholds for the moisture classes is necessary. Nevertheless, the findings of this research point towards a simple method to enable quick scanning in the field, especially for repeated measurements in a region with established calibrations, without the need for extensive databases as they are the case for other methods such as EPO for example (Roger et al., 2003; Roudier et al., 2017).

5.1.3 Zone-based sampling for headland variability

As a basis for future PA applications, field headlands were examined closely, taking into consideration the impacts on the headland area arising from traffic in four zones around the main headland tramline. The results from the generalized linear mixed model showed, that there were significant differences between the zones for fertilizer concentrations, mainly driven by high levels of P and K in the zone around the tramline (zone B). In contrast to nutrients, no significant differences were found for %OM, while in LR, an overall gradient of increasing LR towards the main field was detected. This confirms that a zone-based approach guided by traffic patterns leads to a gain in information about infield variability in the headland area with a relatively low number of samples. The delineation of zones is only driven by traffic patterns which makes it easy to implement and doesn’t need more complex methods such as cluster analysis, PCA or coefficient of variation calculations or yield maps as performed in previous studies (Clay et al., 2017; Ortega and Santibáñez, 2007).

While the delineation is very simple, in theory (as per Figure 3), the real-world setup of fields is often more complex. Figures 32 to 34 show examples of sampled fields with increasingly complex setup of the sampling zones, from ideal in Field 8 to complex in Field 39. Despite the variations in complexity the principle of setup remained the same: the point in Zone A was placed around the middle of the zone between the main tramline and the field edge, the point in Zone B was placed within 1 m of the tramline (on the field edge side), the point for zone C is roughly the width of the sowing application (4 m) from point B, and finally the point for Zone D around 24 m (usually distance between the tramlines) from the point of Zone C.

The distribution of the sampling points is not ideal for an in-depth geostatistical analysis and geospatial mapping, as the number of points per field is very low. But an overview over the field within the limits of few data points is given through example maps of P created with Ordinary Kriging.

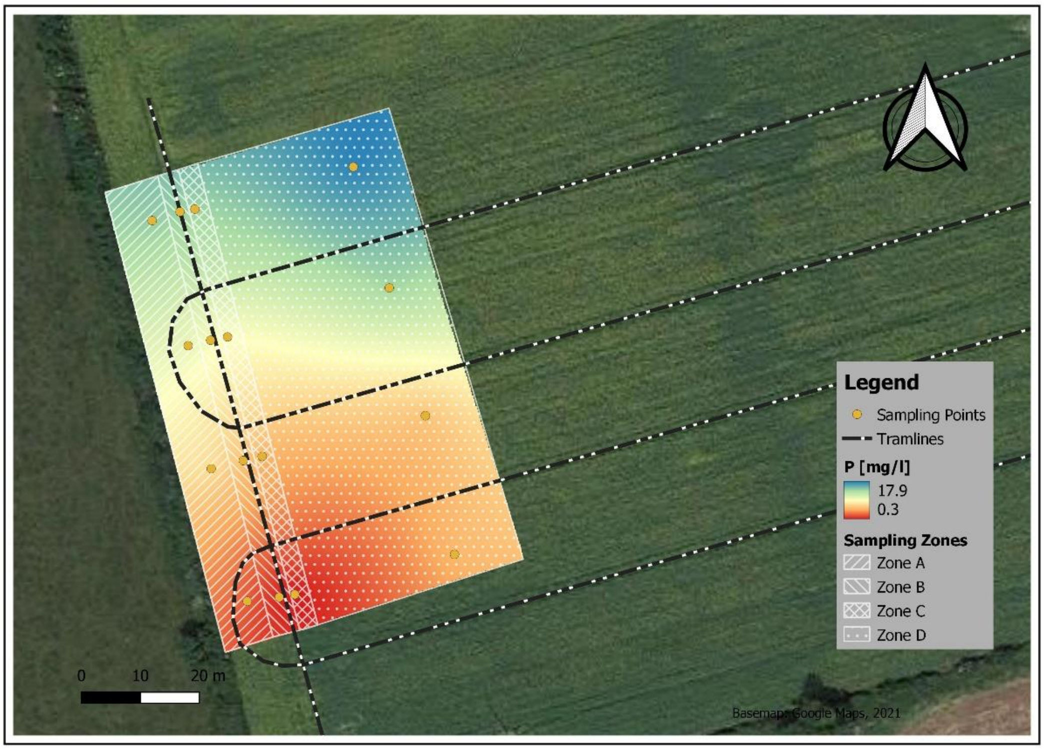

Figure 32 Distribution of P around the sampling points in Field 8 with sampling zones and tramlines. P distribution derived with Ordinary Kriging

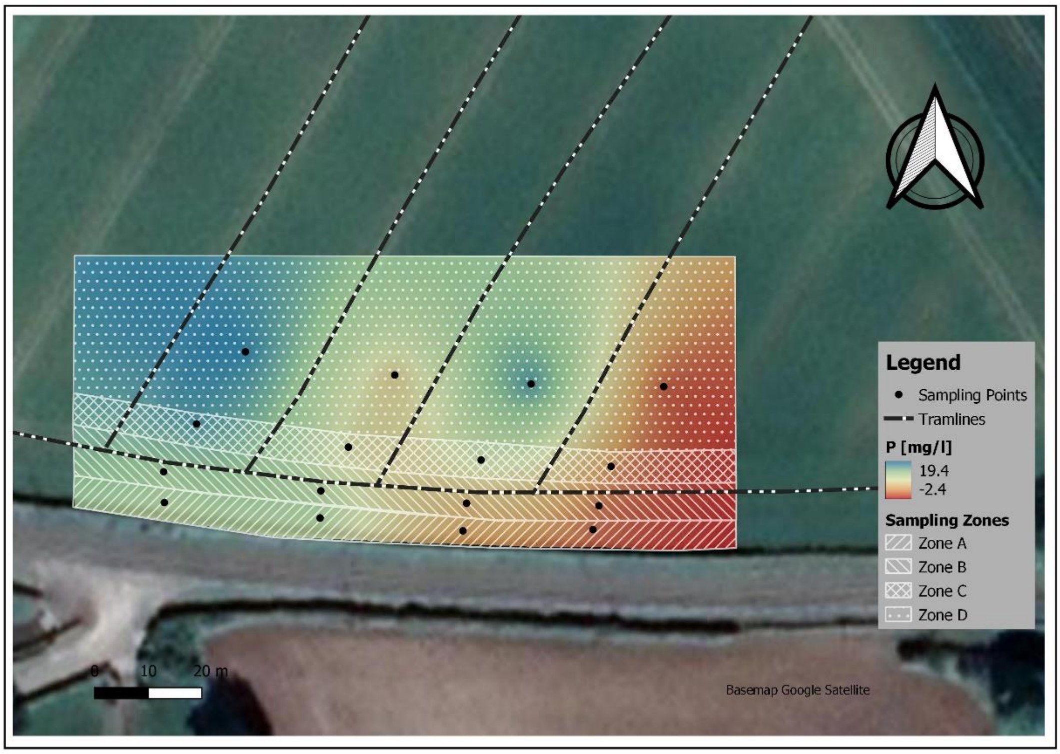

Figure 33 Distribution of P around the sampling points in Field 35 with sampling zones and tramlines. P distribution derived with Ordinary Kriging

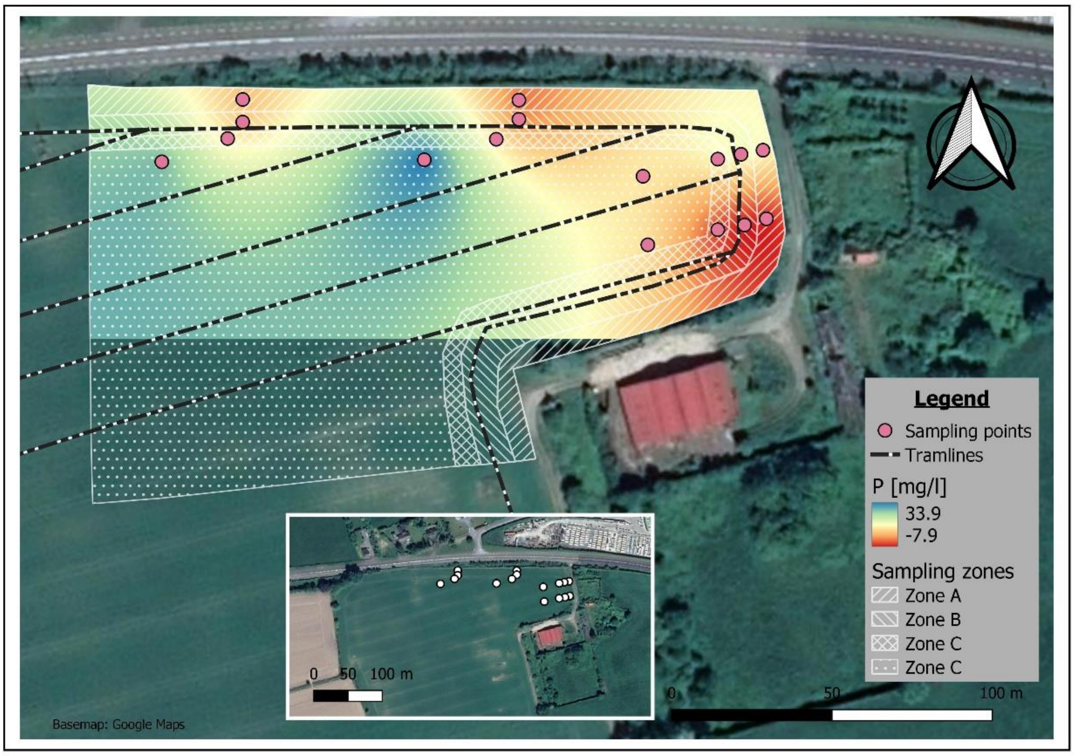

Figure 34 Setup of sampling zones around the main headland tramline in Field 39

The maps show the changes of P throughout the zones, often with high values around the tramline, but they show also a clear variability within the zones, especially in Field 8 and Field 35. This variability has to be taken into consideration in further analyses, and for future applications in PA, a strategy to deal with this issue has to be developed. This could involve sub-dividing the traffic-based zones into smaller units which are controlled by the within-zone variability when it is high. This within-zone variability is more likely to be a geogenic/pedogenic factor, while the zones used in this analysis are caused by anthropogenic factors (i.e. traffic).

In the next step in the development of this approach towards PA, a deeper geostatistical analysis with a higher spatial resolution of sampling points has to be set up. In this analysis the geogenic and anthropogenic variabilities have to be quantified and based on these results the sampling strategy can be refine

5.2 Relevance of the work done

The findings of this research contribute to advancing the use of PA, with special focus on the Irish situation with relatively small fields, which make the proportion of the headland a considerable factor in terms of productivity and yield. The statistical analysis of the zones around the headland tramline showed, that there were significant differences between the zones, which indicates, that treating these zones differently to the rest of the field could have beneficial effects on soil quality and the environment. The detection of values of fertilizer above the recommended agronomic values or index especially at the tramline calls for a close examination of this area and an implementation of management practices that guarantee sustainable soil use also on a small scale.

Besides showing potential for improvement of sustainable management and soil quality, the zoning of the headland area also shows benefits for the future application of proximal soil sensing, here MIR-DRIFTS, in such that several scans within one zone can be averaged and deliver good results which make PA more accessible and promote its use to get the best out of productive agricultural soils with the least environmental impact.

MIR-DRIFTS as alternative for the hazardous Potassium Chromate used in the SMP buffer solution in laboratory extractions promotes the use of “green chemistry” in the laboratory, where more samples can be analysed with hardly any hazardous waste and greatly reduced threats for health and safety of the laboratory analysts. Another advantage of MIR-DRIFTS is, that the spectra only have to be collected once, and then offer unlimited potential of developing new calibrations for a wide array of soil parameters and soil quality indicators.

Advancement in MIR technology has led to the development of handheld instruments with specifications close to benchtop instruments. This opens up a whole new field of application for *in situ* soil spectroscopy. This application though is complicated by the presence of water in the soil in field conditions and additional disturbances through stones, roots, cracks, and varying particle sizes. This research showed one simple method of using correction spectra to eliminate the influence of water, so that spectra collected on samples in field conditions can be corrected and predicted with an existing calibration.

5.3 Development of MIR soil spectroscopy

Since the first application of infrared spectroscopy for soil analysis the technology has progressed considerably. From using single peaks in NIR spectra to utilizing the entire spectrum, from bulky instruments with large moving mirrors to miniature instruments with chip-based Micro-Electro Mechanical Systems (MEMS) FTIR spectrometers (Fathy et al., 2020), the technology has grown to be reliable tool with great potential for future applications. Figure 35 gives an overview over the development of the technology.

The work conducted in this thesis contributed to bringing the MIR technology forward from being established in the research community towards being used as a routine tool both in laboratory and in-field applications. Contributions were specifically made by adding the SMP LR to the pool of parameters for which calibrations exist, by shedding light on the transfer of calibrations between different instruments and by investigating the efficient use of handheld spectrometers in-field and offering solutions for the problems arising from moisture.

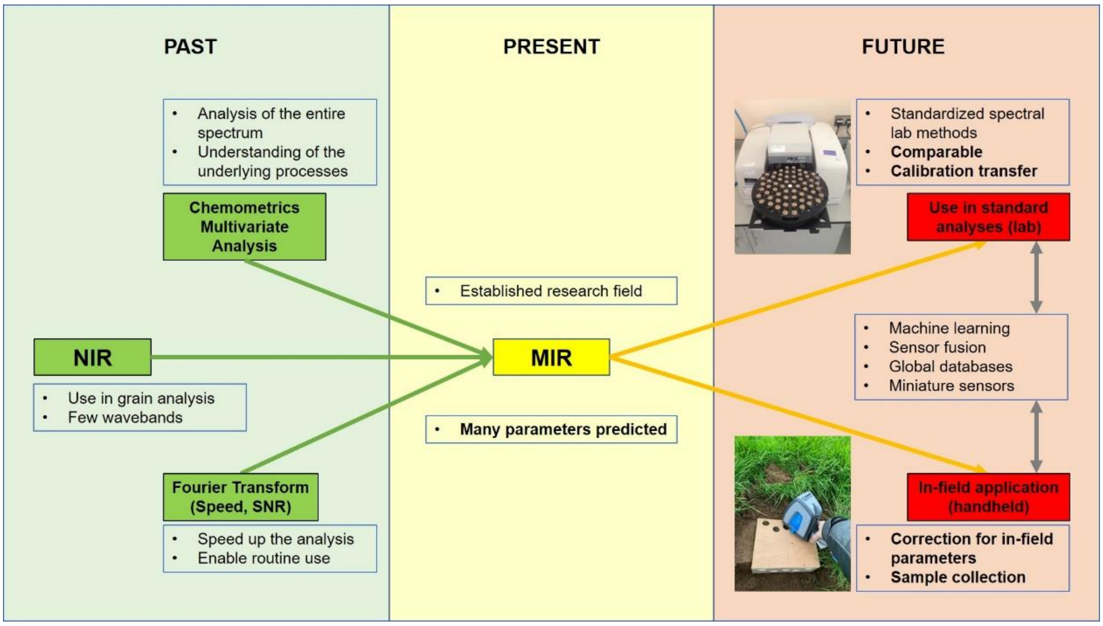

Figure 35 overview over the development of infrared soil spectroscopy towards routine application with the fields where the work of this thesis contributed in bold

For MIR spectroscopy to be used as a routine technology, the main problems which are still to be overcome are a) to find a way to standardize the laboratory analyses so that the results can be compared globally, b) to find efficient ways to record spectra *in situ* and c) to improve the sampling strategy to be able to cover the spatial variability which then can be addressed with PA.

Chapter 6

Conclusion and future work

6.1 Conclusion

Research conducted for this thesis focused on finding ways to get a better understanding of the distribution of soil chemical or soil fertility parameters, especially focused on the headland area in tillage fields. As the transition towards PA requires a large number of samples, commonly used laboratory analyses are too time-consuming too expensive and often involve hazardous chemical compounds such as potassium chromate in the case of the SMP buffer solution, MIR spectroscopy with a benchtop and a handheld instrument was tested as alternative method. For the intermediate time between traditional sampling and PA, zone-based sampling in the headland area was analysed as one possible method for the transition. With the conclusions from the presented work, the research questions posed in the introduction could be answered as follows:

1. Can MIR spectroscopy be used as alternative to laboratory extractions to determine lime requirement?
   - A benchtop model to predict LR can be used as alternative for laboratory extraction, especially for averages of a field
2. How can a handheld MIR spectrometer be applied directly in the field under field-moist conditions?
   - Using a handheld MIR instrument directly on the face of a moist soil pit does not return a signal, but a simple *ex-situ* method consisting of filling soil in a small petri dish and scanning it in a stable position delivers reliable results
   - Spectral distortions from *in situ* soil characteristics can be corrected with moisture content dependant correction spectra
3. Is there variability of soil chemical quality parameters in headlands in a headland zone-based sampling approach?
   - Zone-based sampling in four traffic-based zones around the headland tramline was effective to find statistically significant differences between the zones, especially for nutrient content and LR and can contribute to a more sustainable management of headland areas
   - When the predicted LR values are used in the headland zone-based approach, statistical significance between the zones was detected for almost the same zones as with the laboratory values, which indicates that using zone averages of predicted values is a good approach for future application of MIR in headlands.

6.2 Future work

For a reliable application of MIR for LR analysis, the model should be refined, possibly creating calibrations for more local datasets which could improve the prediction accuracy. Laboratory references and in-house standards for spectral analysis have to be developed to ensure consistent and reliable results. The existing spectral database can be used to develop models for more soil parameters such as %OM, texture, and possibly nutrient content.

Management practices have to be developed to counteract negative influences of headland traffic on soil quality and environment. The zoning of the headland area as used here can be used as a basis for decision making.

Based on the results of the research conducted on correction spectra, this approach has to be broadened for more soils and the correction spectra have to be refined. More soil types, land use and water contents have to be included and soil moisture indicators such as permanent wilting point and field capacity need to be included to be able to compare different fields. Decision support tools have to be developed to determine which correction spectrum should be used for an unknown sample, ideally without the need for further analyses (as they are still needed in the presented case to determine the moisture class).

6.3 Recommendations

The following recommendations arise from the findings of the work done in the frame of this thesis:

- The research of the zone-based sampling approach in the headland area of agricultural fields revealed irregularities especially in fertilizer input around the tramline. To efficiently fertilize the headland area, targeted analysis in traffic-dependant zones and according management practices are required to target that problem.
- Besides the zone-based sampling, the spatial variation of soil quality in the headland can be further quantified using sampling at higher densities, e.g., a grid sampling design.
- The calibration model developed for LR should be used parallel to SMP buffer extractions to refine the analysis and implement its use in standard laboratory practices.
- Parallel to the development of the LR calibration model for the benchtop instrument, the application of handheld MIR instruments should be refined, and a standardized sampling strategy needs to be developed.

References

Adams, F., Evans, C.E., 1962. A Rapid Method for Measuring Lime Requirement of Red-Yellow Podzolic Soils1. Soil Sci. Soc. Am. J. 26, 355. https://doi.org/10.2136/sssaj1962.03615995002600040015x

Adams, M.J., 1995. Chemometrics in Analytical Spectroscopy, RSC Analytical Spectroscopy Monographs. The Royal Society of Chemistry, Cambridge.

Altman, D.G., Bland, J.M., 1983. Measurement in Medicine : The Analysis of Method Comparison. Stat. 32, 307–317. https://doi.org/https://www.jstor.org/stable/2987937

Andrews, S.S., Karlen, D.L., Cambardella, C.A., 2004a. The Soil Management Assessment Framework: A Quantitative Soil Quality Evaluation Method. Soil Sci. Soc. Am. J. 68, 1945–1962. https://doi.org/10.2136/sssaj2009.0029

Andrews, S.S., Karlen, D.L., Cambardella, C.A., 2004b. The Soil Management Assessment Framework : Sci. Soc. Am. J. 68, 1945–1962.

Antille, D.L., Peets, S., Galambošová, J., Botta, G.F., Rataj, V., Macak, M., Tullberg, J.N., Chamen, W.C.T., White, D.R., Misiewicz, P.A., Hargreaves, P.R., Bienvenido, J.F., Godwin, R.J., 2019. Review: Soil compaction and controlled traffic farming in arable and grass cropping systems. Agron. Res. 17, 653–682. https://doi.org/10.15159/AR.19.133

Arshad, M.A., Martin, S., 2002. Identifying critical limits for soil quality indicators in agro-ecosystems. Agric. Ecosyst. Environ. 88, 153–160. https://doi.org/10.1016/S0167-8809(01)00252-3

Awiti, A.O., Walsh, M.G., Shepherd, K.D., Kinyamario, J., 2008. Soil condition classification using infrared spectroscopy: A proposition for assessment of soil condition along a tropical forest-cropland chronosequence. Geoderma 143, 73–84. https://doi.org/10.1016/j.geoderma.2007.08.021

Badalíkova, B., 2010. Influence of soil tillage on soil compaction, in: Soil Engineering. Springer, pp. 19–30.

Barak, P., Jobe, B.O., Krueger, A.R., Peterson, L.A., Laird, D.A., 1997. Effects of long-term soil acidification due to nitrogen fertilizer inputs in Wisconsin. Plant Soil 197, 61–69. https://doi.org/10.1023/A:1004297607070

Barnes, R.J., Dhanoa, M.S., Lister, S.J., 1989. Standard normal variate transformation and de-trending of near-infrared diffuse reflectance spectra. Appl. Spectrosc. 43, 772–777. https://doi.org/10.1366/0003702894202201

Batey, T., 2009. Soil compaction and soil management - A review. Soil Use Manag. 25, 335–345. https://doi.org/10.1111/j.1475-2743.2009.00236.x

Bellon-Maurel, V., Fernandez-Ahumada, E., Palagos, B., Roger, J.M., McBratney, A.B., 2010. Critical review of chemometric indicators commonly used for assessing the quality of the prediction of soil attributes by NIR spectroscopy. TrAC - Trends Anal. Chem. 29, 1073–1081. https://doi.org/10.1016/j.trac.2010.05.006

Bellon-Maurel, V., McBratney, A., 2011. Near-infrared (NIR) and mid-infrared (MIR) spectroscopic techniques for assessing the amount of carbon stock in soils - Critical review and research perspectives. Soil Biol. Biochem. 43, 1398–1410. https://doi.org/10.1016/j.soilbio.2011.02.019

Ben-Dor, E., Banin, A., 1995. Near-Infrared Analysis as a Rapid Method to Simultaneously Evaluate Several Soil Properties. Soil Sci. Soc. Am. J. 59, 364–372. https://doi.org/10.2136/sssaj1995.03615995005900020014x

Ben-Dor, E., Taylor, R.G., Hill, J., Demattê, J.A.M., Whiting, M.L., Chabrillat, S., Sommer, S., 2008. Imaging Spectrometry for Soil Applications. Adv. Agron. 97, 321–392. https://doi.org/10.1016/S0065-2113(07)00008-9

Bengough, A.G., McKenzie, B.M., Hallett, P.D., Valentine, T.A., 2011. Root elongation, water stress, and mechanical impedance: A review of limiting stresses and beneficial root tip traits. J. Exp. Bot. 62, 59–68. https://doi.org/10.1093/jxb/erq350

Bengough, A.G., Mullins, C., 1990. Mechanical impedance to root growth: a review of experimental techniques and root growth responses. J. soil Sci. 41, 341–358. https://doi.org/10.1111/j.1365-2389.1990.tb00070.x

Bennie, A.T.P., Burger, R. du T., 1988. Penetration resistance of fine sandy apedal soils as affected by relative bulk density, water content and texture. South African J. Plant Soil 5, 5–10. https://doi.org/10.1080/02571862.1988.10634239

Bland, J.M., Altman, D.G., 2010. Statistical methods for assessing agreement between two methods of clinical measurement. Int. J. Nurs. Stud. 47, 931–936. https://doi.org/10.1016/j.ijnurstu.2009.10.001

Bland, J.M., Altman, D.G., 2003. Applying the right statistics: Analyses of measurement studies. Ultrasound Obstet. Gynecol. 22, 85–93. https://doi.org/10.1002/uog.122

Blume, H.-P., Brümmer, G.W., Horn, R., Kandeler, E., Kögel-Knabner, I., Kretzschmar, R., Stahr, K., Wilke, B.-M., 2010. Scheffer/Schachtschabel: Lehrbuch der Bodenkunde, 16th ed. Springer-Verlag, Heidelberg.

Bölenius, E., Stenberg, B., Arvidsson, J., 2017. Within field cereal yield variability as affected by soil physical properties and weather variations – A case study in east central Sweden. Geoderma Reg. 11, 96–103. https://doi.org/10.1016/j.geodrs.2017.11.001

Bolker, B.M., Brooks, M.E., Clark, C.J., Geange, S.W., Poulsen, J.R., Stevens, M.H.H., White, J.S.S., 2009. Generalized linear mixed models: a practical guide for ecology and evolution. Trends Ecol. Evol. 24, 127–135. https://doi.org/10.1016/j.tree.2008.10.008

Bradford, J.M., Peterson, G.A., 2000. Conservation tillage. Handb. soil Sci. 247–270.

Bünemann, E.K., Bongiorno, G., Bai, Z., Creamer, R.E., De Deyn, G., de Goede, R., Fleskens, L., Geissen, V., Kuyper, T.W., Mäder, P., Pulleman, M., Sukkel, W., van Groenigen, J.W., Brussaard, L., 2018. Soil quality – A critical review. Soil Biol. Biochem. 120, 105–125. https://doi.org/10.1016/j.soilbio.2018.01.030

Busscher, W.J., Bauer, P.J., Camp, C.R., Sojka, R.E., 1997. Correction of cone index for soil water content differences in a coastal plain soil. Soil Tillage Res. 43, 205–217. https://doi.org/10.1016/S0167-1987(97)00015-9

CAMO Software AS, 2011. The Unscrambler Appendices: Method References. Camo Software AS.

Cécillon, L., Barthès, B.G., Gomez, C., Ertlen, D., Genot, V., Hedde, M., Stevens, A., Brun, J.-J., 2009a. Assessment and monitoring of soil quality using near-infrared reflectance spectroscopy (NIRS). Eur. J. Soil Sci. 60, 770–784. https://doi.org/10.1111/j.1365-2389.2009.01178.x

Cécillon, L., Cassagne, N., Czarnes, S., Gros, R., Vennetier, M., Brun, J.-J., 2009b. Predicting soil quality indices with near infrared analysis in a wildfire chronosequence. Sci. Total Environ. 407, 1200–1205. https://doi.org/10.1016/j.scitotenv.2008.07.029

Central Statistics Office, 2016. Farm Structure Survey 2016 [WWW Document]. URL https://www.cso.ie/en/releasesandpublications/ep/p-fss/farmstructuresurvey2016/da/fs/ (accessed 2.21.20).

Chang, C.-W., Laird, D.A., Mausbach, M.J., Hurburgh, C.R., 2001. Near-Infrared Reflectance Spectroscopy–Principal Components Regression Analyses of Soil Properties. Soil Sci. Soc. Am. J. 65, 480–490. https://doi.org/10.2136/sssaj2001.652480x

Clay, S.A., Bruggeman, S.A., Kitchen, N.R., Clay, D.E., Bruggeman, S., Byamukama, E., 2017. Calculations Supporting Management Zones, in: Clay, D.E., Clay, S.A., Bruggeman, S.A. (Eds.), Practical Mathematics for Precision Farming. American Society of Agronomy, Crop Science Society of America and Soil Science Society of America, Madison, WI, pp. 122–135. https://doi.org/10.2134/practicalmath2017.0024

Cohen, M.J., Dabral, S., Graham, W.D., Prenger, J.P., Debusk, W.F., 2006. Evaluating ecological condition using soil biogeochemical parameters and near infrared reflectance spectra. Environ. Monit. Assess. 116, 427–457. https://doi.org/10.1007/s10661-006-7664-8

Cui, K., Défossez, P., Cui, Y.J., Richard, G., 2010. Soil compaction by wheeling: Changes in soil suction caused by compression. Eur. J. Soil Sci. 61, 599–608. https://doi.org/10.1111/j.1365-2389.2010.01245.x

Dalal, R.C., Henry, R.J., 1986. Simultaneous determination of moisture, organic carbon, and total nitrogen by near infrared reflectance spectrophotometry. Soil Sci. Soc. Am. J. 50, 120–123.

Daly, K., Casey, A., 2003. Eutrophication From Agricultural Sources: Environmental Soil Phosphorus Test. Wexford, Ireland.

Datta, D., 2017. blandr: a Bland-Altman Method Comparison package for R. https://doi.org/10.5281/zenodo.824514

Davis, J.W., 2018. Introduction to Generalized Linear Mixed Models A Count Data Example.

Défossez, P., Richard, G., 2002. Models of soil compaction due to traffic and their evaluation. Soil Tillage Res. 67, 41–64. https://doi.org/10.1016/S0167-1987(02)00030-2

Demattê, J.A.M., Dotto, A.C., Bedin, L.G., Sayão, V.M., Souza, A.B. e., 2019. Soil analytical quality control by traditional and spectroscopy techniques: Constructing the future of a hybrid laboratory for low environmental impact. Geoderma 337, 111–121. https://doi.org/10.1016/j.geoderma.2018.09.010

Department for Environment Food and Rural Affairs, 2010. Fertiliser Manual RB209, 8th ed. The Stationery Office.

Department of Agriculture Food & the Marine, 2018. Nitrates Explanatory Handbook for Good Agricultural Practice for the Protection of Waters Regulations 53.

Department of Agriculture Food & the Marine, 2015. Landscape features - Department of Agriculture, Food & the Marine.

Deverell, R., McDonnell, K., Devlin, G., 2009. The impact of field size on the environment and energy crop production efficiency for a sustainable indigenous bioenergy supply chain in the Republic of Ireland. Sustainability 1, 994–1011. https://doi.org/10.3390/su1040994

Dexter, A.R., 2004. Soil physical quality Part I. Theory, effects of soil texture, density, and organic mailer, and effects on root growth. Geoderma 120, 201–214. https://doi.org/10.1016/j.geodermaa.2003.09.005

Dexter, A.R., 1997. Physical properties of tilled soils. Soil Tillage Res. 43, 41–63. https://doi.org/10.1016/S0167-1987(97)00034-2

Dhawale, N.M., Adamchuk, V.I., Prasher, S.O., Viscarra Rossel, R.A., Ismail, A.A., Kaur, J., 2015. Proximal soil sensing of soil texture and organic matter with a prototype portable mid-infrared spectrometer. Eur. J. Soil Sci. 66, 661–669. https://doi.org/10.1111/ejss.12265

Dickey, E.C., Peterson, T., Eisenhauer, D.E., Jasa, P.J., 1985. Soil Compaction I Where, how bad, a problem. Biol. Syst. Eng. Pap. Publ. 1.

Doran, J.W., Parkin, T.B., 1994. Defining and Assessing Soil Quality. SSSA Spec. Publ. 35, 1–21.

Doran, J.W., Safley, M., Pankhurst, C., Doube, B.M., Gupta, V., others, 1997. Defining and assessing soil health and sustainable productivity. Biol. Indic. soil Heal. 1–28.

Du, C., Zhou, J., 2009. Evaluation of soil fertility using infrared spectroscopy: A review. Environ. Chem. Lett. 7, 97–113. https://doi.org/10.1007/s10311-008-0166-x

Dunne, K.S., Holden, N.M., O'Rourke, S.M., Fenelon, A., Daly, K., 2020. Prediction of phosphorus sorption indices and isotherm parameters in agricultural soils using mid-infrared spectroscopy. Geoderma 358, 113981. https://doi.org/10.1016/j.geoderma.2019.113981

Earl, R., Taylor, J.C., Wood, G.A., Bradley, I., James, I.T., Waine, T., Welsh, J.P., Godwin, R.J., Knight, S.M., 2003. Soil factors and their influence on within-field crop variability, Part I: Field observation of soil variation. Biosyst. Eng. 84, 425–440. https://doi.org/10.1016/S1537-5110(03)00004-7

Emmet-Booth, J.P., Holden, N.M., Fenton, O., Bondi, G., Forristal, P.D., 2020. Exploring the sensitivity of visual soil evaluation to traffic-induced soil compaction. Geoderma Reg. 20, e00243. https://doi.org/10.1016/j.geodrs.2019.e00243

Engel, J., Gerretzen, J., Szymańska, E., Jansen, J.J., Downey, G., Blanchet, L., Buydens, L.M.C., 2013. Breaking with trends in pre-processing? TrAC - Trends Anal. Chem. 50, 96–106. https://doi.org/10.1016/j.trac.2013.04.015

Esbensen, K.H., Swarbrick, B., 2018. Multivariate Data Analysis, 6th ed. Camo Software AS, Oslo, Magnolia TX.

European Chemicals Agency, 2020. Potassium chromate - Substance Information - ECHA [WWW Document]. URL https://echa.europa.eu/substance-information/-/substanceinfo/100.029.218 (accessed 5.17.20).

European Chemicals Agency, 2010a. Member state committee support document for identification of potassium chromate as a substance of very high concern because of its cmr properties. SVHC Support Doc. 1–27.

European Chemicals Agency, 2010b. Potassium dichromate - Authorisation List - ECHA [WWW Document]. URL https://echa.europa.eu/authorisation-list/-/dislist/details/0b0236e1807e157a (accessed 11.24.18).

European Comission, 2012. On the European Innovation Partnership "Agricultural Productivity and Sustainability," COM (2012) 79. Brussels.

European Comission, 2000. Directive 2000/60/EC OF THE EUROPEAN PARLIAMENT AND OF THE COUNCIL of 23 OCTOBER 2000 establishing a framework for Community action in the field of water policy, Official Journal of the European Communities. Brussels.

European Environmental Agency, 2019. Land and soil in Europe. Why we need to use these vital and finite resources sustainably, Eea Signals 2019. https://doi.org/10.2800/779710

European Union, 2017. Good Agricultural Practice for Protection of Waters.

Eurostat, 2016. Share of total utilised agricultural area by physical size of farm [WWW Document]. URL https://ec.europa.eu/eurostat/statistics-explained/images/4/4b/Share_of_total_utilised_agricultural_area%2C_by_physical_size_of_farm%2C_2013_%28%25_of_total%29.png (accessed 3.3.20).

FAO, 2017. Voluntary Guidelines for Sustainable Soil Management, 155th session of the FAO Council, Rome, Italy, 5th December 2016. Rome. https://doi.org/10.1007/978-3-319-68885-5_3

FAO, 2009. Global agriculture towards 2050. Rome.

Fathy, A., Sabry, Y.M., Nazeer, S., Bourouina, T., Khalil, D.A., 2020. On-chip parallel Fourier transform spectrometer for broadband selective infrared spectral sensing. Microsystems Nanoeng. 6. https://doi.org/10.1038/s41378-019-0111-0

Franzen, D.W., 2018. Soil Variability and Fertility Management, in: Shannon, D.K., Clay, D.E., Kitchen, N.R. (Eds.), Precision Agriculture Basics. American Society of Agronomy, Crop Science Society of America, and Soil Science Society of America, pp. 79–92. https://doi.org/10.2134/precisionagbasics.2016.0091

Friedman, D., Hubbs, M., Tugel, A., Seybold, C., Sucik, M., 2001. Guidelines for soil quality assessment in conservation planning. Nat. Resour. Conserv. Serv. Soil Qual. Inst. 1–38.

Gee, G.W., Bauder, J.W., 1986. Particle-size Analysis·, in: Klute, A. (Ed.), Methods of Soil Analysis. Part 1. Physical and Mineralogical Methods. pp. 383–411.

Geladi, P., 2003. Chemometrics in spectroscopy. Part 1. Classical chemometrics. Spectrochim. Acta - Part B At. Spectrosc. 58, 767–782. https://doi.org/10.1016/S0584-8547(03)00037-5

Geladi, P., MacDougall, D., Martens, H., 1985. Linearization and Scatter-Correction for Near-Infrared Reflectance Spectra of Meat. Appl. Spectrosc. 39, 491–500. https://doi.org/10.1366/0003702854248656

Gholizadeh, A., Saberioon, M., Ben-Dor, E., Borůvka, L., 2018. Monitoring of selected soil contaminants using proximal and remote sensing techniques: Background, state-of-the-art and future perspectives. Crit. Rev. Environ. Sci. Technol. 48, 243–278. https://doi.org/10.1080/10643389.2018.1447717

Godwin, R.J., Richards, T.E., Wood, G.A., Welsh, J.P., Knight, S.M., 2003. An economic analysis of the potential for precision farming in UK cereal production. Biosyst. Eng. 84, 533–545. https://doi.org/10.1016/S1537-5110(02)00282-9

Goulding, K.W.T., 2016. Soil acidification and the importance of liming agricultural soils with particular reference to the United Kingdom. Soil Use Manag. 32, 390–399. https://doi.org/10.1111/sum.12270

Greacen, E.L., 1960. Water content and soil strength. J. Soil Sci. 11, 313–333. https://doi.org/10.1111/j.1365-2389.1960.tb01088.x

Griffith, R.W., Goudey, C., Poff, R., 1992. Current application of soil quality standards, in: Proceedings of the Soil Quality Standards Symposium. pp. 1–5.

Håkansson, I., Lipiec, J., 2000. A review of the usefulness of relative bulk density values in studies of soil structure and compaction. Soil Tillage Res. 53, 71–85. https://doi.org/10.1016/S0167-1987(99)00095-1

Hamza, M.A., Anderson, W.K., 2005. Soil compaction in cropping systems: A review of the nature, causes and possible solutions. Soil Tillage Res. 82, 121–145. https://doi.org/10.1016/j.still.2004.08.009

Hedley, C., Roudier, P., Maddi, L., 2015. VNIR Soil Spectroscopy for Field Soil Analysis. Commun. Soil Sci. Plant Anal. 46, 104–121. https://doi.org/10.1080/00103624.2014.988582

Horn, R., Domżżał, H., Słowińska-Jurkiewicz, A., van Ouwerkerk, C., 1995. Soil compaction processes and their effects on the structure of arable soils and the environment. Soil Tillage Res. 35, 23–36. https://doi.org/10.1016/0167-1987(95)00479-C

Hutengs, C., Ludwig, B., Jung, A., Eisele, A., Vohland, M., 2018. Comparison of portable and bench-top spectrometers for mid-infrared diffuse reflectance measurements of soils. Sensors (Switzerland) 18. https://doi.org/10.3390/s18040993

Hutengs, C., Seidel, M., Oertel, F., Ludwig, B., Vohland, M., 2019. In situ and laboratory soil spectroscopy with portable visible-to-near-infrared and mid-infrared instruments for the assessment of organic carbon in soils. Geoderma 355, 113900. https://doi.org/10.1016/j.geoderma.2019.113900

Idowu, O.J., van Es, H.M., Abawi, G.S., Wolfe, D.W., Ball, J.I., Gugino, B.K., Moebius, B.N., Schindelbeck, R.R., Bilgili, A. V., 2008. Farmer-oriented assessment of soil quality using field, laboratory, and VNIR spectroscopy methods. Plant Soil 307, 243–253. https://doi.org/10.1007/s11104-007-9521-0

Janik, L.J., Merry, R.H., Skjemstad, J.O.O., 1998. Can mid infrared diffuse reflectance analysis replace soil extractions? Aust. J. Exp. Agric. 38, 681–696. https://doi.org/10.1071/EA97144

Janik, L.J., Skjemstad, J.O., 1995. Characterization and analysis of soils using mid-infrared partial least-squares .2. Correlations with some laboratory data. Aust. J. Soil Res. 33, 637. https://doi.org/10.1071/SR9950637

Janik, L.J., Skjemstad, J.O., Shepherd, K.D., Spouncer, L.R., 2007. The prediction of soil carbon fractions using mid-infrared-partial least square analysis. Aust. J. Soil Res. 45, 73–81. https://doi.org/10.1071/SR06083

Janik, L.J., Soriano-Disla, J.M., Forrester, S.T., McLaughlin, M.J., 2016. Moisture effects on diffuse reflection infrared spectra of contrasting minerals and soils: A mechanistic interpretation. Vib. Spectrosc. 86, 244–252. https://doi.org/10.1016/j.vibspec.2016.07.005

Ji, W., Adamchuk, V.I., Biswas, A., Dhawale, N.M., Sudarsan, B., Zhang, Y., Viscarra Rossel, R.A., Shi, Z., 2016. Assessment of soil properties in situ using a prototype portable MIR spectrometer in two agricultural fields. Biosyst. Eng. 152, 14–27. https://doi.org/10.1016/j.biosystemseng.2016.06.005

Ji, W., Rossel, R.V., Clay, D.E., Adamchuk, V.I., Gebbers, R., Tremblay, N., Kitchen, N.R., Shannon, D.K., 2018. Proximal Soil and Plant Sensing, in: Shannon, D.K., Clay, David E., Kitchen, N.R. (Eds.), Precision Agriculture Basics. American Society of Agronomy, Crop Science Society of America and Soil Science Society of America, Madison, WI. https://doi.org/10.2134/precisionagbasics.2016.0093

Ji, W., Viscarra Rossel, R.A., Shi, Z., 2015. Accounting for the effects of water and the environment on proximally sensed vis-NIR soil spectra and their calibrations. Eur. J. Soil Sci. 66, 555–565. https://doi.org/10.1111/ejss.12239

JOHN, M.K., 1970. COLORIMETRIC DETERMINATION OF PHOSPHORUS IN SOIL AND PLANT MATERIALS WITH ASCORBIC ACID. Soil Sci. 109, 214–220. https://doi.org/10.1097/00010694-197004000-00002

Johnson, M.G., Lammers, D.A., Anderson, C.P., Rygiewcz, P.T., Kern, J.S., 1990. Sustaining soil quality by protecting the soil resource, in: Proceedings of the Soil Quality Standards Symposium. pp. 72–80.

Kalivas, J.H., 2005. Multivariate Calibration, an Overview. Anal. Lett. 38, 2259–2279. https://doi.org/10.1080/00032710500315904

Karlen, D.L., Ditzler, C.A., Andrews, S.S., 2003. Soil quality: Why and how? Geoderma 114, 145–156. https://doi.org/10.1016/S0016-7061(03)00039-9

Karlen, D.L., Mausbach, M.J., Doran, J.W., Cline, R.G., Harris, R.F., Schumann, G.E., 1997. Soil Quality: A Concept, Definition, and Framework for Evaluation. Soil Sci. Soc. Am. J. 61.

Keesstra, S.D., Bouma, J., Wallinga, J., Tittonell, P., Smith, P., Cerdà, A., Montanarella, L., Quinton, J.N., Pachepsky, Y., Van Der Putten, W.H., Bardgett, R.D., Moolenaar, S., Mol, G., Jansen, B., Fresco, L.O., 2016. The significance of soils and soil science towards realization of the United Nations sustainable development goals. Soil 2, 111–128. https://doi.org/10.5194/soil-2-111-2016

Keller, T., Lamandé, M., Peth, S., Berli, M., Delenne, J.Y., Baumgarten, W., Rabbel, W., Radjaï, F., Rajchenbach, J., Selvadurai, A.P.S., Or, D., 2013. An interdisciplinary approach towards improved understanding of soil deformation during compaction. Soil Tillage Res. 128, 61–80. https://doi.org/10.1016/j.still.2012.10.004

Kissel, D.E., Isaac, R.A., Hitchcock, R., Sonon, L.S., Vendrell, P.F., 2007. Implementation of soil lime requirement by a single-addition titration method. Commun. Soil Sci. Plant Anal. 38, 1341–1352. https://doi.org/10.1080/00103620701328735

Koch, H.J., Heuer, H., Tomanová, O., Märländer, B., 2008. Cumulative effect of annually repeated passes of heavy agricultural machinery on soil structural properties and sugar beet yield under two tillage systems. Soil Tillage Res. 101, 69–77. https://doi.org/10.1016/j.still.2008.07.008

Kooistra, M.J., Tovey, N.K., Soane, B.D., Ouwerkerk, C. van, 1994. Effects of compaction on soil microstructure, in: Soane, B.D., van Ouwerkerk, C. (Eds.), Soil Compaction in Crop Production. Elsevier Science Publishers, B.V., pp. 91–111.

Kulli, B., Gysi, M., Flühler, H., 2003. Visualizing soil compaction based on flow pattern analysis. Soil Tillage Res. 70, 29–40.

Lal, R., Smith, P., Jungkunst, H.F., Mitsch, W.J., Lehmann, J., Ramachandran Nair, P.K., McBratney, A.B., De Moraes Sá, J.C., Schneider, J., Zinn, Y.L., Skorupa, A.L.A., Zhang, H.L., Minasny, B., Srinivasrao, C., Ravindranath, N.H., 2018. The carbon sequestration potential of terrestrial ecosystems. J. Soil Water Conserv. 73, 145A-152A. https://doi.org/10.2489/jswc.73.6.145A

Larson, W.E., Pierce, F.J., 1991. Conservation and enhancement of soil quality. Eval. Sustain. L. Manag. Dev. world Proc. Int. Work. Eval. Sustain. L. Manag. Dev. World, Chiang Rai, Thailand, 15-21 Sept. 1991.

Leenen, M., Welp, G., Gebbers, R., Pätzold, S., 2019. Rapid determination of lime requirement by mid-infrared spectroscopy: A promising approach for precision agriculture. J. Plant Nutr. Soil Sci. 1–11. https://doi.org/10.1002/jpln.201800670

Lipiec, J., Håkansson, I., 2000. Influences of degree of compactness and matric water tension on some important plant growth factors. Soil Tillage Res. 53, 87–94. https://doi.org/10.1016/S0167-1987(99)00094-X

Lipiec, J., Hatano, R., 2003. Quantification of compaction effects on soil physical properties and crop growth. Geoderma 116, 107–136. https://doi.org/10.1016/S0016-7061(03)00097-1

Lipiec, J., Stępniewski, W., 1995. Effects of soil compaction and tillage systems on uptake and losses of nutrients. Soil Tillage Res. 35, 37–52. https://doi.org/10.1016/0167-1987(95)00474-7

Louw, G., Rozanov, A., Wiese, L., van Niekerk, A., 2021. Soil NIR-spectroscopy and object-based landsurface segmentation for fluvial terrace level differentiation. Geomorphology 381, 107668. https://doi.org/10.1016/j.geomorph.2021.107668

Mark, H., Workman, J., 2007. Chemometrics in Spectroscopy, 1st ed, Chemometrics in Spectroscopy. Academic Press, London, Amsterdam. https://doi.org/10.1016/b978-012374024-3/50076-3

Martínez-España, R., Bueno-Crespo, A., Soto, J., Janik, L.J., Soriano-Disla, J.M., 2019. Developing an intelligent system for the prediction of soil properties with a portable mid-infrared instrument. Biosyst. Eng. 177, 101–108. https://doi.org/10.1016/j.biosystemseng.2018.09.013

Masserschmidt, I., Cuelbas, C.J., Poppi, R.J., De Andrade, J.C., De Abreu, C. a, Davanzo, C.U., 1999. Determination of organic matter in soils by FTIR/diffuse reflectance and multivariate calibration. J. Chemom. 13, 265–273. https://doi.org/10.1002/(SICI)1099-128X(199905/08)13:3/4<265::AID-CEM552>3.0.CO;2-E

McCarty, G.W., Reeves, J.B., Follett, R.F., Kimble, J.M., 2002. Mid-Infrared and Near-Infrared Diffuse Reflectance Spectroscopy for Soil Carbon Measurement. Soil Sci. Soc. Am. J. 66, 640. https://doi.org/10.2136/sssaj2002.0640

McLean, E.O., 1982. Soil pH and lime requirement, in: Methods of Soil Analysis. Part 2. Chemical and Microbiological Properties. American Society of Agronomy, Soil Science Society of America, pp. 199–224.

McLean, E.O., 1970. Lime requirements of soils—inactive toxic substances or favorable pH range? Soil Sci. Soc. Am. J. 34, 363–364.

McLean, E.O., Dumford, S.W., Coronel, F., 1966. A Comparison of Several Methods of Determining Lime Requirements of Soils. Soil Sci. Soc. Am. J. 30, 26–30.

Mehlich, A., 1976. New buffer ph method for rapid estimation of exchangeable acidity and lime requirement of soils. Commun. Soil Sci. Plant Anal. 7, 637–652. https://doi.org/10.1080/00103627609366673

Merry, R.H., Janik, L.J., 1999. New Methodology for Lime Requirements. Barton, ACT, Kingston ACT.

Minasny, B., Malone, B.P., McBratney, A.B., Angers, D.A., Arrouays, D., Chambers, A., Chaplot, V., Chen, Z.S., Cheng, K., Das, B.S., Field, D.J., Gimona, A., Hedley, C.B., Hong, S.Y., Mandal, B., Marchant, B.P., Martin, M., McConkey, B.G., Mulder, V.L., O'Rourke, S., Richer-de-Forges, A.C., Odeh, I., Padarian, J., Paustian, K., Pan, G., Poggio, L., Savin, I., Stolbovoy, V., Stockmann, U., Sulaeman, Y., Tsui, C.C., Vågen, T.G., van Wesemael, B., Winowiecki, L., 2017. Soil carbon 4 per mille. Geoderma 292, 59–86. https://doi.org/10.1016/j.geoderma.2017.01.002

Minasny, B., McBratney, A.B., Bellon-Maurel, V., Roger, J.M., Gobrecht, A., Ferrand, L., Joalland, S., 2011. Removing the effect of soil moisture from NIR diffuse reflectance spectra for the prediction of soil organic carbon. Geoderma 167–168, 118–124. https://doi.org/10.1016/j.geoderma.2011.09.008

Mirreh, H.F., Ketchenson, J.W., 1972. Influence of Soil Bulk Density and Matric Pressure on Soil Resistance To Penetration. Can. J. Soil Sci. 52, 477–483.

Morgan, M.F., 1941. Chemical soil diagnosis by the universal soil testing system. CT Agric. Exp. Stn. Bull. 450 579–643.

Mosaddeghi, M.., Hajabbasi, M.., Hemmat, A., Afyuni, M., 2000. Soil compactibility as affected by soil moisture content and farmyard manure in central Iran. Soil Tillage Res. 55, 87–97. https://doi.org/10.1016/S0167-1987(00)00102-1

Mossadeghi-Björklund, M., Arvidsson, J., Keller, T., Koestel, J., Lamandé, M., Larsbo, M., Jarvis, N.J., 2016. Effects of subsoil compaction on hydraulic properties and preferential flow in a Swedish clay soil. Soil Tillage Res. 156, 91–98. https://doi.org/10.1016/j.still.2015.09.013

Mouazen, A.M., Karoui, R., De Baerdemaeker, J., Ramon, H., 2006. Characterization of soil water content using measured visible and near infrared spectra. Soil Sci. Soc. Am. J. 70, 1295–1302. https://doi.org/10.2136/sssaj2005.0297

Naderi-Boldaji, M., Keller, T., 2016. Degree of soil compactness is highly correlated with the soil physical quality index S. Soil Tillage Res. 159, 41–46. https://doi.org/10.1016/j.still.2016.01.010

Naderi-Boldaji, M., Sharifi, A., Alimardani, R., Hemmat, A., Keyhani, A., Loonstra, E.H., Weisskopf, P., Stettler, M., Keller, T., 2013. Use of a triple-sensor fusion system for on-the-go measurement of soil compaction. Soil Tillage Res. 128, 44–53. https://doi.org/10.1016/j.still.2012.10.002

Naderi-Boldaji, M., Weisskopf, P., Stettler, M., Keller, T., 2016. Predicting the relative density from on-the-go horizontal penetrometer measurements at some arable top soils in Northern Switzerland. Soil Tillage Res. 159, 23–32. https://doi.org/10.1016/j.still.2015.12.002

Naes, T., Isaksson, T., Fearn, T., Davies, T., 2004. A User-friendly Guide to Multivariate Calibration and Classification. NIR Publications, Chichester, UK.

National Research Council, 1993. Soil and Water Quality: An Agenda for Agriculture. National Academy Press, Washington, D.C. https://doi.org/10.17226/2132

Ng, W., Minasny, B., Montazerolghaem, M., Padarian, J., Ferguson, R., Bailey, S., McBratney, A.B., 2019. Convolutional neural network for simultaneous prediction of several soil properties using visible/near-infrared, mid-infrared, and their combined spectra. Geoderma 352, 251–267. https://doi.org/10.1016/j.geoderma.2019.06.016

Ni, L.S., Fang, N.F., Shi, Z.H., Tan, W.F., 2019. Mid-infrared spectroscopy tracing of channel erosion in highly erosive catchments on the Chinese Loess Plateau. Sci. Total Environ. 687, 309–318. https://doi.org/10.1016/j.scitotenv.2019.06.116

Nocita, M., Stevens, A., van Wesemael, B., Brown, D.J., Shepherd, K.D., Towett, E., Vargas, R., Montanarella, L., 2015. Soil spectroscopy: An opportunity to be seized. Glob. Chang. Biol. 21, 10–11. https://doi.org/10.1111/gcb.12632

NRCS, 2018. Soil Texture Calculator | NRCS Soils [WWW Document]. URL https://www.nrcs.usda.gov/wps/portal/nrcs/detail/soils/survey/?cid=nrcs142p2_054167 (accessed 3.26.18).

O'Rourke, S.M., Stockmann, U., Holden, N.M., McBratney, A.B., Minasny, B., 2016. An assessment of model averaging to improve predictive power of portable vis-NIR and XRF for the determination of agronomic soil properties. Geoderma 279, 31–44. https://doi.org/10.1016/j.geoderma.2016.05.005

Odlare, M., Svensson, K., Pell, M., 2005. Near infrared reflectance spectroscopy for assessment of spatial soil variation in an agricultural field. Geoderma 126, 193–202. https://doi.org/10.1016/j.geoderma.2004.09.013

Olson, K.R., 1990. Soil physical properties as a measure of cropland productivity, in: Proceedings of the Soil Quality Standards Symposium, San Antonio, Texas, Oct.

Ortega, R.A., Santibáñez, O.A., 2007. Determination of management zones in corn (Zea mays L.) based on soil fertility. Comput. Electron. Agric. 58, 49–59. https://doi.org/10.1016/j.compag.2006.12.011

Padarian, J., Minasny, B., McBratney, A.B., 2019. Using deep learning to predict soil properties from regional spectral data. Geoderma Reg. 16, e00198. https://doi.org/10.1016/j.geodrs.2018.e00198

Paz-Kagan, T., Shachak, M., Zaady, E., Karnieli, A., 2014. A spectral soil quality index (SSQI) for characterizing soil function in areas of changed land use. Geoderma 230–231, 171–184. https://doi.org/10.1016/j.geoderma.2014.04.003

Pierce, F.J., Larson, W.E., Dowdy, R.H., Graham, W.A.P., 1983. Productivity of soils: Assessing long-term changes due to erosion. J. Soil Water Conserv. 38, 39–44.

Reeves, J.B., 2010. Near- versus mid-infrared diffuse reflectance spectroscopy for soil analysis emphasizing carbon and laboratory versus on-site analysis: Where are we and what needs to be done? Geoderma 158, 3–14. https://doi.org/10.1016/j.geoderma.2009.04.005

Reeves, J.B., Francis, B.A., Hamilton, S.K., 2005. Specular reflection and diffuse reflectance spectroscopy of soils. Appl. Spectrosc. 59, 39–46. https://doi.org/10.1366/0003702052940431

Reeves, J.B., McCarty, G.W., Hively, W.D., 2010. Mid- Versus Near-Infrared Spectroscopy for On-Site Analysis of Soil, in: Viscarra Rossel, A.R., McBratney, B.A., Minasny, B. (Eds.), Proximal Soil Sensing. Springer Netherlands, Dordrecht, pp. 133–142. https://doi.org/10.1007/978-90-481-8859-8_11

Rinnan, Å., van den Berg, F., Engelsen, S.B., 2009. Review of the most common pre-processing techniques for near-infrared spectra. TrAC - Trends Anal. Chem. 28, 1201–1222. https://doi.org/10.1016/j.trac.2009.07.007

Roger, J.M., Chauchard, F., Bellon-Maurel, V., 2003. EPO-PLS external parameter orthogonalisation of PLS application to temperature-independent measurement of sugar content of intact fruits. Chemom. Intell. Lab. Syst. 66, 191–204. https://doi.org/10.1016/S0169-7439(03)00051-0

Roudier, P., Hedley, C.B., Lobsey, C.R., Viscarra Rossel, R.A., Leroux, C., 2017. Evaluation of two methods to eliminate the effect of water from soil vis–NIR spectra for predictions of organic carbon. Geoderma 296, 98–107. https://doi.org/10.1016/j.geoderma.2017.02.014

SAS, n.d. PROC GLIMMIX: Syntax :: SAS/STAT(R) 9.3 User's Guide [WWW Document]. URL https://support.sas.com/documentation/cdl/en/statug/63962/HTML/default/viewer.htm#glimmix_toc.htm (accessed 1.29.20).

Savitzky, A., Golay, M.J.E., 1964. Smoothing and Differentiation of Data by Simplified Least Squares Procedures. Anal. Chem. 36, 1627–1639. https://doi.org/10.1021/ac60214a047

Schabenberger, O., 2005. Introducing the Glimmix Procedure for Generalized Linear Mixed Models, in: SUGI 30 Proceedings. pp. 1–20. https://doi.org/http://www2.sas.com/proceedings/sugi30/toc.html#fm

Schrijver, R., Poppe, K., Daheim, C., 2016. Precision agriculture and the future of farming in Europe. Brussels. https://doi.org/10.2861/020809

Servadio, P., Marsili, A., Pagliai, M., Pellegrini, S., Vignozzi, N., 2001. Effects on some clay soil qualities following the passage of rubber-tracked and wheeled tractors in central Italy. Soil Tillage Res. 61, 143–155. https://doi.org/10.1016/S0167-1987(01)00195-7

Shannon, D.K., Clay, D.E., Sudduth, K.A., 2018. An Introduction to Precision Agriculture, in: Shannon, D.K., Clay, D.E., Kitchen, N.R. (Eds.), Precision Agriculture Basics. Madison, WI, pp. 1–12. https://doi.org/10.2134/precisionagbasics.2016.0084

Shepherd, K.D., Walsh, M.G., 2007. Review: Infrared spectroscopy - Enabling an evidence-based diagnostic surveillance approach to agricultural and environmental management in developing countries. J. Near Infrared Spectrosc. 15, 1–19. https://doi.org/10.1255/jnirs.716

Shepherd, K.D., Walsh, M.G., 2002. Development of Reflectance Spectral Libraries for Characterization of Soil Properties. Soil Sci. Soc. Am. J. 66, 988. https://doi.org/10.2136/sssaj2002.0988

Sherman Hsu, C.-P., 1997. Infrared Spectroscopy, in: Settle, F.A. (Ed.), Handbook of Instrumental Techniques for Analytical Chemistry. Prentice Hall PTR, New Jersey, pp. 247–283.

Shi, T., Guo, L., Chen, Y., Wang, W., Shi, Z., Li, Q., Wu, G., 2018. Proximal and remote sensing techniques for mapping of soil contamination with heavy metals. Appl. Spectrosc. Rev. 53, 783–805. https://doi.org/10.1080/05704928.2018.1442346

Shoemaker, H.E., McLean, E.O., Pratt, P.F., 1961. Buffer Methods for Determining Lime Requirement of Soils With Appreciable Amounts of Extractable Aluminum. Soil Sci. Soc. Am. J. 25, 274–277. https://doi.org/10.2136/sssaj1961.03615995002500040014x

Sikora, F.J., 2006. A buffer that mimics the smp buffer for determining lime requirement of soil. Soil Sci. Soc. Am. J. 70, 474–486. https://doi.org/10.2136/sssaj2005.0164

Simo, I., Creamer, R.E., Massey, G., Hamilton, P., Mcdonald, J.A., 2007. EPA STRIVE Programme 2007-2013 Irish Soil Information System Soil Profile Handbook.

Soane, B.D., van Ouwerkerk, C., 1995. Implications of soil compaction in crop production for the quality of the environment. Soil Tillage Res. 35, 5–22. https://doi.org/10.1016/0167-1987(95)00475-8

Soane, B.D., van Ouwerkerk, C., 1994. Soil compaction problems in world agriculture. Soil Compact. Crop Prod. 11, 1–21.

Sørensen, L.K., Dalsgaard, S., 2005. Determination of Clay and Other Soil Properties by Near Infrared Spectroscopy. Soil Sci. Soc. Am. J. 69, 159. https://doi.org/10.2136/sssaj2005.0159

Soriano-Disla, J.M., Janik, L.J., Allen, D.J., McLaughlin, M.J., 2017. Evaluation of the performance of portable visible-infrared instruments for the prediction of soil properties. Biosyst. Eng. 161, 24–36.

https://doi.org/10.1016/j.biosystemseng.2017.06.017

Soriano-Disla, J.M., Janik, L.J., Forrester, S.T., Grocke, S.F., Fitzpatrick, R.W., McLaughlin, M.J., 2019. The use of mid-infrared diffuse reflectance spectroscopy for acid sulfate soil analysis. Sci. Total Environ. 646, 1489–1502. https://doi.org/10.1016/j.scitotenv.2018.07.383

Soriano-Disla, J.M., Janik, L.J., Viscarra Rossel, R.A., MacDonald, L.M., McLaughlin, M.J., 2014. The Performance of Visible, Near-, and Mid-Infrared Reflectance Spectroscopy for Prediction of Soil Physical, Chemical, and Biological Properties. Appl. Spectrosc. Rev. 49, 139–186. https://doi.org/10.1080/05704928.2013.811081

Sparkes, D.L., Jaggard, K.W., Ramsden, S.J., Scott, R.K., 1998. The effect of field margins on the yield of sugar beet and cereal crops. Ann. Appl. Biol. 132, 129–142. https://doi.org/10.1111/j.1744-7348.1998.tb05190.x

Sparks, D.L., 2003. 9 - The Chemistry of Soil Acidity, in: Sparks, D.L. (Ed.), Environmental Soil Chemistry (Second Edition). Academic Press, Burlington, pp. 267–283. https://doi.org/https://doi.org/10.1016/B978-012656446-4/50009-8

Sparling, G.P., Schipper, L.A., Bettjeman, W., Hill, R., 2004. Soil quality monitoring in New Zealand: Practical lessons from a 6-year trial. Agric. Ecosyst. Environ. 104, 523–534. https://doi.org/10.1016/j.agee.2004.01.021

Stenberg, B., Viscarra Rossel, R.A., 2010. Diffuse Reflectance Spectroscopy for High-Resolution Soil Sensing, in: Viscarra Rossel, A.R., McBratney, B.A., Minasny, B. (Eds.), Proximal Soil Sensing. Springer Netherlands, Dordrecht, pp. 29–47. https://doi.org/10.1007/978-90-481-8859-8_3

Stuart, B., 2004. Infrared Spectroscopy: Fundamentals and applications, Journal of Chemical Information and Modeling. JohnWiley & Sons, Ltd.

Teagasc, Plunkett, M., 2016. NMP Online – User Update 2 [WWW Document]. URL https://www.teagasc.ie/media/website/environment/soil/NMP-Online-Update-2_Soil-pH-and--Liming_15th-June-2016.pdf (accessed 8.17.20).

Tekin, Y., Kuang, B., Mouazen, A.M., 2013. Potential of on-line visible and near infrared spectroscopy for measurement of pH for deriving variable rate lime recommendations. Sensors (Switzerland) 13, 10177–10190. https://doi.org/10.3390/s130810177

Teng, H.T., Viscarra Rossel, R.A., Shi, Z., Behrens, T., 2018. Updating a national soil classification with spectroscopic predictions and digital soil mapping. Catena 164, 125–134. https://doi.org/10.1016/j.catena.2018.01.015

The Fertilizer Association of Ireland, 2016. Soil pH & Lime, Technical Bulletin.

Thomas, G.W., Hargrove, W.L., 1984. The Chemistry of Soil Acidity, in: Adams, F. (Ed.), Soil Acidity and Liming, Agronomy Monograph 12. ASA, CSSA, SSSA, Madison, WI.

Tunney, H., Sikora, F.J., Kissel, D., Wolf, A., Sonon, L., Goulding, K.W.T., 2010. A comparison of lime requirements by five methods on grassland mineral soils in Ireland. Soil Use Manag. 26, 126–132. https://doi.org/10.1111/j.1475-2743.2010.00263.x

UN General Assembly, 2015. Transforming our world: the 2030 Agenda for Sustainable Development. A/RES/70/1.

UNEP, 2012. Land Health Surveillance: An evidence-based approach to land ecosystem management, illustrated with a Case Study in the West Africa Sahel. United Nations Envrionment Programme, Nairobi. United Nations Environmental Programme, Nairobi.

Vågen, T.G., Shepherd, K.D., Walsh, M.G., 2006. Sensing landscape level change in soil fertility following deforestation and conversion in the highlands of Madagascar using Vis-NIR spectroscopy. Geoderma 133, 281–294. https://doi.org/10.1016/j.geoderma.2005.07.014

Velasquez, E., Lavelle, P., Andrade, M., 2007. GISQ, a multifunctional indicator of soil quality. Soil Biol. Biochem. 39, 3066–3080. https://doi.org/10.1016/j.soilbio.2007.06.013

Velasquez, E., Lavelle, P., Barrios, E., Joffre, R., Reversat, F., 2005. Evaluating soil quality in tropical agroecosystems of Colombia using NIRS. Soil Biol. Biochem. 37, 889–898. https://doi.org/10.1016/j.soilbio.2004.09.009

Vermeulen, G.D., Tullberg, J.N., Chamen, W.C.T., 2020. Controlled Traffic Farming, in: Dedousis, A., Bartzanas, T. (Eds.), Soil Engineering. Springer Berlin Heidelberg, Berlin, Heidelberg, pp. 101–120.

Viscarra Rossel, R.A., Behrens, T., 2010. Using data mining to model and interpret soil diffuse reflectance spectra. Geoderma 158, 46–54. https://doi.org/10.1016/j.geoderma.2009.12.025

Viscarra Rossel, R.A., McBratney, A.B., 2001. A response-surface calibration model for rapid and versatile site-specific lime-requirement predictions in south-eastern Australia. Aust. J. Soil Res. 39, 185–201. https://doi.org/10.1071/SR99131

Viscarra Rossel, R.A., McBratney, A.B., 1998. Laboratory evaluation of a proximal sensing technique for simultaneous measurement of soil clay and water content. Geoderma 85, 19–39. https://doi.org/10.1016/S0016-7061(98)00023-8

Viscarra Rossel, R.A., Walvoort, D.J.. J., McBratney, A.B., Janik, L.J., Skjemstad, J.O., 2006. Visible, near infrared, mid infrared or combined diffuse reflectance spectroscopy for simultaneous assessment of various soil properties. Geoderma 131, 59–75. https://doi.org/10.1016/j.geoderma.2005.03.007

Viscarra Rossel, R.A., Walvoort, D.J.J., MacBratney, A.B., Janik, L.J., Skjemstad, J.O., 2001. Proximal sensing of soil pH and lime requirement by mid infrared diffuse reflectance spectroscopy, in: Third European Conference on Precision Agriculture (3 Ecpa): Proceedings. pp. 497–502.

Vohland, M., Ludwig, M., Thiele-Bruhn, S., Ludwig, B., 2014. Determination of soil properties with visible to near- and mid-infrared spectroscopy: Effects of spectral variable selection. Geoderma 223–225, 88–96. https://doi.org/10.1016/j.geoderma.2014.01.013

Wadoux, A.M.J.-C., Malone, B., Minasny, B., Fajardo, M., McBratney, A.B., 2021. Selection of the Samples for Laboratory Analysis, in: Soil Spectral Inference with R. Springer Cham, Cham, pp. 143–164. https://doi.org/10.1007/978-3-030-64896-1_8

Wall, D., Plunkett, M. (Eds.), 2016. Major & Micro Nutrient Advice for Productive Agricultural Crops, 4th ed. Teagasc.

Ward, M., Forristal, P.D., McDonnell, K., 2020. Impact of field headlands on wheat and barley performance in a cool Atlantic climate as assessed in 40 Irish tillage fields. Irish J. Agric. Food Res. https://doi.org/10.15212/ijafr-2020-0113

Warkentin, B.P., Fletcher, H.F., 1977. Soil quality for intensive agriculture. Proc. Int. Semin. Soil Environ. Fertil. Manag. Intensive Agric.

Withers, P.J.A., Hodgkinson, R.A., Bates, A., Withers, C.M., 2006. Some effects of tramlines on surface runoff, sediment and phosphorus mobilization on an erosion-prone soil. Soil Use Manag. https://doi.org/10.1111/j.1475-2743.2006.00034.x

Wold, H., 1973. Nonlinear Iterative Partial Least Squares (NIPALS) Modelling: Some Current Developments, Multivariate Analysis–III. ACADEMIC PRESS, INC. https://doi.org/10.1016/b978-0-12-426653-7.50032-6

Wold, S., Sjostrom, M., Eriksson, L., 2001. PLS-regression: a basic tool of chemometrics. Chemom. Intell. Lab. Syst. 58, 109–130. https://doi.org/10.1016/S0169-7439(01)00155-1

Zambon, I., Benedetti, A., Ferrara, C., Salvati, L., 2018. Soil Matters? A Multivariate Analysis of Socioeconomic Constraints to Urban Expansion in Mediterranean

Europe. Ecol. Econ. 146, 173–183. https://doi.org/10.1016/j.ecolecon.2017.10.015

Zeng, R., Zhang, G.L., Li, D.C., Rossiter, D.G., Zhao, Y.G., 2016. How well can VNIR spectroscopy distinguish soil classes? Biosyst. Eng. 152, 117–125. https://doi.org/10.1016/j.biosystemseng.2016.04.019

Digital Appendix

The digital appendix contains the following documents:

Database_PhD_Metzger

Excel table containing information about the field samples and their corresponding laboratory results and MIR-DRIFTS spectra

SAS Output

Output files from the GLIMMIX procedure in SAS for the zone-based comparison

Scientific Articles

Latest version of the three scientific articles for publication as pdf